# ROLE OF MIR-126 IN PLACENTAL DEVELOPMENT AND GLUCOSE METABOLISM

A Dissertation

Presented to the Faculty of the Weill Cornell Graduate School

of Medical Sciences

in Partial Fulfillment of the Requirements for the Degree of

Doctor of Philosophy

by

Abhijeet Sharma

May 2018

# ROLE OF MIR-126 IN PLACENTAL DEVELOPMENT AND GLUCOSE METABOLISM

Abhijeet Sharma, Ph.D.

Cornell University 2018

The placenta is a transient organ that is critical for the growth and development of the mammalian embryo. Placental insufficiencies can lead to preeclampsia in the mother and intra-uterine growth restriction of the fetus. Insults incurred *in utero* have been associated with increased susceptibility to cardiovascular disease and diabetes in adulthood. A functional placenta develops through a delicate interplay of its vascular and trophoblast compartments. However, the genetic basis of trophoblast development and placental angiogenesis is not completely understood. In this thesis, using a mouse model, I have studied the role of a micro-RNA, miR-126, in placental development. Additionally, I also uncovered a novel role for miR-126 in regulating glucose homeostasis in adults.

The first set of studies elucidates the role of miR-126 in the murine placenta. Here, I determined the role of miR-126 in placental development, using a mouse model with a targeted deletion of miR-126. miR-126 has a novel expression domain in trophoblast stem cells and differentiated trophoblast sub-types in the placenta. Loss of miR-126 leads to significant hyperplasia in the junctional zone at embryonic day 15.5 (E15.5) at the expense of the labyrinth, resulting in reduced placental volume for nutrient exchange and intra-uterine growth restriction of the embryos. Junctional zone hyperplasia results from increased numbers of proliferating glycogen trophoblast progenitors at E13.5 that give rise to an expanded glycogen trophoblast population at

E15.5. I also demonstrate that miR-126$^{-/-}$ placentas display aberrant expression of imprinted genes with important roles in glycogen trophoblasts and junctional zone development, including Igf2, H19, and Cdkn1c. Abnormal imprinted gene expression is restricted to the placenta and is accompanied by aberrant DNA methylation at imprint control centers. miR-126$^{-/-}$ placentas also display abnormal expression of the imprinting regulator, *Dnmt1,* through early and mid-gestation and display changes in global methylation at mid-gestation. Collectively, using a miR-126 loss of function mouse model, I have identified a novel role for miR-126 in regulating DNA methylation, imprinted gene expression and glycogen trophoblast proliferation in the placenta.

The second set of studies focused on the role of miR-126 in glucose metabolism. A number of rare autosomal dominant, monogenic forms of diabetes termed maturity onset diabetes (MODY) have been identified in humans. miR-126$^{+/-}$ adult mice display fasting hyperglycemia and hypoinsulinemia. miR-126$^{+/-}$ male mice, but not female mice display sporadic weight-gain defects and severe glucose intolerance during a glucose tolerance test. This indicates that loss of even a single copy of miR-126 is associated with metabolic dysfunction thereby highlighting its importance in maintaining glucose homeostasis.

Collectively, my studies uncovered a novel role for miR-126 in regulating DNA methylation and extra-embryonic energy stores in the placenta. In addition, my studies uncovered a potential novel role for miR-126 in regulating glucose homeostasis in adult mice.

## BIOGRAPHICAL SKETCH

Abhijeet Sharma was born and raised in Bangalore, India. Abhijeet attended Rashtreeya Vidyalaya College of Engineering and obtained his Bachelor of Engineering degree in Biotechnology with distinction in May 2008.

Following his undergraduate studies, Abhijeet pursued his Master's degree at the University of Houston Clear Lake. His research with Dr. Ronald Mills involved characterization of naturally occurring mutations in zinc transporter genes in the model plant system *Arabidopsis thaliana*. He graduated with a Master of Science in Biotechnology in December 2010.

After obtaining his Master's degree, Abhijeet worked as a research technician in Dr. Flint Beal's laboratory in the Department of Neuroscience at Weill Cornell Medical College in February 2011. His research involved characterizing the role of *PGC1α* in the pathogenesis of Huntington's disease and testing the treatment efficacy of a PPAR-agonist Bezafibrate on mouse models of Huntington's disease. His work in the Beal lab resulted in three co-authored publications.

Abhijeet started the Biochemistry, Cell and Molecular Biology graduate program at Weill Cornell Medical College in September 2012. He became a member of Dr. Heidi Stuhlmann's lab in June 2013, and began his thesis research investigating the role of miR-126 in placental development. He also worked on a collaborative project investigating the role of Epidermal Growth Factor Like Domain 7 (Egfl7) as an angiocrine factor in the bone marrow. He has presented his work at the Vincent DuVigneaud Graduate School Symposium at Weill Cornell, as well as at national and

international conferences, including the Society of Developmental Biology (SDB) and the International Federation of Placenta Associations (IFPA). Abhijeet was awarded a NIH travel award for outstanding abstract at IFPA conference in 2016. He was also awarded a seed grant to study non-coding RNA mechanisms in health and disease from NICHD-funded Cornell Center for Reproductive Genomics (CRG) in 2017. During the course of his Ph.D., Abhijeet has mentored undergraduate summer students and first year rotation students. He was also a teaching assistant for the graduate course on Principles of Developmental Biology in 2015.

Abhijeet's graduate work has resulted in a manuscript currently under revision. Following the completion of his Ph.D., Abhijeet plans to continue on to postdoctoral training in scientific research in the field of Cell and Molecular biology.

This work is dedicated to my parents for their endless love, support and encouragement.

## ACKNOWLEDGEMENTS

I want to express my deepest gratitude for all the support I have received throughout my Ph.D. starting with my thesis advisor, Dr. Heidi Stuhlmann. I owe my most sincere thanks to Heidi for her mentorship, guidance and encouragement. Heidi's enthusiasm for science, collaborations and mentoring has been instrumental in shaping the way I think about the same. I am truly indebted to Heidi for the scientist I am today, and the mentor I will be tomorrow.

I would also like to thank my thesis committee members Dr. Todd Evans and Dr. Andrea Ventura for their helpful discussions and periodic scientific guidance.

I am grateful to Dr. Jason Butler for his generosity with time, reagents, collaborations, scientific guidance and career advice. I would also like to thank Dr. Michael Poulos from the Butler lab for providing me with critical scientific expertise and guidance.

I would like to thank present and past members of the Stuhlmann lab including Dr. Lauretta Ann Lacko, Dr. Kathryn Bambino, Dr. Donna Nichol, Samantha Hinds, Lissenya Arguetta and Dr. Clare Burke. I owe special thanks to Laurie for her time, patience, moral support and for being a great friend.

I am grateful to Dr. Effie Apostolou, for her time, guidance and helpful insight on my project and manuscript. I also would like to thank Dr. Tim McGraw and Dr. James Lo and members of their lab for sharing reagents and advice.

Much of my work was made possible by the core facilities at WCMC. I want to thank Lee Cohen-Gould and her team at the WCMC Electron Microscopy Core

Facility. I would like to thank Dr. Paula Cohen and The Center for Reproductive Genomics at Cornell for providing me the NICHD-funded seed grant, which enabled me to use the RNA sequencing core.

I am thankful for the camaraderie and encouragement from my friends at WCMC. I am grateful to have shared my successes and failures and to have received constant support from my peers.

I would like to thank my parents for their unwavering support, for instilling in me scientific curiosity, for providing me with invaluable resources to follow my passion and pursue higher education. I will forever be grateful for their love and sacrifice.

Lastly, I am extremely grateful to my wife. I can unequivocally say that without her scientific and emotional support, I could not have accomplished my graduate work. I want to thank her for always driving me to be a better scientist and person. Her support has allowed me to achieve more than I could have imagined.

## TABLE OF CONTENTS

## LIST OF FIGURES

## LIST OF ABBREVATIONS

| | |
|---|---|
| AKT | Protein Kinase B |
| ART | Assisted reproductive technology |
| BWS | Beckwith Wiedemann syndrome |
| C-TGC | Canal trophoblast giant cell |
| CDKN1C | Cyclin-dependent kinase inhibitor 1C |
| CTCF | CCCTC-binding factor |
| DMR | Differentially methylated region |
| DNMT | DNA methyl transferase |
| EdU | 5-ethynyl-2'-deoxyuridine |
| EGFL7 | Epidermal growth factor like domain 7 |
| EPC | Ecto-placental cone |
| ERG | ETS related gene |
| ERK | Extracellular signal related kinase |
| ESC | Embryonic stem cells |
| ExE | Extra-embryonic ectoderm |
| FGF | Fibroblast Growth Factor |
| GlyT | Glycogen trophoblasts |
| HSC | Hematopoietic stem cells |
| HUVEC | Human umbilical vein endothelial cells |
| ICM | Inner cell mass |
| ICR | Imprint control center |
| IGF2 | Insulin Growth Factor II |
| IUGR | Intra uterine growth restriction |
| JZ | Junctional zone |
| Lab | Labyrinth |
| lncRNA | Long non-coding RNA |
| MAPK | Mitogen-activated Protein Kinase |
| mg | Milligrams |
| miRNA | Micro-RNA |
| mL | Milliliters |
| mm | Millimeters |
| mRNA | Messenger RNA |
| ng | nanogram |
| PAS | Periodic Acid- Schiff |
| PE | Preeclampsia |
| PHLDA2 | Pleckstrin Homology-Like Domain, Family A |
| PI3K | Phosphoionositide 3-Kinase |
| RB | Retinoblastoma |
| S-TGC | Sinusoidal artery trophoblast giant cell |
| SNP | Single Nucleotide Polymorphism |
| SpA-TGC | Spiral artery trophoblast giant cell |
| SPRED1 | Sprouty-related, EVH1 domain-containing protein 1 |

| | |
|---|---|
| SRS | Silver Russel syndrome |
| T2DM | Type II Diabetes Mellitus |
| TET | Ten eleven translocation |
| TGC | Trophoblast giant cell |
| TSC | Trophoblast stem cells |
| UTR | Untranslated region |
| VCAM1 | Vascular cell adhesion protein 1 |
| VEGF | Vascular endothelial growth factor |

## LIST OF SYMBOLS

| | |
|---|---|
| α | alpha |
| β | beta |
| γ | gamma |
| μ | micro |

# Chapter 1- Introduction

## 1.1 Placenta – Structure and function

The placenta is a transient organ that is critical for the survival and growth of mammalian embryos. The placenta forms the interface between maternal and fetal circulations, facilitating exchange of nutrients and gases and disposal of fetal waste. It is a major endocrine organ, secreting hormones critical for maternal physiology during pregnancy and fetal growth during gestation. The placenta also forms the immune barrier for the fetus from the maternal immune system (Rossant and Cross 2001).

A fully developed human placenta is composed of three layers: the maternal decidua, containing maternal vessels that bring blood to and from the implantation site, a middle basal zone, mainly containing trophoblasts that invade maternal vessels to remodel maternal arteries, and a fetal labyrinth layer containing highly branched villous structures of the fetal endothelium which is the site for nutrient, gas and waste exchange (Maltepe et al. 2010).

Placental dysfunction can lead to pregnancy complications such as preeclampsia (PE) and intra uterine growth restriction (IUGR) that increases chances of morbidity and mortality in the mother and the fetus (Rossant and Cross 2001; Maltepe et al. 2010). PE is the leading cause of maternal and fetal morbidity and mortality and is characterized by the sudden onset of maternal hypertension and

proteinuria after 20 weeks gestation. The only treatment for PE is delivery of the fetus (Young et al. 2010). Placental dysfunction is also seen as the leading cause for increase in pre-term deliveries and growth-restricted infants in the past two decades (Goldenberg et al. 2008; Simmons et al. 2010). Infants from induced deliveries are more likely to develop complications like pulmonary dysplasia, hypertension and cerebral palsy. This has resulted in an increase in the number of infants admitted to intensive care nurseries, placing enormous emotional and economic demands on the society (Eichenwald and Stark 2008).

Through a process called fetal programing, environmental insults incurred *in utero* can also result in an increased susceptibility to cardiovascular disease and diabetes later in life (Murphy et al. 2006). Although there have been improvements in neonatal care, early diagnosis and prevention of placental pathologies will have the greatest long-term impact on health care. Studying placental pathologies like preeclampsia and intra-uterine growth restriction requires a thorough understanding of the interplay between transcriptional and epigenetic regulators for human placental development and the effects of environment cues on these processes.

### 1.2 Models of placental development

Human placental development has mostly been studied from analysis on the placenta after delivery or following termination of pregnancy (Maltepe et al. 2010). A number of functional studies have relied on transformed human trophoblast cell lines

or *ex vivo* culture of primary trophoblasts. Several large and small animal models have been extremely beneficial in understanding key features of placental development *in vivo* (Rossant and Cross 2001; Maltepe et al. 2010).

Placentas can be categorized based on morphology and histology. By gross morphology, placentas can be categorized into three distinct types: diffuse (horses, pigs), multicotyledonary (ruminants), zonary (carnivores) and discoid/bidiscoid (rabbits, primates, rodents) (Furukawa et al. 2014). A more functional characterization is based on histology: epitheliochorial (horses, pigs and ruminants), endotheliochorial (carnivores) and hemochorial (rabbits, rodents, primates) (Furukawa et al. 2014). Mice and humans have hemochorial placentas, with the trophoblasts directly in contact with maternal blood (Watson and Cross 2005; Maltepe et al. 2010). Although human and murine placentas have minor differences, both species have similar placental structures and are thought to share molecular mechanisms that control placental development (Watson and Cross 2005). Powerful genetic tools have enabled the use of murine models to study the roles of a single gene or combinations of gene networks in placental development. This has been particularly important in identifying targeted mutations associated with placental defects resulting in embryonic lethality. Mouse mutants have been used to identify several key genes for placental development. Genes such as *Cdx2, Eomes, Esrrb*, that critical for trophoblast stem cell specification and differentiation (Chawengsaksophak et al. 1997; Luo et al. 1997; Riley et al. 1998; Russ et al. 2000), *Ets2*, critical for ectoplacental cone fusion (Yamamoto et al. 1998), *Bmp5, Bmp7, Vcam1*, critical for chorioallantoic fusion (Li et al. 1992; Gurtner et al.

1995; Solloway and Robertson 1999), *Gcm1, Fgfr2, PPARγ* for branching morphogenesis and labyrinth development (Xu et al. 1998; Barak et al. 1999; Giroux et al. 1999; Anson-Cartwright et al. 2000), *Ascl2, H19, Hectd1*, for endocrine trophoblast maintenance (Constancia et al. 2002; Esquiliano et al. 2009; Sarkar et al. 2014) and *Igf2, Gjb2* for nutrient transport (Gabriel et al. 1998; Liang et al. 2010). These studies have also highlighted the importance of signaling interactions between the trophoblasts, the fetal vasculature and the maternal vasculature during placental development.

### 1.3 Murine placental development

Placental development begins at embryonic day 3.5 (E3.5) in the blastocyst when two distinct cell lineages are formed. The outer layer of cells called the trophectoderm are polarized epithelial-like cells with apical microvilli and asymmetric distribution of adherens and tight junctions. The inner cluster of non-polarized cells forms the inner cell mass (ICM) (Rossant and Cross 2001). The trophectodermal layer is specified through a cascade of transcription factors via the hippo-signaling pathway (Watson and Cross 2005). At E4.5, the trophectodermal cells not in contact with the ICM (mural trophectoderm) differentiate into primary trophoblast giant cells (TGCs). Primary TGCs undergo endoreduplication to become polyploid cells and are analogous to human extravillous cytotrophoblasts (Maltepe et al. 2010). From the polar trophectoderm (cells adjacent to the ICM), two cell layers are formed, the extra embryonic ectoderm (ExE) and the ectoplacental cone (EPC). The extraembryonic

ectoderm differentiates into trophoblasts that form the chorion and the labyrinth at later stages (Watson and Cross 2005; Maltepe et al. 2010). Around E8.5, the allantois arising from the posterior end of the mesoderm makes contact with the chorion in a process termed chorio-allantoic fusion (Figure 1.1). Hours after chorio-allantoic fusion takes place, feto-placental blood vessels invade from the allantois and undergo branching morphogenesis to form the fetal part of the placental vasculature (Watson and Cross 2005) (Figure 1.1). In mice, two layers of syncytiotrophoblast are in direct apposition to endothelial cells of the fetal vessels. In the human placenta, the fetal vasculature is in apposition to a monolayer of syncytiotrophoblasts (Maltepe et al. 2010).

Progenitors from ExE and EPC give rise to a wave of postmitotic and polyploid secondary TGCs. The murine placenta has four different secondary TGC subtypes that can be distinguished by their gene expression and location. Spiral artery TGCs (SpA TGCs) invade maternal arteries and replace endothelial cells through a process called spiral artery remodeling and vascular mimicry, resulting in dilation of the arteries (Adamson et al. 2002). Spiral arteries converge to form large canals, lined by canal TGCs (C-TGC), that carry oxygenated blood to the placental labyrinth. The maternal vascular spaces in the labyrinth are lined by sinusoidal TGCs (S-TGCs). After nutrient and waste exchange, blood moves to large lacunae lined by parietal TGCs that connect with the uterine veins (Simmons et al. 2007).

The ectoplacental cone differentiates into several cell types of the junctional zone and some giant cell subtypes. The junctional zone (basal zone in humans) anchors the fetal labyrinth to the maternal decidua and is also a major source of several prolactin and placental lactogens critical for maternal health during gestation (Simmons et al. 2008). Although the function of the junctional zone has not been clearly elucidated, increasing evidence from mouse mutants have highlighted the importance of the junctional zone and the hormones secreted by this layer (Coan et al. 2006; John 2017). The junctional zone contains three major trophoblast subtypes- spongiotrophoblasts, secondary TGCs and glycogen trophoblasts. All trophoblasts subtypes of the junctional zone secrete a number of prolactin and placental lactogen hormones critical for maternal health and metabolic function during gestation (Rossant and Cross 2001). During late gestation, the glycogen trophoblasts migrate into the decidua and release glycogen into the maternal bloodstream. The function of glycogen trophoblasts has not been established. They are speculated to play a role in supporting embryonic growth during late gestation or in parturition (Coan et al. 2006). In human placentas, data suggests that placental glycogen is a defining feature of fetal growth restriction and fetal overgrowth (Akison et al. 2017). Development and differentiation of all the trophoblast lineages rely on a coordinated action of transcriptional, epigenetic and physiological factors in the placenta.

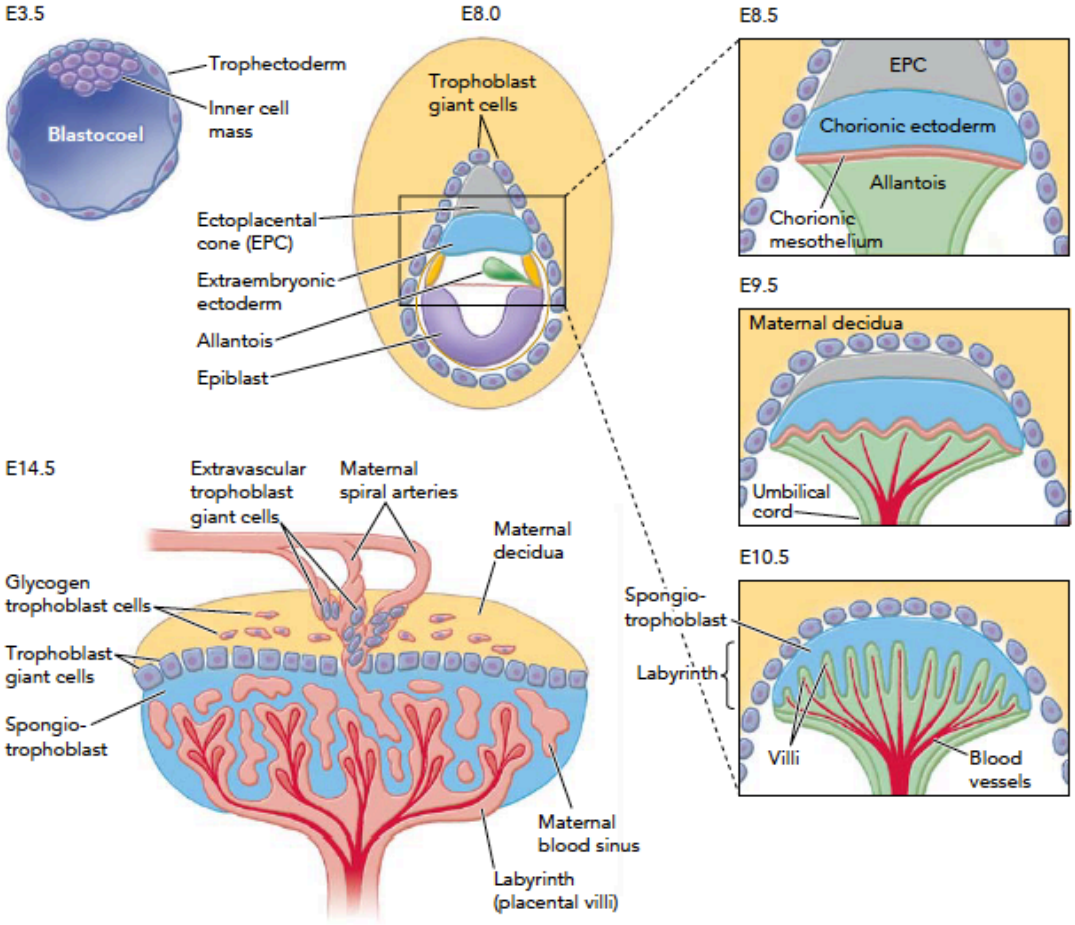


**Figure 1.1 Overview of murine placental development**

Adapted from Rossant and Cross (2005) Physiology 20:180-193

## 1.4 Epigenetic mechanisms- Genomic imprinting

Epigenetic mechanisms involve heritable changes in somatic cells that are independent of changes in nucleotide sequences. DNA methylation at the CpG dinucleotides and histone modifications represent the two major epigenetic marks that control the accessibility of various transcription factors to genes, promoters and enhancers (Jaenisch and Bird 2003).

Genomic imprinting is an epigenetic modification that restricts expression of a gene to one of the two parental alleles. Over a hundred protein-coding genes that play critical roles in growth, development and behavior are imprinted in humans and mice (Morison et al. 2005; Peters 2014). Genomic imprinting does not represent repression of gene expression, but can regulate allelic expression by controlling the promoter, enhancer, splicing junctions and polyadenylation sites (Ferguson-Smith 2011). Imprinted genes appear in clusters spanning several kilobases or megabases in size (Wan and Bartolomei 2008; Sanli and Feil 2015). A large majority of imprinting clusters are also accompanied by long non-coding RNAs (lncRNAs) (Barlow and Bartolomei 2014). Imprinting clusters are controlled by CpG dinucleotides rich imprint control regions (ICR). ICRs carry parent-of origin specific methylation marks acquired during gametogenesis and maintained throughout development. The methylation imprint is established on one parental chromosome and controls expression of some or all imprinted genes in the cluster (Barlow and Bartolomei 2014; Sanli and Feil 2015).

DNA methylation is acquired by *de novo* methyl transferases and maintained by maintenance methyl transferases (Li et al. 1993). In the male germline, paternal specific methylation is acquired in prospermatogonia prior to meiosis (Lucifero et al. 2002). In oocytes, ICRs are methylated at different times during maturation (Koerner et al. 2012). The coordinated action of the de novo methyltransferase DNMT3A and a non-catalytic protein DNMT3L is necessary for placing methylation imprints at ICRs (Cheng and Blumenthal 2010). Methylation at these loci is maintained by the maintenance methyltransferase DNMT1 (Li et al. 1993). DNMT1 catalyzes methylation of hemi-methylated CpG nucleotides at differentially methylated regions (DMRs) of ICRs during cell division (Messerschmidt et al. 2014). Apart from the 5-methyl cytosine, various other proteins and histone modifications are also involved in the maintenance of imprints in somatic cells (Barlow and Bartolomei 2014). KRAB-domain zinc finger protein ZFP57 is one such protein that recruits KAP1, which in turn mediates recruitment of H3-lysine 9 specific histone modifying enzymes (Hirasawa and Feil 2008; Quenneville et al. 2011). ZFP57 mutations in humans are associated with transient neonatal diabetes caused by the loss of DNA methylation at the PLAGL1 gene (Mackay et al. 2008).

After fertilization, despite a massive wave of de-methylation, parental specific imprints are maintained in the inner cell mass and the trophectoderm of blastocysts (Reik et al. 2001; Duffie and Bourc'his 2013). The maintenance of methylation at ICRs is linked to patterns of histone methylation (Kelsey and Feil 2013). Histones at

the DNA methylated alleles of ICRs are marked by histone H3 lysine-9 trimethylation (H3K9me3), H3 lysine-64 tri-methylation (H3K64me3), H4 lysine-20 trimethylation (H4K20me3) and H4 arginine-3 dimethylation (H4R3me2s), and interact with DNA bound heterochromatinprotein-1 gamma (Delaval et al. 2007; Pannetier et al. 2008; Girardot et al. 2014). Throughout development, DNMT1 maintains imprints in dividing cells by catalyzing methylation of hemi-methylated CpG nucleotides at DMRs.

The imprinting cycle is completed by erasure of imprints in primordial germ cells of the early embryo, by passive demethylation (failure to undergo maintenance methylation after DNA replication) or active demethylation, in part through the action of ten-eleven translocation (TET) proteins (Tan and Shi 2012; Li and Zhang 2014).

### 1.5 Roles of imprinted genes during embryonic and placental growth

A large subset of imprinted genes code for factors that regulate embryonic and neonatal growth (Barlow and Bartolomei 2014). Genomic imprinting is thought have evolved through a mechanism termed ‘parental-conflict hypothesis’. The genome of a developing embryo comes from two parents, but embryonic growth and nutrition is reliant on one parent. Paternally expressed genes are proposed to promote embryonic growth and maximize the fitness of an individual embryo. Maternally expressed imprinted genes are proposed to suppress fetal growth ensuring a more equal distribution of maternal resources to all offspring (Moore and Haig 1991). In support

of this hypothesis, a number of studies in transgenic mice with altered expression of imprinted genes have display abnormalities in fetal growth, placental development, maternal lactation and behavior and thermogenesis (Barlow and Bartolomei 2014; John 2017).

Deletion of *Igf2*, a maternally imprinted gene, results in IUGR of the embryos and placentas at mid-gestation (E12.5) and mutant pups are born at 60% of the weight of wild type littermates (DeChiara et al. 1990; DeChiara et al. 1991). Placental defects were shown to be the primary cause of IUGR in the embryos by deleting the promoter of a placental-specific Igf2 transcript (Constancia et al. 2002). Both global and placental specific deletion of *Igf2* also results in reduced numbers of glycogen trophoblasts in the placenta and reduced nutrient transfer to the embryo (Lopez et al. 1996; Constancia et al. 2002; Sferruzzi-Perri et al. 2011). Biallelic expression of Igf2 by deletion of the H19 DMR region results in increased weights of the embryos and placentas and an increase in the glycogen trophoblasts of the placenta (Esquiliano et al. 2009).

Deletion of a paternally imprinted gene Cdkn1C results in overgrowth of embryos at E15.5 and E18.5, but do not maintain their growth trajectory to birth due to placental insufficiencies (Tunster et al. 2011). Apart from widespread labyrinth zone defects, mutant placentas also display defective maturation of glycogen trophoblast progenitors (Coan et al. 2006; Tunster et al. 2011).

Functional studies have also revealed key roles for several placental-specific imprinted genes in nutrient transport, growth and placental hormone expression by regulating the size of the placental endocrine compartment.

During development, Phlda2 is mainly expressed by the placenta. Loss-of-function, gain of function and loss of imprinting mutations have shown that Phlda2 plays a key role in placental growth. Loss of Phlda2 results in placental overgrowth and hypertrophy of the spongiotrophoblast layer (endocrine compartment), resulting in reduced labyrinth compartment and fetal IUGR (Fitzpatrick et al. 2002; Tunster et al. 2010).

The importance of genomic imprinting is highlighted in imprinting disorders observed in humans. Imprinting disorders have diverse sets of clinical phenotypes, but primarily involve growth and neurological development. The two most well characterized growth disorders associated with aberrant imprinting are Beckwith–Wiedemann (BWS) and Silver-Russell syndrome (SRS).

The clinical features of BWS include prenatal and/or postnatal overgrowth, placental overgrowth, macroglossia (enlarged tongue), abdominal wall defects, hypoglycemia, renal abnormalities and predisposition to Wilm's tumors (Maher and Reik 2000; Choufani et al. 2010). BWS has an estimated prevalence of one in 13,700 live births, although cases with subtle phenotypes are thought to go undiagnosed (Engstrom et al. 1988; Gicquel et al. 2005). About 85% of BWS cases are associated

with imprinting defects at 11p15.5 (Li et al. 1998). Around 50% of these cases are associated with hypomethylation at the KvDMR1 locus resulting in decreased concentration of CDKN1C, a growth inhibitor, and 5% are associated with hypermethylation at the H19 DMR resulting in increased IGF2 concentrations, a growth promoter. A majority of BWS cases are sporadic, but approximately 15% are familial, 40% of which are associated with CDKN1C mutations and 20% involving both KCNQ1 and H19 clusters (Catchpoole et al. 1997; Choufani et al. 2010).

SRS is characterized by prenatal and/or postnatal growth restriction accompanied by small triangular shaped face and skeletal asymmetry. The incidence of SRS is around one in 30000 to 100000, although minor forms are speculated to go undiagnosed (Hitchins et al. 2001; Abu-Amero et al. 2008). About 35-65% of SRS cases have been linked to hypomethylation of the H19 DMR, resulting in bi-allelic expression of H19/IGF2 and reduced concentrations of IGF2 and 10% cases resulting from maternal uniparental duplications on chromosome 7. Several SRS patients with hypomethylation at the H19 DMR also exhibit methylation defects at multiple imprinted loci, which is suggestive of a defect in imprint maintenance post fertilization (Azzi et al. 2009; Begemann et al. 2011; Kannenberg et al. 2012).

Several gene expression studies on the global transcriptome in IUGR placentas have demonstrated upregulation of imprinted genes like Phlda2, Peg3, Peg10 and Plagl1 (Abu-Amero et al. 1998; McMinn et al. 2006; Diplas et al. 2009; Piedrahita 2011; Kumar et al. 2012). Consistent results from multiple studies suggest that

imprinted genes are closely associated with the etiology of IUGR in humans.

### 1.6 Assisted reproductive technologies and imprinting disorders

Assisted reproductive technology (ART) can be described as manipulation of one or several steps of conception. ART can include the use of hormones to stimulate the ovary for supernumerary oocyte production, in vitro oocyte maturation, intracytoplasmic sperm injection, *and in vitro* culture of pre implantation embryos and cryopreservation of gametes or embryos. Although ART has been a boon for couples with compromised fertility to conceive children, it has also been associated with IUGR, abnormal placentation and increased risk for imprinting disorders.

Although the effect of ART on imprinting has not been well studied in humans, studies in cattle and sheep born after *in vitro* culture of embryos revealed a high incidence of high birth weight, neonatal respiratory distress, skeletal abnormalities and increased incidence of infant death (Young et al. 1998). Mouse models of ART demonstrate that the procedures affect embryonic development, decrease fetal weight and increase placental weight. ART procedures also cause aberrant expression of imprinted genes including H19, Igf2, Kcnq1ot1, Cdkn1c, Peg3 and Snrnp in the placenta during early placental development and is accompanied by expansion of the junctional zone towards the end of gestation (de Waal et al. 2014; de Waal et al. 2015). These studies also indicate that the placenta is more susceptible to epigenetic aberrations than the fetus. However, the pathways and mechanisms through which

environmental insults during ART result in placental defects have not been identified.

### 1.7 Fetal origins of adult disease

The Barker hypothesis postulates that environmental insults in utero can affect the long-term health of the offspring (Barker 2004a; Barker 2004b). Several studies have shown an association between low birth weight and increased rate of cardiovascular disease and non-insulin dependent diabetes as adults (McMillen and Robinson 2005; Stocker and Cawthorne 2008; Briana and Malamitsi-Puchner 2009; Langley-Evans 2009; Yajnik 2009). Metabolic and endocrine adaptations of the fetus in response to under nutrition or over nutrition are proposed to increase the risk of hypertension, type 2 diabetes, coronary heart disease and hyperlipidemia (de Boo and Harding 2006). Several studies have highlighted the role of low birth weight caused by pre term birth or IUGR in short term and long term consequences on the health of the fetus. It has become increasingly important to develop efficient methods of diagnosing and preventing IUGR, recognizing at risk pregnancies and following up with treatment programs to control disorders arising from these pregnancies.

### 1.8 MicroRNAs

MicroRNAs (miRNAs) are a family of ~21 nucleotide long noncoding RNAs that control gene expression through post-transcriptional and transcriptional gene silencing mechanisms (Bartel 2004). miRNAs bind to complementary bases in the 3'UTRs of

mRNAs and cause degradation or translational inhibition of the transcript (Bartel 2004). miRNAs regulate hundreds of targets, usually acting as switches or fine-tuning mechanisms to control gene expression in various physiological and pathological contexts. miRNAs can act as a 'switch' to downregulate its mRNA target(s) to a level below a functional threshold or/and as a 'fine-tuning' mechanism to adjust gene expression of several targets to reach expression levels required for specific cellular processes (Lewis et al. 2003; Bartel 2004).

After miRNA genes are transcribed, they are processed into 70 nucleotide pre-miRNAs by Drosha inside the nucleus and transported into the cytoplasm by Exportin 5. Dicer processes these transcripts into miRNA-miRNA* duplexes and one strand is assembled into the RNA-induced silencing complex (RISC). The miRNA strand binds to its target by sequence complementarity and suppresses expression by mRNA cleavage (He and Hannon 2004). Based on their genomic location, miRNAs can be classified into intergenic and intronic. Intergenic miRNAs are located in un-annotated regions of the genome and transcribed from their unique promoters. Intronic miRNAs are believed to be transcribed along with and share promoters with the host gene (Lee et al. 2002; Kim and Kim 2007). Although there is some evidence that intronic miRNAs can be independently transcribed, a larger majority are processed from the host gene transcript. Co-expression and co-regulation of intronic miRNA with its host gene is proposed to have an antagonistic or synergistic effect. Intronic miRNAs can repress activity of genes activated by the host gene to have an antagonistic effect or

tune gene expression of transcripts to have a synergistic function with the host gene (Lutter et al. 2010).

Functional characterization of several miRNAs *in vivo*, through knock-out mouse models, has shown that miRNAs unlike transcription factors are not master regulators of gene expression, but act as a rheostats that fine tune gene expression of regulatory networks to confer robustness to cells under environmental variability (Vidigal and Ventura 2015). With some exceptions (miR-205) (Wang et al. 2013), most individual miRNA knock-out mice have a modest or no apparent phenotype.

### 1.9 Role of Egfl7/miR-126 in angiogenesis

miR-126 is an intronic miRNA located in intron 7 of the gene *Egfl7*. Egfl7 is selectively expressed by actively proliferating endothelial cells during physiological and pathological angiogenesis (Soncin et al. 2003; Fitch et al. 2004). Egfl7 is also expressed in embryonic stem cells (ESCs), trophoblast stem cells (TSCs), primordial germ cells, neural stem cells and pre-implantation embryos beginning at the 8-cell stage (Fitch et al. 2004; Campagnolo et al. 2008; Lacko et al. 2014). The first Egfl7 knock out models demonstrated vascular defects and partial embryonic lethality (Parker et al. 2004; Schmidt et al. 2007). However, along with deletion of Egfl7, miR-126 expression was significantly reduced. A later study using an Eglf7-specific knockout with intact miR-126 expression does not display an overt phenotype during embryonic development (Kuhnert et al. 2008). However, recent studies in our lab have

demonstrated a critical role for Egfl7 for placental vascularization and embryonic growth (Lacko et al. 2017). Egfl7$^{-/-}$ placentas display gross defects in chorioallantoic branching morphogenesis, placental vascular patterning and >50% reduction in fetal blood space resulting in IUGR of the embryos. Eglf7$^{-/-}$ placental endothelial cells are deficient in migration, cord formation, and sprouting (Lacko et al. 2017).

miR-126, present in intron 7 of Egfl7, has complete sequence conservation in vertebrates and has an expression pattern similar to EGFL7. The role of miR-126 in vascular development was studied in loss of function zebrafish and mouse models. miR-126 knock down in zebrafish resulted in loss of vascular integrity and hemorrhaging during embryonic development (Fish et al. 2008; Wang et al. 2008). miR-126$^{-/-}$ mice in which Egfl7 is intact display partial embryonic lethality and vascular defects in the embryo during development (Kuhnert et al. 2008; Wang et al. 2008). miR-126$^{-/-}$ embryos displayed systemic edema, multifocal hemorrhages and demise, with highest percentage of embryos with vascular defects from E13.5 – E15.5. Electron microscopy showed extensive blood vessel rupture and lack of tight cell interactions in endothelial cells of miR-126$^{-/-}$ embryos. At E15.5 miR-126$^{-/-}$ embryos also displayed reduced numbers of BrdU+ PECAM+ proliferating endothelial cells. However, 60% of miR-126$^{-/-}$ survived to adulthood and displayed no major histological abnormalities. From this data, the authors conclude that miR-126 is essential for maintenance of vascular integrity during embryogenesis, but not essential for vascular homeostasis after birth (Wang et al. 2008).

The angiogenic response of endothelial cells (ECs) in miR-126$^{-/-}$ was tested using aortic ring and matrigel plug assays. Aortic rings isolated from 4-week old miR-126$^{-/-}$ mice cultured on matrigel with endothelial growth medium containing FGF-2 and VEGF and supplemented with 3% mouse serum displayed impaired endothelial outgrowth when compared to wild-type littermates (Wang et al. 2008). Since neoangiogenesis is critical for cardiac repair following myocardial infarction, the response of wild type and miR-126$^{-/-}$ mice following induced myocardial infarction was tested. 3 weeks following surgical ligation of the left coronary artery, only 50% of miR-126$^{-/-}$ survived, compared to survival rate of 70% of wild type littermates, with no surviving miR-126$^{-/-}$ 3 weeks after the procedure (Wang et al. 2008). Similar to the mouse model, impaired angiogenic response was observed in the miR-126 morpholino injected zebrafish (Fish et al. 2008).

The molecular targets of miR-126 controlling angiogenic response were identified from gene expression profiles of kidney ECs from wild type and miR-126$^{-/-}$ mice (Wang et al. 2008). Functional assays using gain and loss of function of miR-126 in primary endothelial cells and human umbilical vein endothelial cells (HUVECs) showed Spred-1 and PIK3R2 as direct targets of miR-126 (Wang et al. 2008). The results from the zebrafish and mouse models reveal an essential role for miR-126 in regulating developmental angiogenesis and vascular integrity *in vivo* (Fish et al. 2008; Wang et al. 2008). miR-126 regulates the angiogenic actions of VEGF and FGF by inhibiting Spred-1 and PIK3R2, inhibitors of the MAPK and AKT pathway respectively (Fish et al. 2008; Wang et al. 2008). miR-126 not only responds to

angiogenic growth factor stimuli, but also activates angiogenesis in response to the physiological stimulus of blood flow.

miR-126 has also been shown to regulate endothelial-hematopoietic interactions and hematopoiesis. Inhibition of miR-126 in endothelial cells leads to increased SDF-1/CXCL12 expression, resulting in increased migration of Sca-$1^{+}$/$Lin^{-}$ progenitor cells (van Solingen et al. 2011). miR-126 is also expressed in human hematopoietic cells (HSCs) and early progenitors. Loss of function and gain of function studies in HSCs have demonstrated a pivotal role for miR-126 in restraining cell cycle progression in vitro and in vivo by regulating multiple targets of PI3K/AKT/GSK3 pathway (Lechman et al. 2012)

## 1.10 Summary and significance

Normal placental development is crucial for the health of the mother and the fetus during gestation and for the long-term health of the fetus. Abnormal placentation contributes to the development and progression of a number of disease pathologies like preeclampsia, intra uterine growth restriction and gestational diabetes.

A number of mouse models have been used to elucidate pathways and genes regulating development and intricate interactions of the vascular and trophoblast compartments of the placenta. A large number of studies have described the roles of

protein coding genes, however, the roles of miRNAs in placental development have not been well studied.

miR-126 is a vascular specific intronic miRNA that plays a critical role in regulating angiogenesis during embryonic development. Due the functional role of miR-126 and its host gene Egfl7 in angiogenesis, we hypothesized that miR-126 plays an important role in placental development. To test this, I used a miR-126 loss-of-function congenic mouse model. In this dissertation, in chapters 2 and 3, I describe a novel role for miR-126 in regulating the glycogen trophoblast proliferation in the placenta and demonstrate a functional role for miR-126 in regulating DNA methylation and genomic imprinting. In chapter 4, I will describe metabolic defects in miR-126$^{+/-}$ adult mice with potential roles for miR-126 in insulin secretion.

## REFERENCES


Abu-Amero S, Monk D, Frost J, Preece M, Stanier P, Moore GE. 2008. The genetic aetiology of Silver-Russell syndrome. *J Med Genet* 45: 193-199.

Abu-Amero SN, Ali Z, Bennett P, Vaughan JI, Moore GE. 1998. Expression of the insulin-like growth factors and their receptors in term placentas: a comparison between normal and IUGR births. *Mol Reprod Dev* 49: 229-235.

Adamson SL, Lu Y, Whiteley KJ, Holmyard D, Hemberger M, Pfarrer C, Cross JC. 2002. Interactions between trophoblast cells and the maternal and fetal circulation in the mouse placenta. *Dev Biol* 250: 358-373.

Akison LK, Nitert MD, Clifton VL, Moritz KM, Simmons DG. 2017. Review: Alterations in placental glycogen deposition in complicated pregnancies: Current preclinical and clinical evidence. *Placenta* 54: 52-58.

Anson-Cartwright L, Dawson K, Holmyard D, Fisher SJ, Lazzarini RA, Cross JC. 2000. The glial cells missing-1 protein is essential for branching morphogenesis in the chorioallantoic placenta. *Nat Genet* 25: 311-314.

Azzi S, Rossignol S, Steunou V, Sas T, Thibaud N, Danton F, Le Jule M, Heinrichs C, Cabrol S, Gicquel C et al. 2009. Multilocus methylation analysis in a large cohort of 11p15-related foetal growth disorders (Russell Silver and Beckwith Wiedemann syndromes) reveals simultaneous loss of methylation at paternal and maternal imprinted loci. *Hum Mol Genet* 18: 4724-4733.

Barak Y, Nelson MC, Ong ES, Jones YZ, Ruiz-Lozano P, Chien KR, Koder A, Evans RM. 1999. PPAR gamma is required for placental, cardiac, and adipose tissue development. *Mol Cell* 4: 585-595.

Barker DJ. 2004a. Developmental origins of adult health and disease. *J Epidemiol Community Health* 58: 114-115.

-. 2004b. The developmental origins of chronic adult disease. *Acta Paediatr Suppl* 93: 26-33.

Barlow DP, Bartolomei MS. 2014. Genomic imprinting in mammals. *Cold Spring Harb Perspect Biol* 6.

Bartel DP. 2004. MicroRNAs: genomics, biogenesis, mechanism, and function. *Cell* 116: 281-297.

Begemann M, Spengler S, Kanber D, Haake A, Baudis M, Leisten I, Binder G, Markus S, Rupprecht T, Segerer H et al. 2011. Silver-Russell patients showing a broad range of ICR1 and ICR2 hypomethylation in different tissues. *Clin Genet* 80: 83-88.

Briana DD, Malamitsi-Puchner A. 2009. Intrauterine growth restriction and adult disease: the role of adipocytokines. *Eur J Endocrinol* 160: 337-347.

Campagnolo L, Moscatelli I, Pellegrini M, Siracusa G, Stuhlmann H. 2008. Expression of EGFL7 in primordial germ cells and in adult ovaries and testes. *Gene Expr Patterns* 8: 389-396.

Catchpoole D, Lam WW, Valler D, Temple IK, Joyce JA, Reik W, Schofield PN, Maher ER. 1997. Epigenetic modification and uniparental inheritance of H19 in Beckwith-Wiedemann syndrome. *J Med Genet* 34: 353-359.

Chawengsaksophak K, James R, Hammond VE, Kontgen F, Beck F. 1997. Homeosis and intestinal tumours in Cdx2 mutant mice. *Nature* 386: 84-87.

Cheng X, Blumenthal RM. 2010. Coordinated chromatin control: structural and functional linkage of DNA and histone methylation. *Biochemistry* 49: 2999-3008.

Choufani S, Shuman C, Weksberg R. 2010. Beckwith-Wiedemann syndrome. *Am J Med Genet C Semin Med Genet* 154C: 343-354.

Coan PM, Conroy N, Burton GJ, Ferguson-Smith AC. 2006. Origin and characteristics of glycogen cells in the developing murine placenta. *Dev Dyn* 235: 3280-3294.

Constancia M, Hemberger M, Hughes J, Dean W, Ferguson-Smith A, Fundele R, Stewart F, Kelsey G, Fowden A, Sibley C et al. 2002. Placental-specific IGF-II is a major modulator of placental and fetal growth. *Nature* 417: 945-948.

de Boo HA, Harding JE. 2006. The developmental origins of adult disease (Barker) hypothesis. *Aust N Z J Obstet Gynaecol* 46: 4-14.

de Waal E, Mak W, Calhoun S, Stein P, Ord T, Krapp C, Coutifaris C, Schultz RM, Bartolomei MS. 2014. In vitro culture increases the frequency of stochastic epigenetic errors at imprinted genes in placental tissues from mouse concepti produced through assisted reproductive technologies. *Biol Reprod* 90: 22.

de Waal E, Vrooman LA, Fischer E, Ord T, Mainigi MA, Coutifaris C, Schultz RM, Bartolomei MS. 2015. The cumulative effect of assisted reproduction procedures on placental development and epigenetic perturbations in a mouse model. *Hum Mol Genet* 24: 6975-6985.

DeChiara TM, Efstratiadis A, Robertson EJ. 1990. A growth-deficiency phenotype in heterozygous mice carrying an insulin-like growth factor II gene disrupted by targeting. *Nature* 345: 78-80.

DeChiara TM, Robertson EJ, Efstratiadis A. 1991. Parental imprinting of the mouse insulin-like growth factor II gene. *Cell* 64: 849-859.

Delaval K, Govin J, Cerqueira F, Rousseaux S, Khochbin S, Feil R. 2007. Differential histone modifications mark mouse imprinting control regions during spermatogenesis. *EMBO J* 26: 720-729.

Diplas AI, Lambertini L, Lee MJ, Sperling R, Lee YL, Wetmur J, Chen J. 2009. Differential expression of imprinted genes in normal and IUGR human placentas. *Epigenetics* 4: 235-240.

Duffie R, Bourc'his D. 2013. Parental epigenetic asymmetry in mammals. *Curr Top Dev Biol* 104: 293-328.

Eichenwald EC, Stark AR. 2008. Management and outcomes of very low birth weight. *N Engl J Med* 358: 1700-1711.

Engstrom W, Lindham S, Schofield P. 1988. Wiedemann-Beckwith syndrome. *Eur J Pediatr* 147: 450-457.

Esquiliano DR, Guo W, Liang L, Dikkes P, Lopez MF. 2009. Placental glycogen stores are increased in mice with H19 null mutations but not in those with insulin or IGF type 1 receptor mutations. *Placenta* 30: 693-699.

Ferguson-Smith AC. 2011. Genomic imprinting: the emergence of an epigenetic paradigm. *Nat Rev Genet* 12: 565-575.

Fish JE, Santoro MM, Morton SU, Yu S, Yeh RF, Wythe JD, Ivey KN, Bruneau BG, Stainier DY, Srivastava D. 2008. miR-126 regulates angiogenic signaling and vascular integrity. *Dev Cell* 15: 272-284.

Fitch MJ, Campagnolo L, Kuhnert F, Stuhlmann H. 2004. Egfl7, a novel epidermal growth factor-domain gene expressed in endothelial cells. *Dev Dyn* 230: 316-324.

Fitzpatrick GV, Soloway PD, Higgins MJ. 2002. Regional loss of imprinting and growth deficiency in mice with a targeted deletion of KvDMR1. *Nat Genet* 32: 426-431.

Furukawa S, Kuroda Y, Sugiyama A. 2014. A comparison of the histological structure of the placenta in experimental animals. *J Toxicol Pathol* 27: 11-18.

Gabriel HD, Jung D, Butzler C, Temme A, Traub O, Winterhager E, Willecke K. 1998. Transplacental uptake of glucose is decreased in embryonic lethal connexin26-deficient mice. *J Cell Biol* 140: 1453-1461.

Gicquel C, Rossignol S, Cabrol S, Houang M, Steunou V, Barbu V, Danton F, Thibaud N, Le Merrer M, Burglen L et al. 2005. Epimutation of the telomeric

imprinting center region on chromosome 11p15 in Silver-Russell syndrome. *Nat Genet* 37: 1003-1007.

Girardot M, Hirasawa R, Kacem S, Fritsch L, Pontis J, Kota SK, Filipponi D, Fabbrizio E, Sardet C, Lohmann F et al. 2014. PRMT5-mediated histone H4 arginine-3 symmetrical dimethylation marks chromatin at G + C-rich regions of the mouse genome. *Nucleic Acids Res* 42: 235-248.

Giroux S, Tremblay M, Bernard D, Cardin-Girard JF, Aubry S, Larouche L, Rousseau S, Huot J, Landry J, Jeannotte L et al. 1999. Embryonic death of Mek1-deficient mice reveals a role for this kinase in angiogenesis in the labyrinthine region of the placenta. *Curr Biol* 9: 369-372.

Goldenberg RL, Culhane JF, Iams JD, Romero R. 2008. Epidemiology and causes of preterm birth. *Lancet* 371: 75-84.

Gurtner GC, Davis V, Li H, McCoy MJ, Sharpe A, Cybulsky MI. 1995. Targeted disruption of the murine VCAM1 gene: essential role of VCAM-1 in chorioallantoic fusion and placentation. *Genes Dev* 9: 1-14.

He L, Hannon GJ. 2004. MicroRNAs: small RNAs with a big role in gene regulation. *Nat Rev Genet* 5: 522-531.

Hirasawa R, Feil R. 2008. A KRAB domain zinc finger protein in imprinting and disease. *Dev Cell* 15: 487-488.

Hitchins MP, Stanier P, Preece MA, Moore GE. 2001. Silver-Russell syndrome: a dissection of the genetic aetiology and candidate chromosomal regions. *J Med Genet* 38: 810-819.

Jaenisch R, Bird A. 2003. Epigenetic regulation of gene expression: how the genome integrates intrinsic and environmental signals. *Nat Genet* 33 Suppl: 245-254.

John RM. 2017. Imprinted genes and the regulation of placental endocrine function: Pregnancy and beyond. *Placenta*.

Kannenberg K, Urban C, Binder G. 2012. Increased incidence of aberrant DNA methylation within diverse imprinted gene loci outside of IGF2/H19 in Silver-Russell syndrome. *Clin Genet* 81: 366-377.

Kelsey G, Feil R. 2013. New insights into establishment and maintenance of DNA methylation imprints in mammals. *Philos Trans R Soc Lond B Biol Sci* 368: 20110336.

Kim YK, Kim VN. 2007. Processing of intronic microRNAs. *EMBO J* 26: 775-783.

Koerner MV, Pauler FM, Hudson QJ, Santoro F, Sawicka A, Guenzl PM, Stricker SH, Schichl YM, Latos PA, Klement RM et al. 2012. A downstream CpG island controls transcript initiation and elongation and the methylation state of the imprinted Airn macro ncRNA promoter. *PLoS Genet* 8: e1002540.

Kuhnert F, Mancuso MR, Hampton J, Stankunas K, Asano T, Chen CZ, Kuo CJ. 2008. Attribution of vascular phenotypes of the murine Egfl7 locus to the microRNA miR-126. *Development* 135: 3989-3993.

Kumar N, Leverence J, Bick D, Sampath V. 2012. Ontogeny of growth-regulating genes in the placenta. *Placenta* 33: 94-99.

Lacko LA, Hurtado R, Hinds S, Poulos MG, Butler JM, Stuhlmann H. 2017. Altered feto-placental vascularization, feto-placental malperfusion, and fetal growth restriction in mice with Egfl7 loss-of-function. *Development*.

Lacko LA, Massimiani M, Sones JL, Hurtado R, Salvi S, Ferrazzani S, Davisson RL, Campagnolo L, Stuhlmann H. 2014. Novel expression of EGFL7 in placental trophoblast and endothelial cells and its implication in preeclampsia. *Mech Dev* 133: 163-176.

Langley-Evans SC. 2009. Nutritional programming of disease: unravelling the mechanism. *J Anat* 215: 36-51.

Lechman ER, Gentner B, van Galen P, Giustacchini A, Saini M, Boccalatte FE, Hiramatsu H, Restuccia U, Bachi A, Voisin V et al. 2012. Attenuation of miR-126 activity expands HSC in vivo without exhaustion. *Cell Stem Cell* 11: 799-811.

Lee Y, Jeon K, Lee JT, Kim S, Kim VN. 2002. MicroRNA maturation: stepwise processing and subcellular localization. *EMBO J* 21: 4663-4670.

Lewis BP, Shih IH, Jones-Rhoades MW, Bartel DP, Burge CB. 2003. Prediction of mammalian microRNA targets. *Cell* 115: 787-798.

Li E, Beard C, Jaenisch R. 1993. Role for DNA methylation in genomic imprinting. *Nature* 366: 362-365.

Li E, Bestor TH, Jaenisch R. 1992. Targeted mutation of the DNA methyltransferase gene results in embryonic lethality. *Cell* 69: 915-926.

Li E, Zhang Y. 2014. DNA methylation in mammals. *Cold Spring Harb Perspect Biol* 6: a019133.

Li M, Squire JA, Weksberg R. 1998. Molecular genetics of Wiedemann-Beckwith syndrome. *Am J Med Genet* 79: 253-259.

Liang L, Guo WH, Esquiliano DR, Asai M, Rodriguez S, Giraud J, Kushner JA, White MF, Lopez MF. 2010. Insulin-like growth factor 2 and the insulin receptor, but not insulin, regulate fetal hepatic glycogen synthesis. *Endocrinology* 151: 741-747.

Lopez MF, Dikkes P, Zurakowski D, Villa-Komaroff L. 1996. Insulin-like growth factor II affects the appearance and glycogen content of glycogen cells in the murine placenta. *Endocrinology* 137: 2100-2108.

Lucifero D, Mertineit C, Clarke HJ, Bestor TH, Trasler JM. 2002. Methylation dynamics of imprinted genes in mouse germ cells. *Genomics* 79: 530-538.

Luo J, Sladek R, Bader JA, Matthyssen A, Rossant J, Giguere V. 1997. Placental abnormalities in mouse embryos lacking the orphan nuclear receptor ERR-beta. *Nature* 388: 778-782.

Lutter D, Marr C, Krumsiek J, Lang EW, Theis FJ. 2010. Intronic microRNAs support their host genes by mediating synergistic and antagonistic regulatory effects. *BMC Genomics* 11: 224.

Mackay DJ, Callaway JL, Marks SM, White HE, Acerini CL, Boonen SE, Dayanikli P, Firth HV, Goodship JA, Haemers AP et al. 2008. Hypomethylation of multiple imprinted loci in individuals with transient neonatal diabetes is associated with mutations in ZFP57. *Nat Genet* 40: 949-951.

Maher ER, Reik W. 2000. Beckwith-Wiedemann syndrome: imprinting in clusters revisited. *J Clin Invest* 105: 247-252.

Maltepe E, Bakardjiev AI, Fisher SJ. 2010. The placenta: transcriptional, epigenetic, and physiological integration during development. *J Clin Invest* 120: 1016-1025.

McMillen IC, Robinson JS. 2005. Developmental origins of the metabolic syndrome: prediction, plasticity, and programming. *Physiol Rev* 85: 571-633.

McMinn J, Wei M, Schupf N, Cusmai J, Johnson EB, Smith AC, Weksberg R, Thaker HM, Tycko B. 2006. Unbalanced placental expression of imprinted genes in human intrauterine growth restriction. *Placenta* 27: 540-549.

Messerschmidt DM, Knowles BB, Solter D. 2014. DNA methylation dynamics during epigenetic reprogramming in the germline and preimplantation embryos. *Genes Dev* 28: 812-828.

Moore T, Haig D. 1991. Genomic imprinting in mammalian development: a parental tug-of-war. *Trends Genet* 7: 45-49.

Morison IM, Ramsay JP, Spencer HG. 2005. A census of mammalian imprinting. *Trends Genet* 21: 457-465.

Murphy VE, Smith R, Giles WB, Clifton VL. 2006. Endocrine regulation of human fetal growth: the role of the mother, placenta, and fetus. *Endocr Rev* 27: 141-169.

Pannetier M, Julien E, Schotta G, Tardat M, Sardet C, Jenuwein T, Feil R. 2008. PR-SET7 and SUV4-20H regulate H4 lysine-20 methylation at imprinting control regions in the mouse. *EMBO Rep* 9: 998-1005.

Parker LH, Schmidt M, Jin SW, Gray AM, Beis D, Pham T, Frantz G, Palmieri S, Hillan K, Stainier DY et al. 2004. The endothelial-cell-derived secreted factor Egfl7 regulates vascular tube formation. *Nature* 428: 754-758.

Peters J. 2014. The role of genomic imprinting in biology and disease: an expanding view. *Nat Rev Genet* 15: 517-530.

Piedrahita JA. 2011. The role of imprinted genes in fetal growth abnormalities. *Birth Defects Res A Clin Mol Teratol* 91: 682-692.

Quenneville S, Verde G, Corsinotti A, Kapopoulou A, Jakobsson J, Offner S, Baglivo I, Pedone PV, Grimaldi G, Riccio A et al. 2011. In embryonic stem cells, ZFP57/KAP1 recognize a methylated hexanucleotide to affect chromatin and DNA methylation of imprinting control regions. *Mol Cell* 44: 361-372.

Reik W, Dean W, Walter J. 2001. Epigenetic reprogramming in mammalian development. *Science* 293: 1089-1093.

Riley P, Anson-Cartwright L, Cross JC. 1998. The Hand1 bHLH transcription factor is essential for placentation and cardiac morphogenesis. *Nat Genet* 18: 271-275.

Rossant J, Cross JC. 2001. Placental development: lessons from mouse mutants. *Nat Rev Genet* 2: 538-548.

Russ AP, Wattler S, Colledge WH, Aparicio SA, Carlton MB, Pearce JJ, Barton SC, Surani MA, Ryan K, Nehls MC et al. 2000. Eomesodermin is required for mouse trophoblast development and mesoderm formation. *Nature* 404: 95-99.

Sanli I, Feil R. 2015. Chromatin mechanisms in the developmental control of imprinted gene expression. *Int J Biochem Cell Biol* 67: 139-147.

Sarkar AA, Nuwayhid SJ, Maynard T, Ghandchi F, Hill JT, Lamantia AS, Zohn IE. 2014. Hectd1 is required for development of the junctional zone of the placenta. *Dev Biol* 392: 368-380.

Schmidt M, Paes K, De Maziere A, Smyczek T, Yang S, Gray A, French D, Kasman I, Klumperman J, Rice DS et al. 2007. EGFL7 regulates the collective migration of endothelial cells by restricting their spatial distribution. *Development* 134: 2913-2923.

Sferruzzi-Perri AN, Vaughan OR, Coan PM, Suciu MC, Darbyshire R, Constancia M, Burton GJ, Fowden AL. 2011. Placental-specific Igf2 deficiency alters developmental adaptations to undernutrition in mice. *Endocrinology* 152: 3202-3212.

Simmons DG, Fortier AL, Cross JC. 2007. Diverse subtypes and developmental origins of trophoblast giant cells in the mouse placenta. *Dev Biol* 304: 567-578.

Simmons DG, Rawn S, Davies A, Hughes M, Cross JC. 2008. Spatial and temporal expression of the 23 murine Prolactin/Placental Lactogen-related genes is not associated with their position in the locus. *BMC Genomics* 9: 352.

Simmons LE, Rubens CE, Darmstadt GL, Gravett MG. 2010. Preventing preterm birth and neonatal mortality: exploring the epidemiology, causes, and interventions. *Semin Perinatol* 34: 408-415.

Solloway MJ, Robertson EJ. 1999. Early embryonic lethality in Bmp5;Bmp7 double mutant mice suggests functional redundancy within the 60A subgroup. *Development* 126: 1753-1768.

Soncin F, Mattot V, Lionneton F, Spruyt N, Lepretre F, Begue A, Stehelin D. 2003. VE-statin, an endothelial repressor of smooth muscle cell migration. *EMBO J* 22: 5700-5711.

Stocker CJ, Cawthorne MA. 2008. The influence of leptin on early life programming of obesity. *Trends Biotechnol* 26: 545-551.

Tan L, Shi YG. 2012. Tet family proteins and 5-hydroxymethylcytosine in development and disease. *Development* 139: 1895-1902.

Tunster SJ, Tycko B, John RM. 2010. The imprinted Phlda2 gene regulates extraembryonic energy stores. *Mol Cell Biol* 30: 295-306.

Tunster SJ, Van de Pette M, John RM. 2011. Fetal overgrowth in the Cdkn1c mouse model of Beckwith-Wiedemann syndrome. *Dis Model Mech* 4: 814-821.

van Solingen C, de Boer HC, Bijkerk R, Monge M, van Oeveren-Rietdijk AM, Seghers L, de Vries MR, van der Veer EP, Quax PH, Rabelink TJ et al. 2011. MicroRNA-126 modulates endothelial SDF-1 expression and mobilization of Sca-1(+)/Lin(-) progenitor cells in ischaemia. *Cardiovascular research* 92: 449-455.

Vidigal JA, Ventura A. 2015. The biological functions of miRNAs: lessons from in vivo studies. *Trends Cell Biol* 25: 137-147.

Wan LB, Bartolomei MS. 2008. Regulation of imprinting in clusters: noncoding RNAs versus insulators. *Adv Genet* 61: 207-223.

Wang D, Zhang Z, O'Loughlin E, Wang L, Fan X, Lai EC, Yi R. 2013. MicroRNA-205 controls neonatal expansion of skin stem cells by modulating the PI(3)K pathway. *Nat Cell Biol* 15: 1153-1163.

Wang S, Aurora AB, Johnson BA, Qi X, McAnally J, Hill JA, Richardson JA, Bassel-Duby R, Olson EN. 2008. The endothelial-specific microRNA miR-126 governs vascular integrity and angiogenesis. *Dev Cell* 15: 261-271.

Watson ED, Cross JC. 2005. Development of structures and transport functions in the mouse placenta. *Physiology (Bethesda)* 20: 180-193.

Xu X, Weinstein M, Li C, Naski M, Cohen RI, Ornitz DM, Leder P, Deng C. 1998. Fibroblast growth factor receptor 2 (FGFR2)-mediated reciprocal regulation loop between FGF8 and FGF10 is essential for limb induction. *Development* 125: 753-765.

Yajnik CS. 2009. Nutrient-mediated teratogenesis and fuel-mediated teratogenesis: two pathways of intrauterine programming of diabetes. *Int J Gynaecol Obstet* 104 Suppl 1: S27-31.

Yamamoto H, Flannery ML, Kupriyanov S, Pearce J, McKercher SR, Henkel GW, Maki RA, Werb Z, Oshima RG. 1998. Defective trophoblast function in mice with a targeted mutation of Ets2. *Genes Dev* 12: 1315-1326.

Young BC, Levine RJ, Karumanchi SA. 2010. Pathogenesis of preeclampsia. *Annu Rev Pathol* 5: 173-192.

Young LE, Sinclair KD, Wilmut I. 1998. Large offspring syndrome in cattle and sheep. *Rev Reprod* 3: 155-163.

# Chapter 2 – Novel role for miR-126 in regulating glycogen trophoblast proliferation in the murine placenta

## 2.1 Rationale

The placenta is critical for the development and survival of the mammalian embryo. It is responsible for nutrient, gas and waste exchange, as well as immunological and endocrine functions critical during pregnancy (Watson and Cross 2005). The murine placenta develops from two major lineages, the trophectoderm and the extraembryonic mesoderm (Rossant and Cross 2001). Dysregulation of placental development can lead to abnormal placentation with adverse consequences for the mother and the fetus. Placental pathologies like preeclampsia and intra uterine growth restriction can lead to embryonic and maternal demise (Rossant and Cross 2001).

miRNAs have been shown to play critical roles in human placental development. Several functional studies have revealed key roles for miRNAs in trophoblast proliferation, invasion, migration, hormone production and angiogenesis (Lee et al. 2011; Ishibashi et al. 2012; Luo et al. 2012; Fu et al. 2013b; Li et al. 2013). Placental disorders like PE and IUGR are also associated with aberrant miRNA expression (Fu et al. 2013a) (Tsochandaridis et al. 2015). However, most of these functional studies rely on transformed trophoblast cell lines or cultures of primary trophoblast cells. To completely understand the roles played by miRNAs in placental development and disease, in vivo models are necessary.

Human and murine placentas are hemochorial, in which maternal blood comes in direct contact with the chorion. They are also thought to share molecular mechanisms controlling placental development (Watson and Cross 2005). Powerful genetic tools have enabled the use of murine models to study the roles of a single gene or combinations of gene networks in placental development. This has been particularly important in identifying targeted mutations associated with placental defects resulting in embryonic lethality.

In this chapter I will describe a novel expression domain for miR-126 in the trophoblasts of the placenta and a functional role for miR-126 in regulating glycogen trophoblast proliferation. This data is part of a manuscript in revision (miR-126 regulates glycogen trophoblast proliferation and DNA methylation in the murine placenta. Abhijeet Sharma, Lauretta A. Lacko and Heidi Stuhlmann. In revision, Development).

## 2.2 Abstract

A functional placenta develops through a delicate interplay of its vascular and trophoblast compartments. Placental insufficiencies can lead to adverse outcomes for the mother and the fetus. We have identified a novel expression domain for the endothelial-specific microRNA miR-126 in trophoblasts of murine and human placentas. Here, we determine the role of miR-126 in placental development using a mouse model with a targeted deletion of miR-126. miR-126$^{-/-}$ mice in a congenic

C57BL/6J background die in utero. Loss-of miR-126 leads to significant hyperplasia in the junctional zone at E15.5 at the expense of the labyrinth, resulting in reduced placental volume for nutrient exchange and intra-uterine growth restriction of the embryos. Junctional zone hyperplasia results from increased numbers of proliferating glycogen trophoblast progenitors at E13.5 that give rise to an expanded glycogen trophoblast population at E15.5.

## 2.3 Introduction

A recent study revealed a novel expression domain for the endothelial specific gene *Egfl7* in the trophectoderm and trophoblasts of the placenta(Lacko et al. 2014). miR-126 is a microRNA (miRNA) that is embedded in intron 7 of *Egfl7* and shares upstream regulatory elements with *Egfl7* (Kuhnert et al. 2008; Wang et al. 2008). miR-126 knock-out mice display vascular leakage, hemorrhaging and partial embryonic lethality (Kuhnert et al. 2008; Wang et al. 2008). The vascular defects can be attributed to diminished sprouting and adhesion of endothelial cells resulting from reduced PI3K and MAPK signaling. Studies in zebrafish and mice revealed that, miR-126 modulates developmental angiogenesis by post transcriptionally regulating gene expression of Spred1 and Pik3r2, inhibitors of Akt and Erk signaling (Fish et al. 2008; Wang et al. 2008). However, the expression of miR-126 in the placenta and function of miR-126 during placental development has not been investigated.

Here, the role of miR-126 in placental development was examined using the miR-126$^{-/-}$ mouse model developed by Dr. Eric Olson's laboratory (Wang et al. 2008). In a congenic background, we show that the endothelial specific miRNA, miR-126 displays a novel expression domain in the trophoblasts of the murine placenta. miR-126$^{-/-}$ placentas have increased numbers of proliferating glycogen trophoblast progenitor cells during mid-gestation, leading to an expanded junctional zone and reduced size of the fetal labyrinth of the placenta, all of which results in late gestational intra uterine growth restriction of the embryos.

## 2.4 Results and Discussion

### 2.4.1 Embryonic lethality of miR-126$^{-/-}$ embryos and late gestational intra-uterine growth restriction in a C57BL/6J background

Previous studies showed that miR-126$^{-/-}$ mice in a mixed genetic background display angiogenic defects, including leaky vessels, hemorrhaging, and partial embryonic lethality with incomplete penetrance (Kuhnert et al. 2008; Wang et al. 2008) To explore the function of miR-126 in a congenic background, miR-126$^{+/-}$ mice were backcrossed for ten generations into a C57BL/6J background. Intercrosses of congenic miR-126$^{+/-}$ mice failed to produce any surviving miR-126$^{-/-}$ pups at postnatal day10 (P10) (Fig 2.1A). To determine the time of demise of miR-126$^{-/-}$ embryos, litters from miR-126$^{+/-}$ intercrosses were genotyped at different gestational stages. Only 6% (3 out of 52) of embryos at embryonic day 18.5 (E18.5) and 12% (14 out of

112) at E15.5 were miR-126$^{-/-}$. However, at E12.5, miR-126$^{-/-}$ embryos were observed at the expected 25% ratio (24 out of 98) (Fig. 2.1A). Vascular defects, including hemorrhaging at E12.5 and systemic edema at E15.5 (Kuhnert et al. 2008; Wang et al. 2008) were observed with complete penetrance in miR-126$^{-/-}$ embryos in a congenic C57BL/6J background (Fig 2.1B). A fraction of miR-126$^{+/-}$ embryos (~50%) displayed similar vascular defects. The sizes and weights of embryos and placentas at E12.5 and E15.5 were measured. miR-126$^{-/-}$ embryos at E15.5 had significantly lower crown-to-rump lengths and reduced wet weights when compared to miR-126$^{+/+}$ littermates (Fig 2.1D), consistent with late gestational intra-uterine growth restriction (IUGR). No significant differences in weights and crown to rump lengths between miR-126$^{-/-}$ and miR-126$^{+/+}$ embryos were detected at E12.5 (Fig 2.1C). Furthermore, no significant differences in placental lengths and weights were detected at E12.5 or E15.5 (Fig 2.1C,D).

### 2.4.2 miR-126 is expressed by trophoblast and endothelial cells of the placenta.

During embryonic development, Egfl7 and miR-126 expression is restricted to the endothelium (Fitch et al. 2004; Parker et al. 2004; Wang et al. 2008; Bambino et al. 2014). Interestingly, during placental development *Egfl7* is expressed in the trophectoderm, in trophoblast stem cells (TSCs) and in junctional zone trophoblasts, in addition to maternal and fetal endothelial cells (Lacko et al. 2014).

Expression levels of miR-126-3p were comparable in E12.5 placentas and

A

| Age | Pups (litters) | | miR126$^{+/+}$ | miR126$^{+/-}$ | miR126$^{-/-}$ |
|---|---|---|---|---|---|
| P10 | 346 (44) | Observed | 173 (50%) | 172 (50%) | 0 (0%) |
| | | Expected | 87 (25%) | 172 (50%) | 87 (25%) |
| E18.5 | 52 (7) | Observed | 15 (29%) | 34 (65%) | 3 (6%) |
| | | Expected | 14 (25%) | 28 (50%) | 14 (25%) |
| E15.5 | 112 (17) | Observed | 39 (35%) | 59 (53%) | 14 (12%) |
| | | Expected | 30 (25%) | 59 (50%) | 30 (25%) |
| E12.5 | 98 (12) | Observed | 21 (21%) | 49 (50%) | 24 (25%) |
| | | Expected | 24 (25%) | 50 (50%) | 24 (25%) |

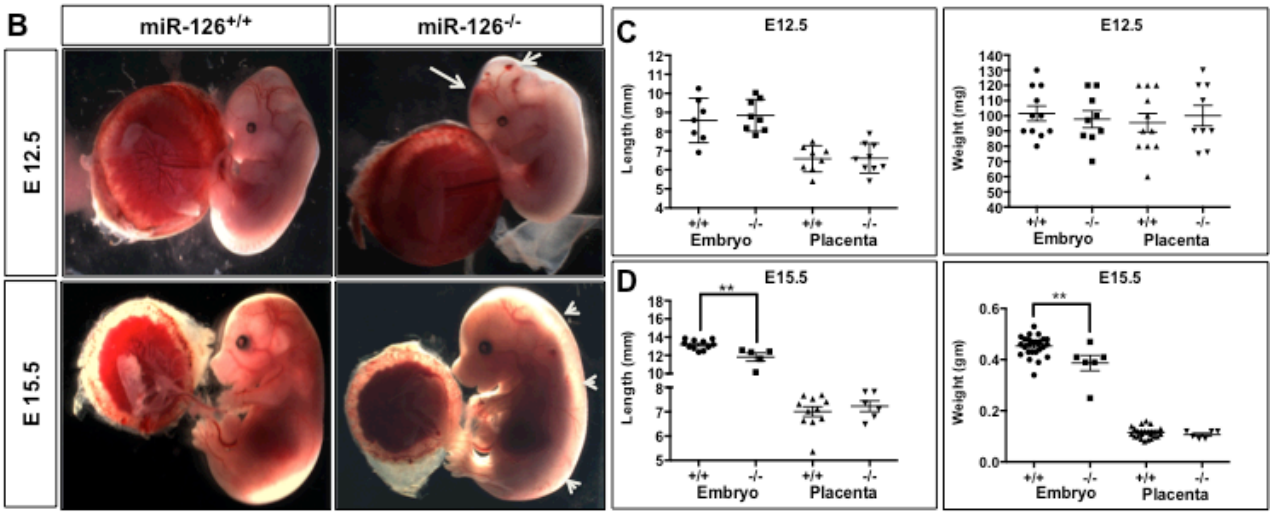


**Figure 2.1 miR-126$^{-/-}$ mice in a congenic C57BL/6J background die in utero and display late gestational IUGR**. Genotypes of offspring from miR-126$^{+/-}$ intercrosses. The observed and expected numbers of mice and embryos for each genotype at each developmental stage are shown **(A)**. Representative images of miR-126$^{+/+}$ and miR-126$^{-/-}$ littermate embryos and placentas at E12.5 and E15.5 **(B)**. Lengths (mm) and wet weights (mg) of embryos and placentas from miR-126$^{+/+}$ (n=7) and miR-126$^{-/-}$ (n=8) conceptuses at E12.5. Error bars indicate SEM **(C)**. Lengths (mm) and wet weights (mg) of embryos and placentas from miR-126$^{+/+}$ (n=25) and miR-126$^{-/-}$ (n=6) conceptuses at E15.5. Error bars indicate SEM. (** p≤0.01) **(D)**.

embryos and undetectable in miR-126$^{-/-}$ embryos and placentas, as determined by quantitative RT-PCR (Fig. 2.2A). Expression levels of miR-126 were comparable in TSCs and embryonic stem cells (ESCs) (Figure 2.2B). To visualize localization of miR-126 in the murine placenta, *in situ* hybridization was performed using a miR-126 specific LNA probe. miR-126$^{-/-}$ littermate placentas were used as controls for probe specificity. At E12.5, miR-126 is localized in the trophoblast giant cells (Fig. 2.2C, top panel, green arrow) and spongiotrophoblasts (Fig. 2.2C, top panel, red arrow) of the junctional zone. miR-126 expression was also detected in endothelial cells (Fig. 2.2C, bottom panel, green arrow) and syncytiotrophoblasts of the fetal labyrinth (Fig. 2.2C, bottom panel, red arrow). No positive signal was detected in miR126$^{-/-}$ placentas demonstrating specificity of the probe (Fig. 2.2C). miR-126 expression could also be seen in syncytiotrophoblasts (Fig. 2.2D, top panel, red arrow), cytotrophoblasts (Fig. 2.2D, bottom panel, blue arrow) and fetal endothelial cells (Fig. 2.2D, bottom panel, black arrow) in sections of term human placentas. No positive signal was detected in tissue hybridized with a scrambled LNA probe (Fig. 2.2D). Together, these findings demonstrate a novel expression domain for miR-126 in trophoblast stem cells and several trophoblast cell subtypes in murine and human placentas, in addition to its expression in fetal endothelial cells.

### 2.4.3 Hyperplasia of the junctional zone in miR-126$^{-/-}$ placentas at E15.5

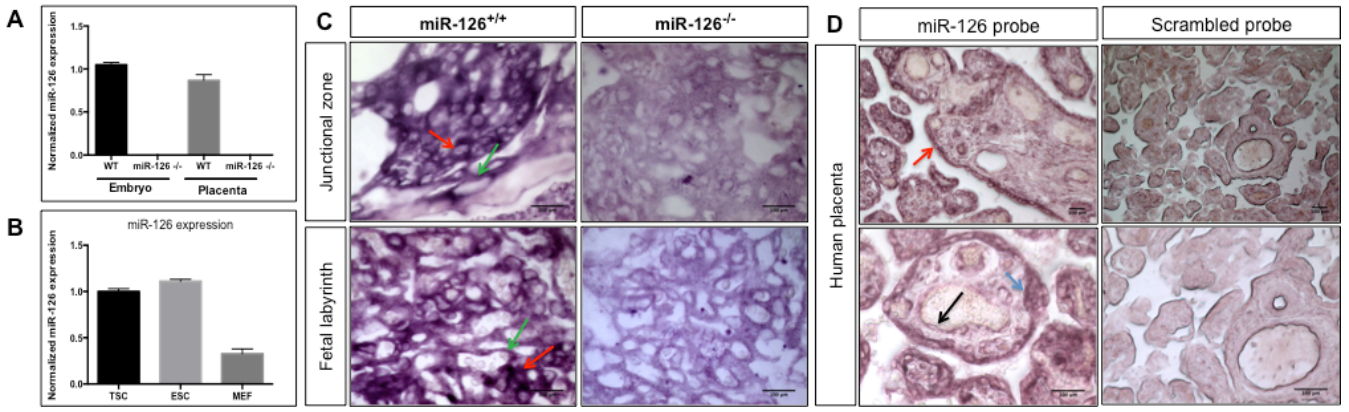


**Figure 2.2 Trophoblasts and endothelial cells of murine and term human placentas express miR-126.** Quantification of miR-126-3p expression in miR-126$^{+/+}$ (n=3) and miR-126$^{-/-}$ (n=3) embryos and placentas at E12.5 by quantitative RT PCR. Error bars indicate SEM. Expression levels are normalized to levels in miR-126$^{+/+}$ embryos **(A).** Quantification of miR-126-3p levels in trophoblast stem cells (TSC), embryonic stem cells (ESC) and mouse embryonic fibroblasts (MEF) by quantitative RT PCR (n=3; technical replicates). Error bars indicate SEM **(B)**. Representative images of sections from E12.5 miR-126$^{+/+}$ and miR-126$^{-/-}$ placentas hybridized with a DIG-labeled miR-126 LNA probe. Top panels: miR-126 specific expression is detected in the junctional zone in trophoblast giant cells (green arrow) and spongiotrophoblasts (red arrow) of miR-126$^{+/+}$, but not miR-126$^{-/-}$ placentas. Bottom panels: miR-126 specific expression is detected in the fetal labyrinth in endothelial cells (green arrow) and syncytial trophoblasts (red arrow) of miR-126$^{+/+}$, but not miR-126$^{-/-}$ placentas. Bar = 100 µm **(C)**. Representative images of human term placenta sections hybridized with a DIG- labeled miR-126, or a DIG-labeled scrambled LNA probe. Top Panels: miR-126 specific expression is detected in the syncytiotrophoblasts (red arrow) in sections stained with DIG-labeled miR-126 LNA probe, but not in sections hybridized with DIG-labeled scrambled LNA probe. Bottom panels: miR-126 specific expression is detected in fetal endothelial cells (black arrow) and cytotrophoblasts (blue arrow) in sections hybridized with DIG-labeled miR-126 LNA probe, but not in sections stained with DIG-labeled scrambled LNA probe. Bar = 100 µm **(D).**

Placental sections from miR-126$^{-/-}$ (n=3) and miR-126$^{+/+}$ (n=4) littermates were immunostained with Tpbpa antibodies to mark junctional zone (JZ) trophoblasts, and CD31 antibodies to mark endothelial cells of the fetal labyrinth (Lab) and the maternal decidua. Visual inspection showed an enlarged JZ in miR-126$^{-/-}$ placentas (Fig. 2.3A). Quantitative analysis showed a significant increase of the junctional zone area concomitant with a significant decrease in fetal labyrinth area in miR-126$^{-/-}$ placentas (Fig. 2.3B). This is further illustrated by a significantly reduced Lab/JZ ratio in miR-126$^{-/-}$ placentas (Fig. 2.3C). The increase in junctional zone area is a result of significantly increased numbers of Tpbpa$^{+}$ trophoblast cells in miR-126$^{-/-}$ placentas compared to miR-126$^{+/+}$ littermates (Fig. 2.3D). In contrast, there were no significant differences in the size of the decidua or of the total placental area between miR-126$^{+/+}$ and miR-126$^{-/-}$ placentas (Fig. 2.3B). Together, this data is consistent with a reduced labyrinth area as a potential cause for the observed IUGR and reduced viability of miR-126$^{-/-}$ embryos at E15.5 (Fig. 2.1A and 2.1D). Consistent with the absence of IUGR in miR-126$^{-/-}$ conceptuses at E12.5, placental labyrinth and junctional zone areas in miR-126$^{-/-}$ and miR-126$^{+/+}$ conceptuses were similar in size at E12.5 (Fig 2.4).

Unexpectedly, in contrast to the vascular defects observed in miR-126$^{-/-}$ embryos, the vasculature in the fetal labyrinth of miR-126$^{-/-}$ placentas appeared normal (Fig. 2.5A). No significant differences in the average vessel area (Fig. 2.5B), the numbers of Erg$^{+}$ endothelial cells (Fig. 2.5D) or Erg$^{+}$EdU$^{+}$ proliferating endothelial

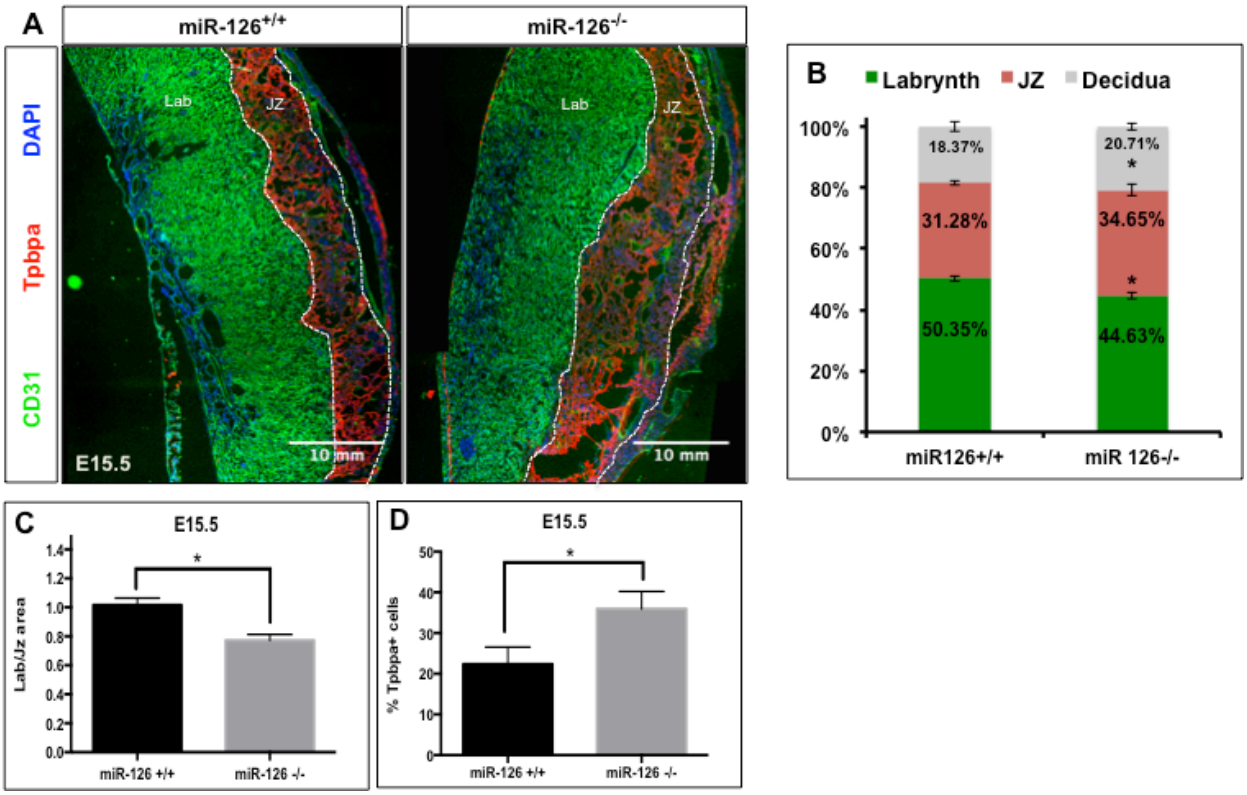


**Figure 2.3 miR-126$^{-/-}$ placentas at E15.5 display expanded junctional zones and reduced fetal labyrinths.** Representative images of E15.5 miR126$^{+/+}$ and miR-126$^{-/-}$ placental sections, immunostained with antibodies against CD31 (green) to mark the endothelium of the labyrinth (Lab) and maternal arteries, and Tpbpa (red) to mark trophoblasts of the junctional zone (JZ). Dotted white lines indicate the junctional zone/labyrinth and junctional zone/decidua boundaries **(A)**. Quantification of the areas of the fetal labyrinth (CD31, green), junctional zone (Tpbpa, red) and the decidua (gray) as a fraction of the total area (fetal labyrinth+ junctional zone+ decidua) of miR-126$^{+/+}$ (n=4) and miR-126$^{-/-}$ (n=3) placentas. Error bars indicate SEM (* p≤0.05) **(B)**. Ratio of labyrinth (Lab) to junctional zone (JZ) area in miR-126$^{+/+}$ and miR-126$^{-/-}$ placentas at E15.5. Measurements obtained from placentas shown in panel B were used. For miR-126$^{+/+}$ placentas the ratio is set artificially at 1. Error bars indicate SEM (* p≤0.05) **(C)**. Quantification of Tpbpa$^{+}$ cells in miR-126$^{+/+}$ (n=4) and miR-126$^{-/-}$ (n=3) placentas at E15.5. Error bars indicate SEM (* p≤0.05) **(D)**.

cells (Fig. 2.5E) were observed between miR-126$^{+/+}$ and miR-126$^{-/-}$ placentas at E12.5.

### 2.4.4 Increased numbers of glycogen trophoblasts in miR-126$^{-/-}$ placentas at E15.5

The observed expansion of the junctional zone trophoblasts in miR-126$^{-/-}$ placentas at E15.5 suggested an increase in the numbers of spongiotrophoblasts, glycogen trophoblasts, or both as the underlying cause. To identify the affected cell type(s), we performed co-immunostaining of E15.5 miR-126$^{+/+}$ and miR-126$^{-/-}$ placentas with antibodies for Tpbpa and p57$^{Kip2}$ (Fig. 2.6A). Spongiotrophoblasts and glycogen trophoblast cells (GlyTs) of the junctional zone express the trophoblast specific gene Tpbpa (Adamson et al. 2002). Placental GlyTs but not spongiotrophoblasts express the imprinted gene p57$^{Kip2}$ (Cdkn1c) (Georgiades et al. 2002; Coan et al. 2006). Large clusters of GCs (Tpbpa$^{low}$p57$^{Kip2+}$) were detected in the junctional zones of miR-126$^{-/-}$ and miR-126$^{+/+}$ placentas (Fig. 2.6A, arrows). Quantification of GlyTs and spongiotrophoblasts showed that miR-126$^{-/-}$ placentas contain significantly increased numbers of Tpbpa$^{low}$p57$^{Kip2+}$ GCs in the junctional zone (Fig. 2.6B). In contrast, no significant difference in the numbers of Tpbpa$^{high}$p57$^{Kip2-}$ spongiotrophoblasts was detected (Fig. 2.6C). We next analyzed glycogen content in GlyT clusters by performing periodic acid-schiff (PAS) staining on sections from paraffin-embedded placental tissue at E15.5. Visual inspection revealed larger PAS positive GlyT clusters in miR-126$^{-/-}$ placentas compared to miR-126$^{+/+}$ placentas (Fig. 2.6D). We also

quantified the glycogen content in the placental tissue by colorimetry (Kemp and Van Heijningen 1954). miR-126$^{-/-}$ placental tissue contained significantly increased amounts of glycogen when compared to miR-126$^{+/+}$ littermates (Fig. 2.6E). Together, these results indicate that miR-126$^{-/-}$ placentas contain increased numbers of terminally differentiated glycogen trophoblasts that results in a significantly increased junctional zone area at E15.5.

### 2.4.5 Increased numbers of proliferating glycogen cell progenitors in miR-126$^{-/-}$ placentas at E13.5

To determine if the increased number of GlyTs in the junctional zone was a result of increased cell proliferation, we performed an EdU proliferation assay. EdU was intravenously injected into E15.5 pregnant females from miR-126$^{+/-}$ intercrosses, followed by co-immunostaining of placental sections with antibodies for p57$^{Kip2}$ and Tpbpa. Few proliferating cells were detected in the junctional zone at E15.5 (Fig. 2.7A). This is consistent with a previous study reporting a 4-fold increase in spongiotrophoblasts and a 250-fold increase in glycogen trophoblasts between E12.5 and E16.5, with proliferation ceasing by E16.5 (Coan et al. 2006). To quantify proliferating progenitor cells at the time of trophoblast cell proliferation in the junctional zone, EdU injections and immunostaining of placentas were performed at E13.5 (Fig. 2.8A).

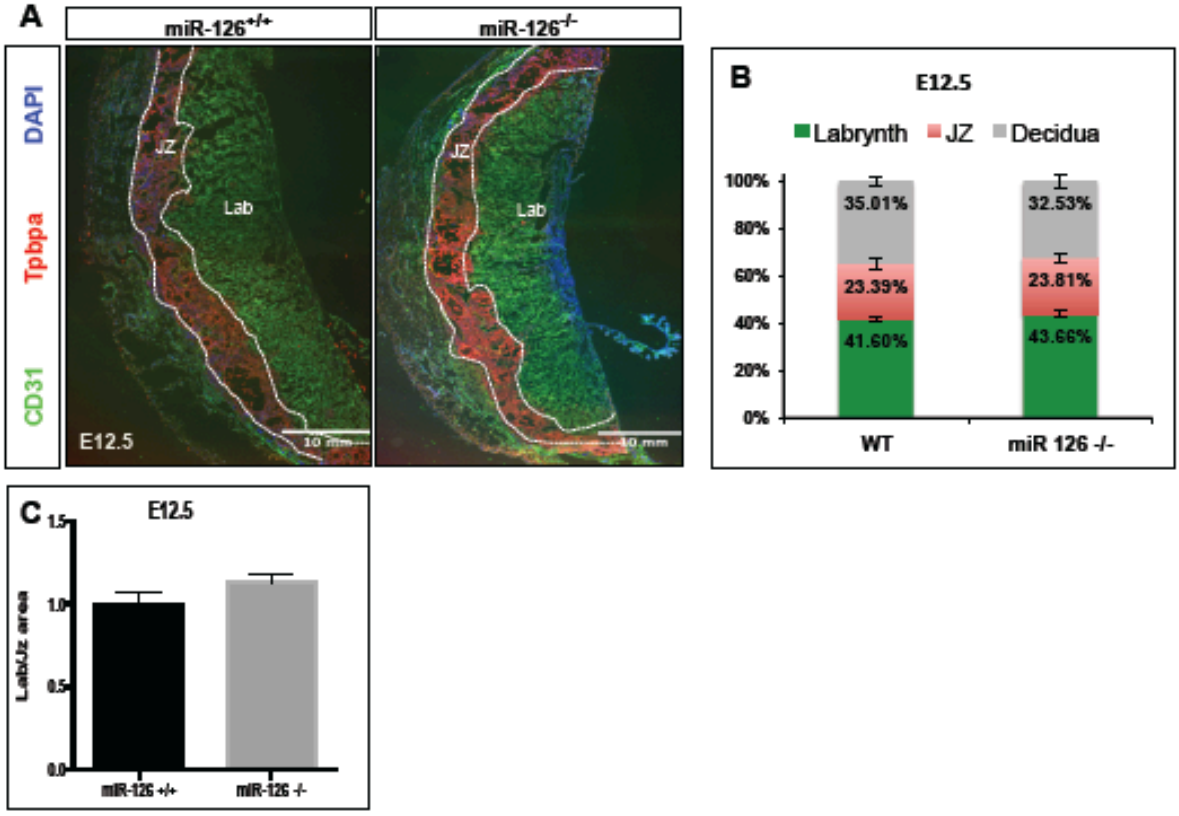


**Figure 2.4 miR-126$^{-/-}$ placentas at E12.5 do not display junctional zone hypertrophy.** Representative images of E12.5 miR126$^{+/+}$ and miR-126$^{-/-}$ placentas immunostained with antibodies against CD31 to mark the endothelium of the labyrinth (Lab) and maternal arteries and Tpbpa to mark trophoblasts of the junctional zone (JZ). Bar = 100mm. **(A)**. Quantification of the areas of the fetal labyrinth (CD31, green), junctional zone (Tpbpa, red) and the decidua (gray) as a fraction of the total area (fetal labyrinth+ junctional zone + decidua) of miR-126$^{+/+}$ (n=4) and miR-126$^{-/-}$ (n=4) placentas (3 sec1ons 100µm apart at the placental midline. Error bars indicate SEM **(B)**. Ratio of labyrinth to junctional zone area in miR-126$^{+/+}$ and miR-126$^{-/-}$ placentas at E12.5. Measurements obtained from placentas shown in panel B were used. For miR-126$^{+/+}$ placentas the ratio is set artificially at 1. Error bars indicate SEM. **(C)**.

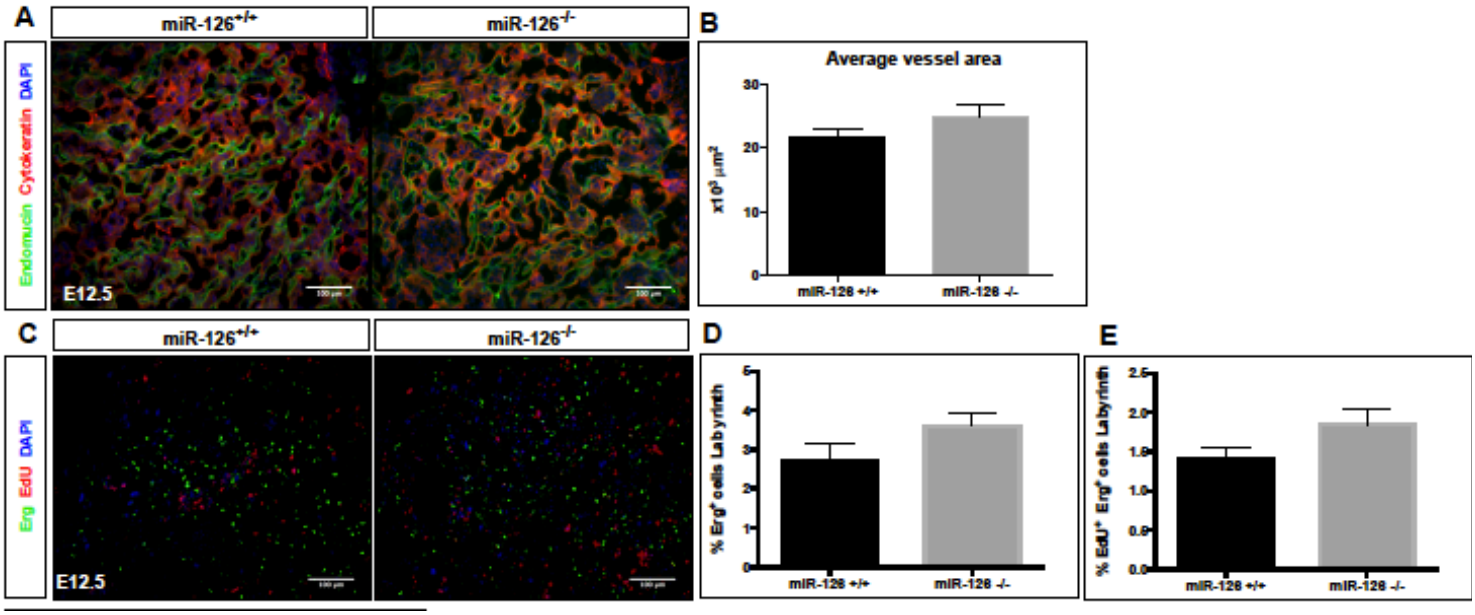


**Figure 2.5 miR-126$^{-/-}$ placentas at E12.5 do not display overt vascular phenotypes.** Representative images of the fetal labyrinth from E12.5 miR126$^{+/+}$ and miR-126$^{-/-}$ placentas immunostained with antibodies against ENDOMUCIN to mark the fetal endothelium of the labyrinth and CYTOKERATIN to mark trophoblasts **(A)**. Quantification of the average area of fetal vessels in the fetal labyrinth of miR-126$^{+/+}$ (n=4) and miR-126$^{-/-}$ (n=4) placentas. Error bars indicate SEM **(B)**. Representative images of E12.5 miR126$^{+/+}$ and miR-126$^{-/-}$ placentas immunostained with an ERG antibody to mark the fetal endothelium of the labyrinth and EdU to mark proliferating cells (ClickiT chemistry) **(C)**. Quantification of Erg$^{+}$ endothelial cells in the fetal labyrinth zone of miR-126$^{+/+}$ (n=4) and miR-126$^{-/-}$ (n=4) placentas. Error bars indicate SEM **(D)**. Quantification of EdU$^{+}$ Erg$^{+}$ proliferating endothelial cells in the fetal labyrinth zone of miR-126$^{+/+}$ (n=4) and miR-126$^{-/-}$ (n=4) placentas. Error bars indicate SEM **(E)**.

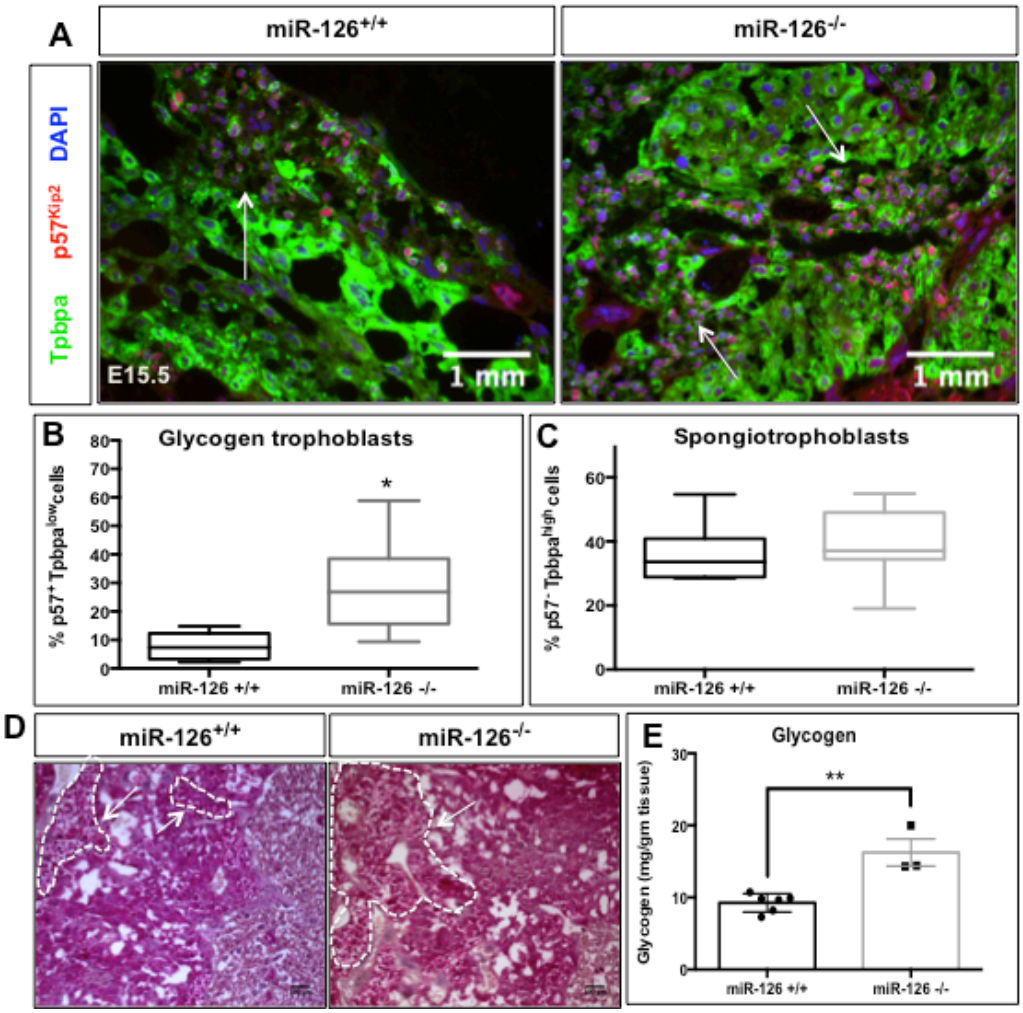


**Figure 2.6 Increased numbers of glycogen trophoblasts in miR-126$^{-/-}$ placentas at E15.5.** Representative immunofluorescence images of section from miR-126$^{+/+}$ and miR-126$^{-/-}$ E15.5 placentas co-immunostained with a p57$^{Kip2}$ antibody to mark glycogen trophoblast cells and a Tpbpa antibody to mark junctional zone trophoblasts. Arrows indicate clusters of Tpbpa$^{low}$p57$^{+}$ glycogen trophoblast cells in the junctional zone. Bar = 1 mm **(A)**. Quantification of Tpbpa$^{low}$p57$^{+}$ glycogen trophoblast cells in the junctional zone of miR-126$^{+/+}$ (n=4) and miR-126$^{-/-}$ (n=3) placentas. Data are shown as % of total number of cells in each image. Error bars indicate SEM (* p≤0.05) **(B)**. Quantification of Tpbpa$^{high}$p57$^{-}$ spongiotrophoblasts in the junctional zone **(C)**. PAS stain of representative paraffin sections from miR126$^{+/+}$ and miR-126$^{-/-}$ E15.5 placentas. Arrows indicate glycogen trophoblast clusters in the junctional zone **(D)**. Quantification of glycogen content in miR-126$^{+/+}$ (n=6) and miR-126$^{-/-}$ (n=3) placentas. Error bars indicate SEM. (** p≤0.01) **(E)**.

Quantification of glycogen progenitors and proliferating glycogen progenitors in the junctional zone revealed that miR-126$^{-/-}$ placentas (n=4) contain a significantly higher fraction of Tpbpa$^{+}$p57$^{Kip2+}$ glycogen trophoblast progenitors (Fig. 2.8B) and, most importantly, a significantly higher proportion of EdU$^{+}$Tpbpa$^{+}$p57$^{Kip2+}$ proliferating glycogen progenitors (Fig. 2.8C) when compared to miR-126$^{+/+}$ placentas (n=4). No significant differences in the fraction of Tpbpa$^{+}$ (spongiotrophoblasts) (Fig. 2.8D) or Tpbpa$^{+}$ EdU$^{+}$ trophoblasts (proliferating spongiotrophoblasts) were detected in the junctional zone between miR-126$^{+/+}$ and miR-126$^{-/-}$ placentas (Fig. 2.8E). These results indicate that loss-of miR-126 leads to increased numbers of proliferating glycogen trophoblast progenitors at E13.5, resulting in increased numbers of differentiated GlyTs and an expanded junctional zone in E15.5 placentas, concomitant with a reduced fetal labyrinth area.

**Discussion**

The results presented in this study reveal a novel role for miR-126 in regulating GlyT proliferation placental development. Loss-of-miR-126 resulted in a mutant phenotype that was restricted to the trophoblasts of the placenta. miR-126$^{-/-}$ placentas contain increased numbers of proliferating GlyT progenitors resulting in hyperplasia of the junctional zone at the expense of the fetal labyrinth, concomitant with late gestational IUGR of the embryos. This phenotype was unexpected, since miR-126$^{-/-}$ embryos and adult mice display vascular phenotypes and defects in angiogenesis (Kuhnert et al. 2008; Wang et al. 2008) and expression of miR-126 was thought to be endothelial

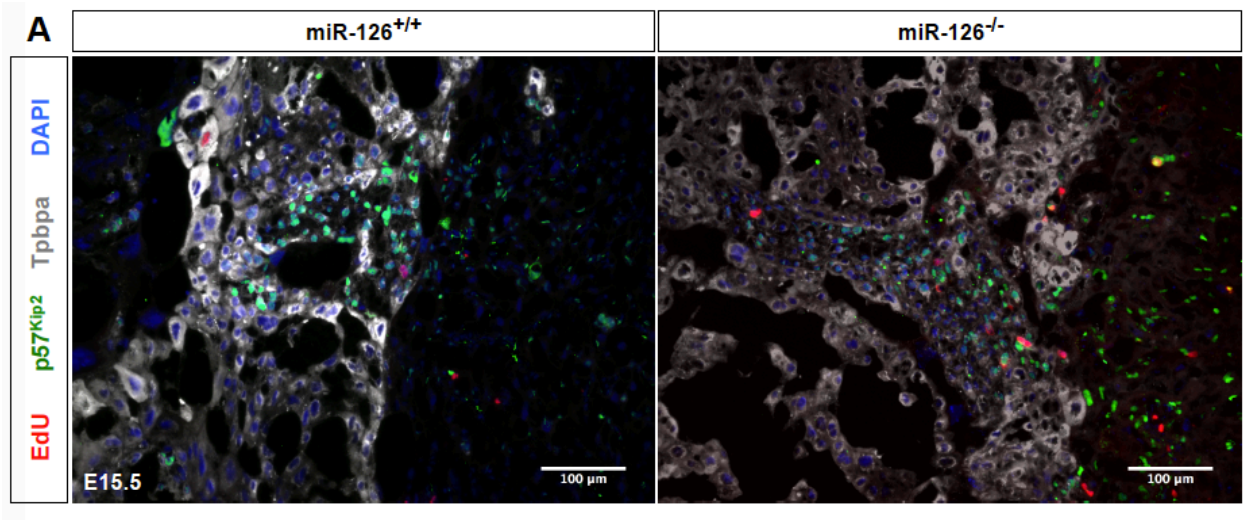


**Figure 2.7 Reduced numbers of proliferating cells in the junctional zone of placentas at E15.5.** Representative images of sections of miR-126$^{+/+}$ and miR-126$^{-/-}$ placentas at E15.5, immunostained with p57$^{Kip2}$ antibody, Tpbpa antibody and EdU (ClickiT chemistry) **(A)**

cell-specific. In contrast, vascular phenotypes were absent in the fetal labyrinth of miR-126$^{-/-}$ placentas (Fig. 2.5). This result may reflect the fact that the endothelial cell lineage in the fetal labyrinth is derived from the extraembryonic mesoderm of the allantois whereas all embryonic and adult endothelial cells are derived from the mesoderm of the embryo proper. In support, the transcriptome of the placental endothelium is unique when compared to that of other vascular beds (Nolan et al. 2013). Mice with loss-of-function of the host gene *Egfl7* display vascular patterning defects in the fetal labyrinth but lack an overt phenotype in the embryonic or adult vasculature (Lacko et al. 2017). The integration of microRNAs into introns of protein coding genes provides a common mechanism to coordinate expression and the regulatory functions of microRNAs with the gene networks regulated by the host gene (Wang et al. 2008; Liu and Olson 2010). Co-expression of miR-126 and Egfl7 in the endothelium in embryos and adult mice is controlled by a 5' 5.4-kb regulatory region that contains conserved consensus sequences for binding of Ets transcription factors (Wang et al. 2008; Bambino et al. 2014). miR-126 is generated from a retained intron in a subset of Egfl7 pre-mRNAs (Wang et al. 2008). In the placenta, miR-126 and *Egfl7* are co-expressed in the trophoblast lineage, in addition to its expression in the fetal and maternal endothelium. Specifically, we detected miR-126 transcripts, Egfl7 transcripts and protein in junctional zone trophoblasts of the murine placenta and in cytotrophoblasts and syncytiotrophoblasts of term human placenta, and in mouse TSCs (Lacko et al. 2014).

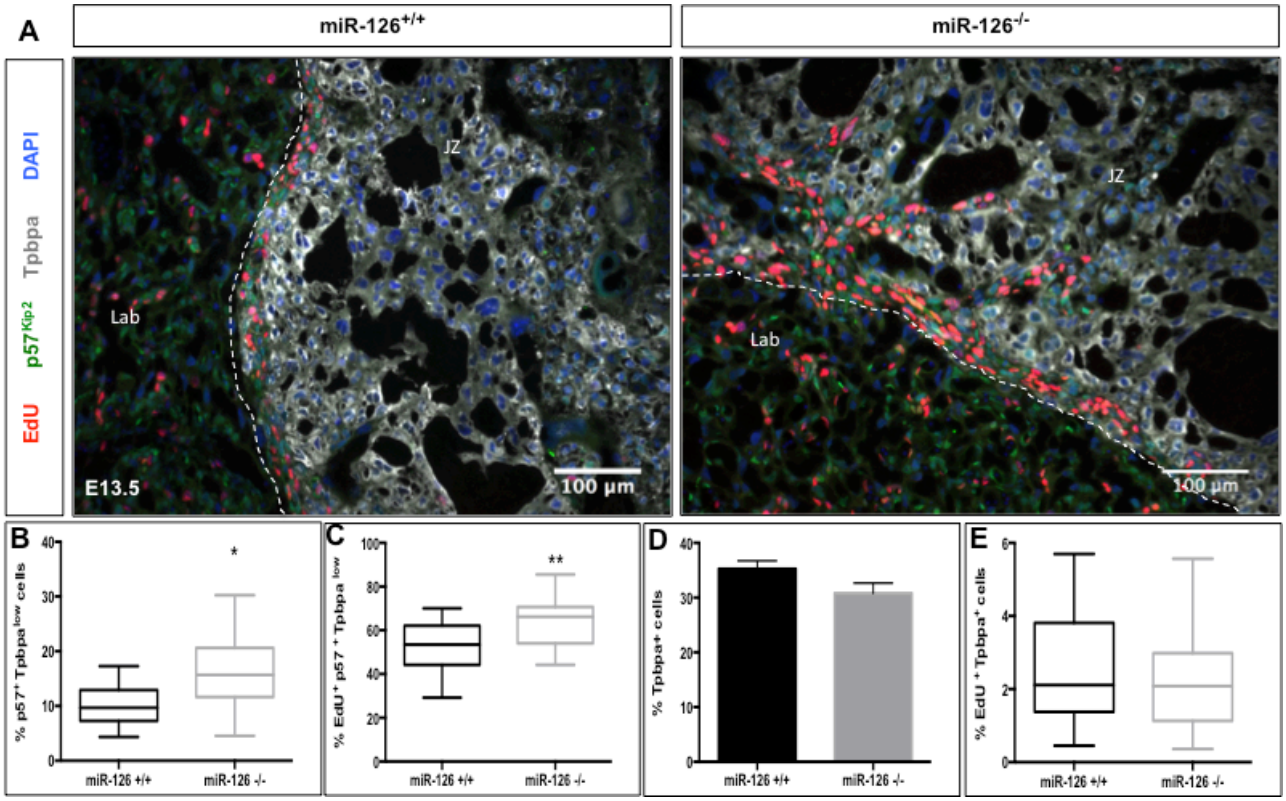


**Figure 2.8: Increased numbers of proliferating glycogen trophoblast progenitors in E13.5 miR-126$^{-/-}$ placentas at E13.5.** Representative images of sections of miR-126$^{+/+}$ and miR-126$^{-/-}$ placentas at E13.5, immunostained with p57$^{Kip2}$ antibody, Tpbpa antibody and EdU (ClickiT chemistry). Dotted white line indicates the boundary between the junctional zone and labyrinth. Bar = 100mm **(A)**. Quantification of Tpbpa$^{+}$p57$^{+}$ glycogen trophoblasts in the junctional zone of miR-126$^{+/+}$ (n=4) and miR-126$^{-/-}$ (n=4) placentas. Error bars indicate SEM. (* p≤0.05) **(B)**. Quantification of EdU$^{+}$Tpbpa$^{+}$p57$^{+}$ proliferating glycogen trophoblast progenitor cells in the junctional zone of miR-126$^{+/+}$ (n=4) and miR-126$^{-/-}$ (n=4) placentas. Error bars indicate SEM. (** p≤0.01) **(C)**. Quantification of Tpbpa$^{+}$ trophoblasts in the junctional zone **(D)**. Quantification of EdU$^{+}$Tpbpa$^{+}$ proliferating cells in the junctional zone **(E)**.

Our study is the first to implicate a role for a microRNA in GlyT proliferation and regulation of imprinted gene expression specifically in the placenta. The function of the GlyT lineage in the placenta is largely unknown; however, their migration into the decidua during late gestation and subsequent release of glucose into the maternal bloodstream supports the hypothesis that they are important for supplementing maternal nutrient resources and regulating embryonic growth during late gestation (Coan et al. 2006).

## 2.5 Materials and methods

### Mice and genotyping

All animal protocols were approved and are in accordance with the Institutional Animal Care and Use Committee (IACUC) at Weill Cornell Medical College of Cornell University. miR-126$^{+/-}$ mice (Wang et al. 2008) in a mixed genetic background were obtained from Dr. Eric Olsen (UT Southwestern Medical Center) and backcrossed for 10 generations into a congenic C57Bl6/J background. Genotyping was done by genomic PCR on DNA from yolk sac or tail biopsies, using the following primers:

126wild-forward: 5'- GGGCCACTTTACCCTGAAGAG -3';

126wild-reverse: 5'-GCTGACCGCGCATTATTACTC-3';

126floxed-reverse: 5' – GACGGTATCGATAAAGCTAGC-3'.

For timed pregnancies, the day of a vaginal plug was designated as embryonic day 0.5. All experimental embryos and placentas were isolated from litters of miR-126$^{+/-}$ x

miR-126$^{+/-}$ crosses. Embryonic sizes were calculated by crown to rump length measurements and placental sizes were calculated by measurements along the diameter of the placenta.

**Quantitative real-time PCR**

Embryos and placentas (E12.5) were isolated in cold PBS and flash frozen in liquid nitrogen. RNA was isolated using Trizol (Invitrogen). For analysis of miR-126 expression, 10ng of RNA was reverse transcribed using TaqMan MicroRNA Reverse Transcription Kit (Life Technologies #4366596) with RT primers specific for miR126-3p (*002228*) and control snoRNA234 *(0001234)*. Real Time PCR was performed using TaqMan Universal PCR Master Mix (Life Technologies #4324018) and TaqMan probes for miR126-3p and control snoRNA234.

***In situ* hybridization**

In situ hybridization was performed as previously described (Nielsen 2012). Briefly, OCT embedded mouse and human placenta sections were post-fixed with 4% PFA for 10mins and washed with PBS. Slides were treated with an acetylation solution (500µl 6N HCl, 670µl triethanolamine, 300µl acetic anhydride in 48.5ml DEPC-treated water) for 5min at RT. Sections were pre-hybridized in hybridization buffer (50% formamide, 5x SSC, 500µg/µl yeast tRNA, 5mM EDTA, 1X Denhardt' solution) for 4hr at 55$^0$C, and incubated with a DIG-labeled LNA miR-126 LNA probe (Exiqon) for 4hr at 55$^0$C. Slides were washed twice with 0.1x SSC at 60$^0$C and 4 times with 2x SSC at RT, blocked for 1hr using a blocking buffer (10% blocking reagent, 20% heat

inactivated goat serum in MABT) and incubated overnight at $4^0$C with alkaline phosphatase-conjugated anti-DIG antibody (1:1600, Roche). Sections were washed with MABT and NTMT (100 mM NaCl, 100 mM Tris–HCl pH9.5, 50 mM $MgCl_2$, 1% Tween20, 20 µM Levamisole, in $H_2O$). Signal was detected using NBT-BCIP (Roche) at RT. Sections were post-fixed in 4% paraformaldehyde and imaged using an Axioplan 2 imaging microscope (Carl Zeiss) with 20X and 40X objectives.

**Histology and Immunohistochemistry**

Placentas were isolated in ice-cold PBS, fixed in 4% paraformaldehyde overnight, and embedded in an OCT: 30% sucrose mixture. Cryosections were permeabilized in 0.5% Triton-X/0.1% Saponin/PBS (TSP) and blocked with 1% donkey serum in 0.1% TSP/PBS (PBS–TSP). Sections were incubated overnight at 4°C with primary antibodies - CD31 (BD Biosciences, 553370, 5µg/ml); Cytokeratin (DAKO Z0622, 10µg/ml); Tpbpa (Abcam, ab104401, 10µg/µl); p57 (Santa Cruz, sc-1039, 20µg/µl); Erg (Abcam, ab110639, 0.17µg/ml) -, followed by incubation with secondary antibodies (Alexa488-donkey-α-rat, Alexa488-donkey-α-rabbit, Alexa488-donkey-α-goat and Alexa594-donkey-α-rabbit, Jackson Immunoresearch, 1.5 µg/ml), and mounted with Prolong Gold + DAPI. Images were acquired using an Axioplan 2 imaging microscope with 20X and 40X objectives.

**Measurement of labyrinth and junctional zone areas**

Labyrinth and junctional zone areas were quantified from 6 images each of CD31 and Tpbpa immunostained cryosections from miR-$126^{+/+}$ (n=4) and miR-$126^{-/-}$ (n=3)

placentas derived from at least two litters of miR-126$^{+/-}$ x miR-126$^{+/-}$ crosses. The area stained positive for CD31 was quantified as the fetal labyrinth area, and the area stained positive for Tpbpa was quantified as the junctional zone area. Labyrinth and junctional zone regions were traced using ImageJ software and the percentage area was quantified.

**PAS staining**

Placentas were isolated, fixed in 4% paraformaldehyde, dehydrated through a series of alcohols, and embedded in paraffin. Sections were deparaffinized and hydrated through a series of alcohols to distilled water, stained with 1% Periodic acid for 5 minutes, and rinsed in distilled water. Sections were then stained with Schiff's reagent (Sigma) at room temperature for 30 minutes, washed in running tap water for 5 minutes, counterstained with Hematoxylin, and mounted with Permount (Fisher Scientific). Images were acquired using an Axioplan 2 imaging microscope with a 20X objective.

**EdU Labeling**

Proliferating cells were labeled using the Click-iT EdU Imaging Kit (Life Technologies, C10339), as previously described (Lacko et al. 2017). Briefly, pregnant female miR-126$^{+/-}$ mice were subjected to intraperitoneal injection of EdU at 50 μg per gram of body weight at day 13.5 and day 15.5 of gestation. After 60 minutes, mice were euthanized and placentas were isolated and fixed in 4% paraformaldehyde overnight. Tissue was embedded in an OCT: 30% sucrose mixture and sectioned for

further processing. EdU detection was carried out according to the manufacturer's protocol. Antibody staining was then performed as described above. Approximately every 10th section was used for quantification of labeling, for a total of four sections per placenta (n=4 per genotype), and analyzed using ImageJ, Metamorph (Molecular Devices) and Prism (GraphPad) software.

**Cell counts**

Glycogen trophoblast and proliferating cells were quantified from 10-15 high magnification images of miR-126$^{+/+}$ (n=4) and miR-126$^{-/-}$ (n=4) immunostained placentas from at least two litters of miR-126$^{+/-}$ x miR-126$^{+/-}$ crosses. p57$^{Kip2+}$Tpbpa$^{low}$ cells in the junctional zone of E13.5 and E15.5 placentas and EdU$^{+}$ p57$^{Kip2+}$Tpbpa$^{low}$ cells in the junctional zone of E13.5 were quantified using MetaMorph imaging software. Trophoblast giant cells were excluded based on the size of their nuclei.

**Quantification of total glycogen from placental tissue**

Total glycogen content in placentas was measured using previously described methods (Kemp and Van Heijningen 1954). Briefly, placentas were weighed, and boiled for 20 min in a 30% KOH solution saturated with $Na_2SO_4$. After cooling on ice, glycogen was precipitated by adding 1.2 volumes of 95% ethanol. Samples were spun at 1000xg for 30min at 4$^{o}$C, and the glycogen pellet was dissolved in ddH20. A phenol-sulfuric acid colorimetric method was used to determine glycogen content (Kemp and Van Heijningen 1954).

## REFERENCES


Adamson SL, Lu Y, Whiteley KJ, Holmyard D, Hemberger M, Pfarrer C, Cross JC. 2002. Interactions between trophoblast cells and the maternal and fetal circulation in the mouse placenta. *Dev Biol* 250: 358-373.

Bambino K, Lacko LA, Hajjar KA, Stuhlmann H. 2014. Epidermal growth factor-like domain 7 is a marker of the endothelial lineage and active angiogenesis. *Genesis* 52: 657-670.

Coan PM, Conroy N, Burton GJ, Ferguson-Smith AC. 2006. Origin and characteristics of glycogen cells in the developing murine placenta. *Dev Dyn* 235: 3280-3294.

Fish JE, Santoro MM, Morton SU, Yu S, Yeh RF, Wythe JD, Ivey KN, Bruneau BG, Stainier DY, Srivastava D. 2008. miR-126 regulates angiogenic signaling and vascular integrity. *Dev Cell* 15: 272-284.

Fitch MJ, Campagnolo L, Kuhnert F, Stuhlmann H. 2004. Egfl7, a novel epidermal growth factor-domain gene expressed in endothelial cells. *Dev Dyn* 230: 316-324.

Fu G, Brkic J, Hayder H, Peng C. 2013a. MicroRNAs in Human Placental Development and Pregnancy Complications. *Int J Mol Sci* 14: 5519-5544.

Fu G, Ye G, Nadeem L, Ji L, Manchanda T, Wang Y, Zhao Y, Qiao J, Wang YL, Lye S et al. 2013b. MicroRNA-376c impairs transforming growth factor-beta and nodal signaling to promote trophoblast cell proliferation and invasion. *Hypertension* 61: 864-872.

Georgiades P, Ferguson-Smith AC, Burton GJ. 2002. Comparative developmental anatomy of the murine and human definitive placentae. *Placenta* 23: 3-19.

Ishibashi O, Ohkuchi A, Ali MM, Kurashina R, Luo SS, Ishikawa T, Takizawa T, Hirashima C, Takahashi K, Migita M et al. 2012. Hydroxysteroid (17-beta) dehydrogenase 1 is dysregulated by miR-210 and miR-518c that are aberrantly expressed in preeclamptic placentas: a novel marker for predicting preeclampsia. *Hypertension* 59: 265-273.

Kemp A, Van Heijningen AJ. 1954. A colorimetric micro-method for the determination of glycogen in tissues. *Biochem J* 56: 646-648.

Kuhnert F, Mancuso MR, Hampton J, Stankunas K, Asano T, Chen CZ, Kuo CJ. 2008. Attribution of vascular phenotypes of the murine Egfl7 locus to the microRNA miR-126. *Development* 135: 3989-3993.

Lacko LA, Hurtado R, Hinds S, Poulos MG, Butler JM, Stuhlmann H. 2017. Altered feto-placental vascularization, feto-placental malperfusion, and fetal growth restriction in mice with Egfl7 loss-of-function. *Development*.

Lacko LA, Massimiani M, Sones JL, Hurtado R, Salvi S, Ferrazzani S, Davisson RL, Campagnolo L, Stuhlmann H. 2014. Novel expression of EGFL7 in placental trophoblast and endothelial cells and its implication in preeclampsia. *Mech Dev* 133: 163-176.

Lee DC, Romero R, Kim JS, Tarca AL, Montenegro D, Pineles BL, Kim E, Lee J, Kim SY, Draghici S et al. 2011. miR-210 targets iron-sulfur cluster scaffold homologue in human trophoblast cell lines: siderosis of interstitial trophoblasts as a novel pathology of preterm preeclampsia and small-for-gestational-age pregnancies. *Am J Pathol* 179: 590-602.

Li P, Guo W, Du L, Zhao J, Wang Y, Liu L, Hu Y, Hou Y. 2013. microRNA-29b contributes to pre-eclampsia through its effects on apoptosis, invasion and angiogenesis of trophoblast cells. *Clin Sci (Lond)* 124: 27-40.

Liu N, Olson EN. 2010. MicroRNA regulatory networks in cardiovascular development. *Dev Cell* 18: 510-525.

Luo L, Ye G, Nadeem L, Fu G, Yang BB, Honarparvar E, Dunk C, Lye S, Peng C. 2012. MicroRNA-378a-5p promotes trophoblast cell survival, migration and invasion by targeting Nodal. *J Cell Sci* 125: 3124-3132.

Nielsen BS. 2012. MicroRNA in situ hybridization. *Methods Mol Biol* 822: 67-84.

Nolan DJ, Ginsberg M, Israely E, Palikuqi B, Poulos MG, James D, Ding BS, Schachterle W, Liu Y, Rosenwaks Z et al. 2013. Molecular signatures of tissue-specific microvascular endothelial cell heterogeneity in organ maintenance and regeneration. *Dev Cell* 26: 204-219.

Parker LH, Schmidt M, Jin SW, Gray AM, Beis D, Pham T, Frantz G, Palmieri S, Hillan K, Stainier DY et al. 2004. The endothelial-cell-derived secreted factor Egfl7 regulates vascular tube formation. *Nature* 428: 754-758.

Rossant J, Cross JC. 2001. Placental development: lessons from mouse mutants. *Nat Rev Genet* 2: 538-548.

Tsochandaridis M, Nasca L, Toga C, Levy-Mozziconacci A. 2015. Circulating microRNAs as clinical biomarkers in the predictions of pregnancy complications. *Biomed Res Int* 2015: 294954.

Wang S, Aurora AB, Johnson BA, Qi X, McAnally J, Hill JA, Richardson JA, Bassel-Duby R, Olson EN. 2008. The endothelial-specific microRNA miR-126 governs vascular integrity and angiogenesis. *Dev Cell* 15: 261-271.

Watson ED, Cross JC. 2005. Development of structures and transport functions in the mouse placenta. *Physiology (Bethesda)* 20: 180-193.

## Chapter 3- Gene expression and signaling in miR-126$^{-/-}$ placentas

### 3.1 Rationale

A number of genetic and epigenetic determinants control trophoblast differentiation and placental development (Maltepe et al. 2010; Lefebvre 2012). Genomic imprinting is an epigenetic modification that regulates gene expression from a single allele based on parental origin (Plasschaert and Bartolomei 2014). The importance of maintaining genomic imprints for placental development is highlighted in murine models where imprinted gene deletions and uniparental duplications result in placental abnormalities and embryonic growth defects (Lopez et al. 1996; Georgiades et al. 2001; Esquiliano et al. 2009; Tunster et al. 2010; Oh-McGinnis et al. 2011). Human infants with naturally occurring imprinting disorders like Beckwith–Wiedemann and Silver-Russell syndromes have abnormal placentas (Maher and Reik 2000; Gicquel et al. 2005; Schonherr et al. 2007). Genomic imprinting also affects nutrient availability and tissue development in utero (Tunster et al. 2013; Green et al. 2015). Interestingly, several known regulators of junctional zone trophoblast development are imprinted genes that are located in the Igf2 and Kcnq1ot1 clusters on the distal end of chromosome 7 (Fig. 3.1) (Ferguson-Smith et al. 2001; Lefebvre 2012). Genomic imprinting is regulated by the maintenance DNA methyl transferase, *Dnmt1*. Dnmt1 catalyzes methylation of hemi-methylated CpG nucleotides at differentially methylated regions (DMRs) of imprint control centers (Messerschmidt et al. 2014). Dnmt1o (oocyte specific) deficiency results in partial loss of DNA methylation and placental defects, including an expanded spongiotrophoblast volume,

aberrant glycogen trophoblast migration and reduced surface area for maternal fetal gas exchange (Himes et al. 2013).

In the previous chapter, I have described defects in glycogen trophoblast progenitor proliferation in miR-126$^{-/-}$ placentas that result in junctional zone expansion, reduced fetal labyrinth and IUGR of the embryos. In this chapter, I will describe a role for miR-126 in regulating imprinted gene expression by modulating DNA methylation as a possible mechanism for aberrant glycogen trophoblast proliferation. The results described in this chapter are from studies designed and performed by myself. They are part of a manuscript in revision (miR-126 regulates glycogen trophoblast proliferation and DNA methylation in the murine placenta Abhijeet Sharma, Lauretta A. Lacko and Heidi Stuhlmann. In revision. Development).

### 3.2 Abstract

miR-126$^{-/-}$ placentas display an expanded junctional zone at E15.5 resulting from increased numbers of proliferating glycogen trophoblast progenitors. Several imprinted genes have been implicated in regulating glycogen trophoblast development. We show that miR-126$^{-/-}$ placentas display aberrant expression of imprinted genes with important roles in glycogen trophoblasts and junctional zone development, including Igf2, H19, Cdkn1c, Ascl2 and Phlda2. Abnormal imprinted gene expression is restricted to the placenta and is accompanied by methylation defects at several CpGs at ICRs of Kcnq1ot1 and H19. miR-126$^{-/-}$ placentas also

display dysregulated expression of the imprinting regulator, *Dnmt1,* and changes in global methylation. Our findings uncover a novel role for miR-126 in regulating expression of imprinted genes and DNA methylation in the placenta to regulate the extra-embryonic energy stores in the placenta.

### 3.3 Introduction

A number of imprinted genes with roles in development of the junctional zone and glycogen trophoblasts (GlyTs) are located in two distinct clusters on mouse chromosome 7. Allele specific expression of imprinted genes in these clusters is regulated by differentially methylated regions (DMRs) function as imprint control centers (ICRs). A number of these imprinted genes are also implicated in the etiology of Beckwith–Wiedemann syndrome (BWS), Silver–Russell syndrome (SRS) and IUGR in humans, characterized by growth abnormalities of the embryo and placenta (Maher and Reik 2000; Constancia et al. 2002; Gicquel et al. 2005; Schonherr et al. 2007; Esquiliano et al. 2009).

Two independent ICRs, IC1 and IC2 on chromosome 7 control imprinting at the H19/Igf2 and Kcnq1 clusters through different mechanisms. The IC1 DMR controls paternal expression of Igf2 and maternal expression of H19 in embryos and placentas (Fig. 3.1). Allele specific expression is maintained by binding of the CTCF insulator protein to 4 target sites at the ICR. On the paternal allele, methylation at the ICR prevents CTCF binding, abrogates H19 expression and activates *Igf2* expression

through the distal enhancer. On the maternal allele, insulator CTCF proteins bind the ICR, inhibiting access of the distal enhancer to Igf2 and activating *H19* expression (Bell and Felsenfeld 2000; Hark et al. 2000).

At the IC2 cluster, the lncRNA Kcnq1ot1 is expressed only from the paternal allele and methylation of its promoter on the maternal allele acts as the ICR to maintain allelic expression (Smilinich et al. 1999). Kcnq1ot1 expression on the paternal allele is functionally linked to silencing of 8-10 genes in cis (Mancini-Dinardo et al. 2006). Genes near the Kcnq1ot1 promoter (Kcnq1, Cdkn1C, Slc22a18, Phlda2) are imprinted in the embryo and placenta in mice and humans. In contrast, genes located farther away from the promoter (Ascl2, Cd81, Tssc4, Osbpl5) are imprinted only in the placenta (Fig. 3.1). Kcnq1ot1 maintains imprinting of both ubiquitously imprinted and placental-specific imprinted genes through DNA methylation at the ICR and repressive histone methylation (Lewis et al. 2004; Mohammad et al. 2010). The ubiquitously imprinted genes are repressed on the paternal chromosome by DNA methylation at the DMR 610bp from TSS of Kcnq1ot1 (Mohammad et al. 2010). Deletion of Dnmt1 or the DMR results in loss of imprinting of the ubiquitously imprinted genes in the embryo and the placenta (Lewis et al. 2004; Mohammad et al. 2010). However, imprinting of the placental specific genes is intact. Maintenance of imprinting of placental specific imprinted genes is proposed to involve repressive histone marks placed by epigenetic modifiers recruited by Kcnq1ot1 (Lewis et al. 2004).

*Igf2* and *Cdkn1C* are expressed by the GlyTs (Redline et al. 1993; Georgiades et al. 2002) and *Ascl2* and *Phlda2* are expressed in the ectoplacental cone, during early development, but are later exclusively expressed by spongiotrophoblasts and syncytiotrophoblasts respectively (Guillemot et al. 1994; Frank et al. 1999; Oh-McGinnis et al. 2011). IGF2P0$^{-/-}$ (placenta-specific) placentas and IGF2$^{-/-}$ (global) placentas display significantly reduced GlyTs (Constancia et al. 2002; Sferruzzi-Perri et al. 2011). Biallelic expression of Igf2 through the deletion of the H19 DMR also leads to an increase in GlyT number and placental glycogen (Esquiliano et al. 2009). *Cdkn1c* mouse mutants display abnormal GlyT progenitor differentiation accompanied by decreased glycogen in the placenta (Coan et al. 2006; Tunster et al. 2011). Phlda2$^{-/-}$ placentas have increased junctional zone volume (Tunster et al. 2010). *Phlda2* overexpression also results in abnormal GlyTs and reduced glycogen content in the placenta (Tunster et al. 2010). Biallelic expression of Phlda2 also affects junctional zone formation in the placenta (Salas et al. 2004). *Ascl2*$^{-/-}$ placentas are devoid of GlyTs (Oh-McGinnis et al. 2011).

In zebrafish and mouse embryos, miR-126 modulates PI3K and MAPK signaling to control proliferation and migration of endothelial cells to modulate angiogenesis (Fish et al. 2008; Wang et al. 2008). miR-126 also regulates cell proliferation of colon and breast cancer cells (Guo et al. 2008; Zhang et al. 2008; Zhou et al. 2013), and human hematopoietic stem cells (Lechman et al. 2012) by targeting members of the PI3K and MAPK pathways. Based on the fact that miR-126 has perfect sequence

conservation, miR-126 potentially has a conserved role in regulating PI3K and MAPK pathways.

To understand the mechanism through which miR-126 regulates GlyT development, gene expression of several imprinted genes implicated in GlyT and junctional zone development was analyzed. To minimize biases in gene expression from changes in cellular composition of the placenta, analyses were performed on E12.5 placentas, where there are no significant differences in junctional zone area. We show a dysregulation of imprinted gene expression in miR-126$^{-/-}$ placentas accompanied by changes in DNA methylation at ICRs and dysregulation of Dnmt1. PI3K and MAPK signaling pathways were also analyzed in the placenta. We show significantly reduced AKT and ERK signaling in miR-126$^{-/-}$ placentas. The results of this study identify potential signaling mechanisms through which miR-126 regulates junctional zone trophoblast development in the murine placenta.

## 3.4 Results and discussion

### 3.4.1 miR-126 regulates imprinted gene expression and DNA methylation at DMRs on chromosome 7 in the placenta

To identify the molecular pathways through which miR-126 affects glycogen trophoblast expansion, expression levels of genes that are known regulators of GlyT development were analyzed. The Igf2 cluster contains the imprinted genes *Igf2* and

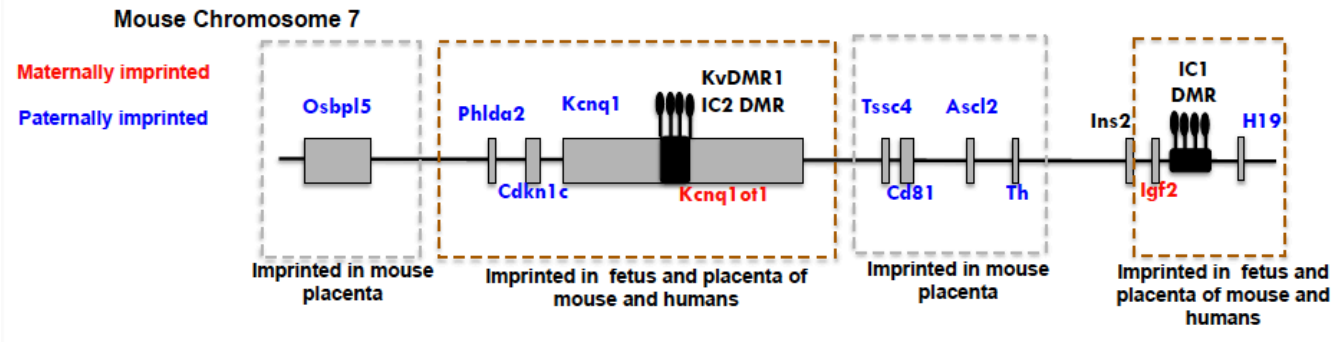


**Figure 3.1 Imprinted genes on the distal end of chromosome 7.** Imprinted genes on chromosome 7 are organized into two clusters. The distal end contains genes Igf2, H19 and Ins2, regulated by the imprint control center IC1. Binding of insulator CTCF proteins at IC1 DMR activates H19 expression on the maternal chromosome. Methylation of IC1 on the paternal chromosome prevents CTCF binding and activates Igf2 expression. The second cluster containing 8-10 genes regulated by IC2 DMR (KvDMR1). LncRNA Kcnq1ot1 suppresses genes in cis on the paternal chromosome. Methylation of IC2 on the maternal chromosome turns-off Kcnq1ot1 expression. Genes closer to IC2 are ubiquitously imprinted in the embryo and the placenta. Genes further away from IC2 DMR are imprinted only in the mouse placenta.

*H19* and *Ins2*. Deletion of *Igf2* or *H19* results in altered glycogen trophoblast numbers (Lopez et al. 1996; Esquiliano et al. 2009). The Kcnq1ot1 cluster contains *Cdkn1c* ($p57^{Kip2}$), *Phlda2, Kcnq1*, *Ascl2, Ospbl5, Cd81* and *Tssc4*. Loss of *Cdkn1c* leads to glycogen trophoblast differentiation defects (Tunster et al. 2011). *Phlda2* deletion results in spongiotrophoblast hypertrophy and increased JZ area (Tunster et al. 2010). *Ascl2* hypomorphs have reduced spongiotrophoblasts and no GlyTs (Oh-McGinnis et al. 2011).

We analyzed expression levels of the imprinted genes implicated in JZ and GlyT development located in these two clusters in E12.5 placentas (n=4) by qRT-PCR (Fig. 3.3). miR-$126^{-/-}$ placentas show significantly reduced expression of Igf2 and significantly elevated H19 expression (Fig. 3.2A) when compared to miR-$126^{+/+}$ placentas. However, Igf2 and H19 expression is unchanged between miR-$126^{-/-}$ and miR-$126^{+/+}$ embryos (Fig. 3.4A).

We next investigated if aberrant imprinted gene expression is associated with changes in DNA methylation at imprinted loci. DNA methylation at IC1 and IC2 from genomic DNA isolated from E12.5 miR-$126^{-/-}$ and miR-$126^{+/+}$ (n=2) littermate placentas was analyzed by pyrosequencing. At the IC1 locus, CTCF insulator proteins cooperatively bind to the DMR to maintain imprinting. miR-$126^{-/-}$ placentas display significantly increased methylation at several CpGs of the DMR corresponding to CTCF target sites 3 and 4 (-2.9kb to -1.7kb from H19 TSS) (Fig. 3.2B), but is unchanged at DMRs corresponding to CTCF target sites 1 and 2 (-4.6kb to -3.5kb

from H19 TSS) (Fig. 3.2C). Deletions of CTCF sites in tandem have highlighted their role in maintaining imprinting at this locus. Previous studies have shown that deletion of three CTCF target sites (sites 2,3,4) results in a reactivation of H19 and loss of Igf2 expression on the paternal allele and a reciprocal effect on the maternal allele (Thorvaldsen et al. 1998; Thorvaldsen et al. 2002). A mouse model carrying deletion of CTCF target sites 2 and 3 displays changes in pup weights and loss of imprinting in this region (Ideraabdullah et al. 2014). Mice with mutations in CTCF target site 4 alone also display loss of imprinting in endodermal and mesodermal tissues (Pant et al. 2004). Together, these data suggest that changes in methylation at the CTCF target sites results in bi-allelic expression of Igf2 and H19 in miR-126$^{-/-}$ placentas at E12.5.

We next investigated expression levels of imprinted genes in the IC2 cluster. Expression of imprinted genes in this cluster is controlled by transcription of the long non-coding RNA Kcnq1ot1 that runs antisense to *Kcnq1*. miR-126$^{-/-}$ placentas have significantly reduced expression of Kcnq1ot1 and no significant difference in Kcnq1 expression (Fig. 3.3A). Expression of Cdkn1c is significantly reduced, whereas Phlda2 expression levels were unaffected in miR-126$^{-/-}$ placentas at E12.5 (Fig. 3.3A). Expression of Kcnq1ot1, Cdkn1c and Phlda2 were unchanged between miR-126$^{-/-}$ and miR-126$^{+/+}$ embryos (Fig. 3.4B). At the IC2 locus, a DMR adjacent to transcriptional start site (TSS) of Kcnq1ot1 regulates imprinting of genes close to the cluster. There were no significant differences in methylation levels of the CpGs at IC2 (Fig. 3.3B).

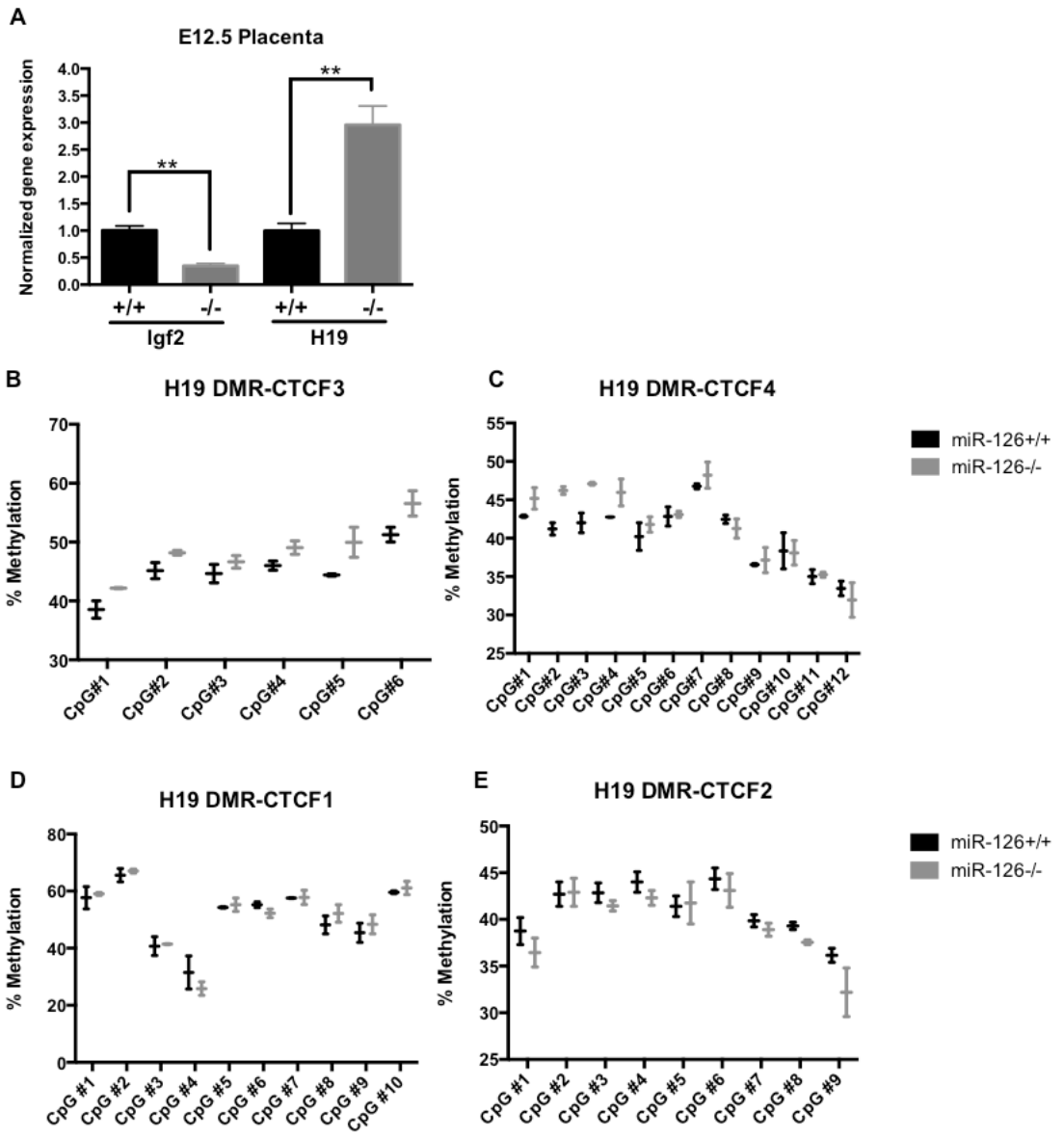


**Figure 3.2 miR-126 regulates imprinted gene expression and DNA methylation at the H19/Igf2 imprinting cluster in the placenta.** Gene expression levels of maternally imprinted gene *Igf2* and paternally imprinted gene *H19* in E12.5 placentas by quantitative RT PCR (n=3, from two litters for each genotype). Error bars indicate SEM. (** $p \leq 0.01$) **(A).** Percent methylation of CpGs at CTCF binding site 3 of imprint control center IC1 **(B)**. Percent methylation of CpGs at CTCF binding site 4 of imprint control center IC1 **(C)**. Percent methylation of CpGs at CTCF binding site 1 of imprint control center IC1 **(D)**. Percent methylation of CpGs at CTCF binding site 2 of imprint control center IC1 **(E).**

We next investigated if imprinted genes in other genomic locations are also dysregulated in miR-126$^{-/-}$ placentas. *Peg3* is an imprinted gene located in the centromeric region of chromosome 7 that regulates transcription of several placental-specific gene families (Kim et al. 2013). *Grb10* is an imprinted gene on chromosome 11 whose deletion leads to placental defects and IUGR in embryos (Charalambous et al. 2010). Expression levels of both Peg3 and Grb10 are significantly downregulated in miR-126$^{-/-}$ placentas at E12.5 (Fig. 3.3C). Global DNA methylation levels in E12.5 placentas were tested by DNA dot blot assay with an anti-5methyl cytosine antibody. miR-126$^{-/-}$ placentas display reduced methylation when compared to miR-126$^{+/+}$ littermate placentas (Fig. 3.3D).These results indicate that loss of miR-126 results in a global dysregulation of methylation and imprinted gene expression in the placenta but not in the embryo.

### 3.4.2 miR-126 regulates Dnmt1 expression in the placenta and trophoblast stem cells

Deletion of the DNA maintenance methylase, *Dnmt1,* results in aberrant imprinted gene expression in the placenta (Lewis et al. 2004; Weaver et al. 2010). We investigated if dysregulation *Dnmt1* was the cause for global changes in DNA methylation and imprinted gene expression observed in miR-126$^{-/-}$ placentas. Interestingly, *Dnmt1* expression was significantly dysregulated at the mRNA and protein levels in miR-126$^{-/-}$ placentas at several developmental stages analyzed. *Dnmt1*

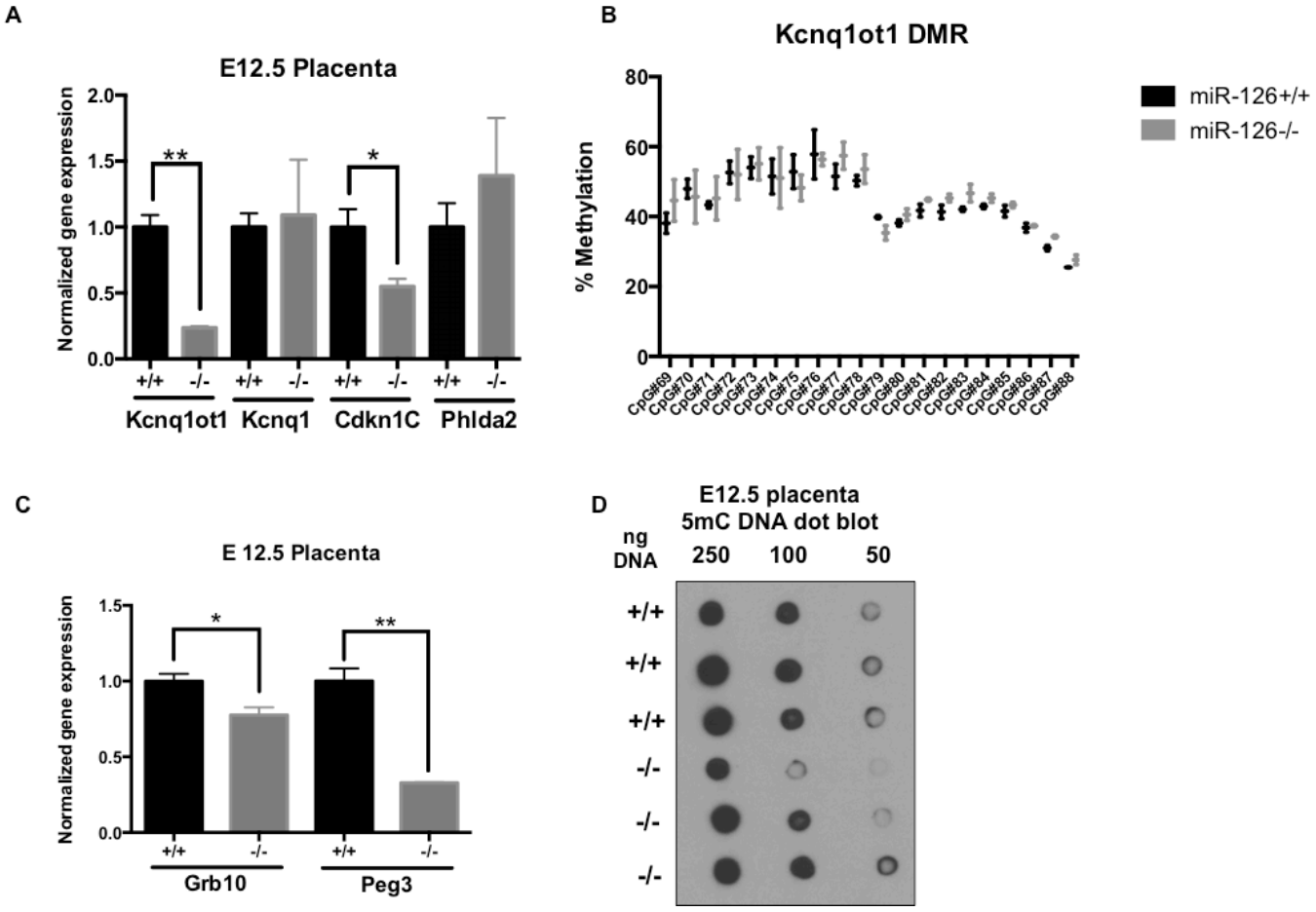


**Figure 3.3 miR-126 regulates imprinted gene expression and DNA methylation in the placenta at E12.5.** Gene expression levels of maternally imprinted gene Kcnq1ot1 and paternally imprinted genes Kcnq1, Cdkn1C and Phlda2 in E12.5 placentas by quantitative RT PCR (n=3, from two litters for each genotype). Error bars indicate SEM. (* $p \leq 0.05$) (** $p \leq 0.01$) **(A)**. Percent methylation of CpGs at Kcnq1ot1 imprint control center **(B)**. Gene expression levels of imprinted genes Grb10 and Peg3 in E12.5 placentas by quantitative RT PCR (n=3, from two litters for each genotype). Error bars indicate SEM. (* $p \leq 0.05$) (** $p \leq 0.01$) **(C)**. DNA dot blot using an anti-5methyl cytosine antibody on total genomic DNA (250, 100, 50ng) from miR-126$^{+/+}$ and miR-126$^{-/-}$ placentas (n =3, from two litters for each genotype) **(D)**.

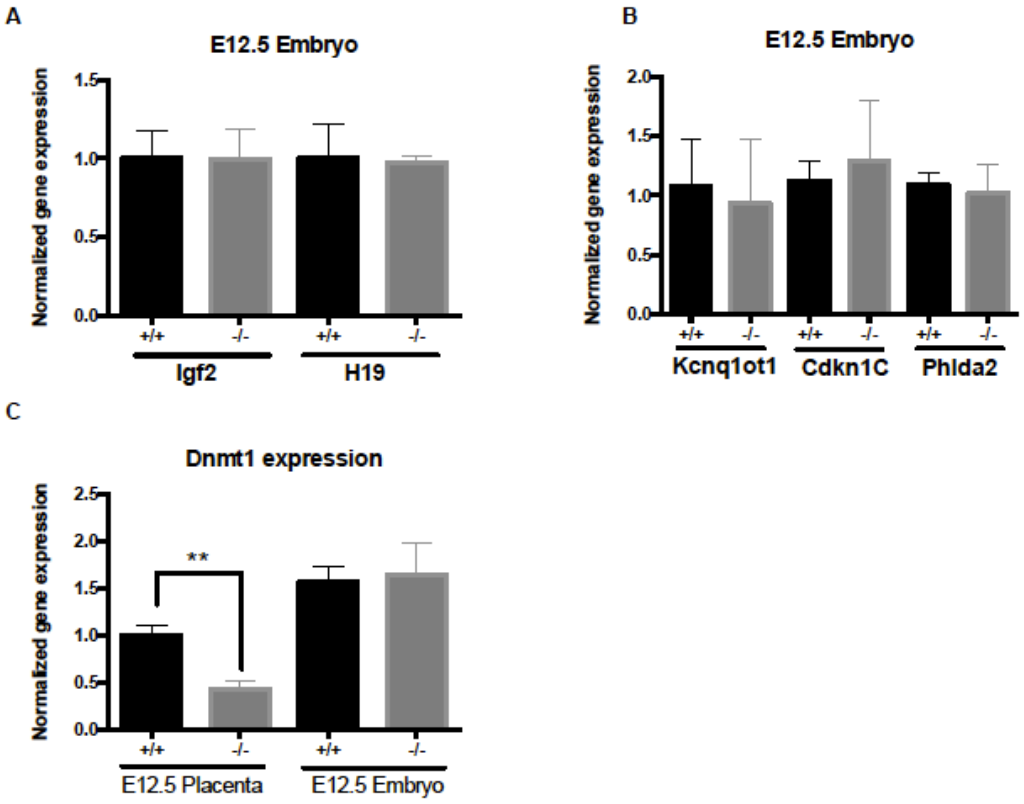


**Figure 3.4 miR-126$^{-/-}$ embryos do not display changes in expression of imprinted genes and Dnmt1.** Gene expression levels of maternally imprinted gene *Igf2* and paternally imprinted gene *H19* in E12.5 embryos by quantitative RT PCR (n=3, from two litters for each genotype). Error bars indicate SEM **(A)**. Gene expression levels of maternally imprinted gene Kcnq1ot1 and paternally imprinted genes Cdkn1C and Phlda2 in E12.5 embryos by quantitative RT PCR (n=3, from two litters for each genotype). Error bars indicate SEM **(B)**. Gene expression levels of *Dnmt1* in E12.5 embryos and placentas by quantitative RT PCR (n =3, from two litters for each genotype) **(C)**

mRNA expression level in miR-126$^{-/-}$ placentas is significantly increased at E10.5, significantly reduced at E12.5 and unchanged at E15.5 when compared to miR-126$^{+/+}$ placentas (Fig. 3.5A). At the protein level, DNMT1 expression in miR-126$^{-/-}$ placentas is reduced at E10.5, unchanged at E12.5 and reduced at E15.5 (Fig. 3.5B). miR-126$^{-/-}$ placentas at E12.5 also displayed significantly reduced expression of Dnmt3a, but no significant change in expression levels of Dnmt3b, Tet1, Tet2 and Tet3 (Figure 3.6A,B). We also observed upregulation of Dnmt1 expression in miR-126$^{-/-}$ trophoblast stem cells that did not reach significance (Fig. 3.5C).

Collectively, these data suggest that miR-126 controls *Dnmt1* expression in a dynamic manner in the trophoblasts of the placenta at the transcriptional and the post-translational level to regulate DNA methylation and glycogen trophoblast development.

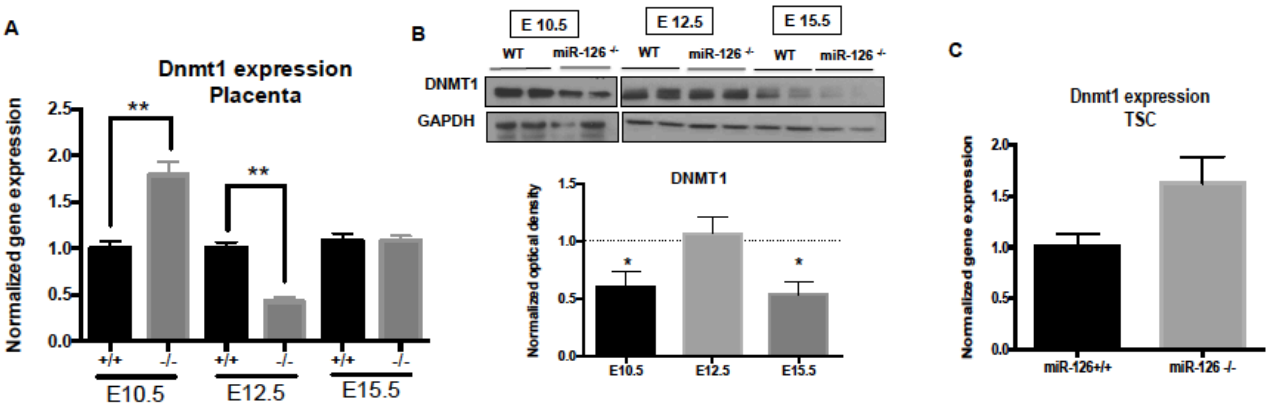


**Figure 3.5 miR-126 regulates Dnmt1 expression in the placenta and trophoblast stem cells.** Gene expression levels of *Dnmt1* in E10.5, E12.5 and E15.5 placentas by quantitative RT PCR (n =3, from two litters for each genotype) **(A)**. Western blot analysis and quantification of protein expression by optical density of tissue lysates from E10.5, E12.5 and E15.5 placentas. Membranes were probed with antibodies against DNMT1 and GAPDH (loading control) (n = 2, from two litters for each genotype, quantification from two independent experiments) **(B)**. Gene expression levels of *Dnmt1* in miR-126$^{-/-}$ and miR-126$^{+/+}$ trophoblast stem cells (TSC) by quantitative RT PCR (n =3, from two litters for each genotype) **(C)**.

### 3.4.3 miR-126 regulates AKT and ERK signaling in the placenta

In endothelial cells of the developing embryo, miR-126 modulates angiogenesis by binding to and degrading inhibitors of the PI3K and MAPK signaling pathways (Fish et al. 2008; Wang et al. 2008). Akt1$^{-/-}$ embryos and placentas display growth impairment *in utero* (Yang et al. 2003; Kent et al. 2012) and Akt1$^{-/-}$ placentas have severely reduced glycogen trophoblasts (Kent et al. 2012). PI3K and MAPK signaling was investigated in E12.5 and E15.5 placentas. miR-126$^{-/-}$ placental lysates displayed reduced pAKT and pERK expression at E12.5 when compared to miR-126$^{+/+}$ littermates (Fig. 3.7A,B). Interestingly, miR-126$^{-/-}$ placentas also display significantly increased AKT1 expression (Fig. 3.7A). There is no significant difference in pAKT, AKT1 and pERK expression in placentas at E15.5 (Fig. 3.7A,B). Glycogen synthase kinase-3 (GSK 3) is a regulator of glycogen synthesis and is negatively regulated by PI3K-mediated activation of AKT. There were no significant differences in expression levels of pGSK3β and GSK3β in miR-126$^{-/-}$ placentas at E12.5 or E15.5 when compared to miR-126$^{+/+}$ littermates (Fig. 3.7C).

To identify potential direct targets of miR-126 in the placenta, expression levels of genes that are validated targets of miR-126 in other cell types (Spred1, Vcam1, Egfl7, Pik3r2, CrkII) were analyzed. miR-126 inhibits translation of Spred1, Vcam1 and Pik3r2 in endothelial cells (Fish et al. 2008; Harris et al. 2008; Wang et al. 2008) and Eglf7 in lung cancer cells (Sun et al. 2010). Paradoxically, expression levels of Spred1 were significantly reduced in miR-126$^{-/-}$ placentas (Fig. 3.7D). There was

no significant difference in expression levels of Vcam1, Egfl7 (Fig. 3.7D) and Pik3r2 (Fig. 3.7 E) in miR-126$^{-/-}$ placentas. miR-126 has been shown to regulate HSC proliferation by inhibiting CrkII expression (Lechman et al. 2012). CRKII, an adaptor protein for PI3K signaling was significantly up regulated in miR-126$^{-/-}$ placentas at E12.5 and E15.5 (Fig. 3.7E).

**Discussion**

The distal portion of mouse chromosome 7 contains several imprinted genes (*Igf2, H19, Kcnq1ot1, Cdkn1c, Phlda2, Ascl2*) that are organized into two distinct, independently regulated clusters. Gain and loss-of function mutants of these imprinted genes, as well as mutants with bi-allelic gene expression, display defects in glycogen cell proliferation and differentiation (Constancia et al. 2002; Salas et al. 2004; Esquiliano et al. 2009; Tunster et al. 2010; Oh-McGinnis et al. 2011; Sferruzzi-Perri et al. 2011; Tunster et al. 2011), similar to the phenotypes observed in miR-126$^{-/-}$ placentas. miR-126$^{-/-}$ placentas display aberrant expression of Igf2, H19, Cdkn1c, Ascl2, Phlda2 and Kcnq11ot1 at E12.5 accompanied by changes in DNA methylation at some CpGs of imprint control centers.

The absence of more robust changes in DNA methylation at both imprinted loci could potentially be due to contaminating cell types with biallelic expression of imprinted genes. Although some imprinted genes are known to be expressed by GlyTs (Igf2, Cdkn1C), a detailed analysis of imprinting has not been performed in all of the trophoblast cell subtypes of the placenta. Recent evidence also suggests that the

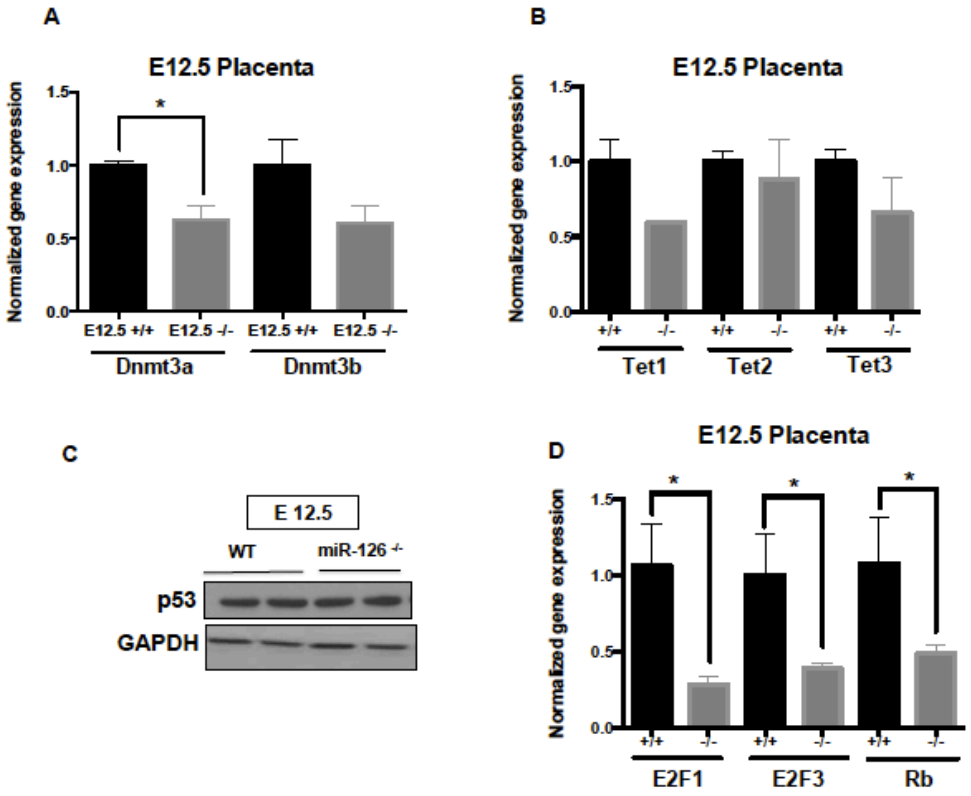


**Figure 3.6 Gene expression analyses of regulators of DNA methylation.** Gene expression levels *Dnmt3a* and *Dnmt3b* in E12.5 placentas by quantitative RT PCR (n=3, from two litters for each genotype). Error bars indicate SEM. (* $p \leq 0.05$) **(A)**. Gene expression levels *Tet1, Tet2* and *Tet3* in E12.5 placentas by quantitative RT PCR (n=3, from two litters for each genotype). Error bars indicate SEM **(B)**. Western blot analysis of tissue lysates from E12.5 placentas. Membranes were probed with antibodies against p53 and GAPDH (loading control) **(C)**. Gene expression levels *E2f1, E2f3* and *Retinoblastoma (Rb)* in E12.5 placentas by quantitative RT PCR (n=3, from two litters for each genotype). Error bars indicate SEM. (* $p \leq 0.05$) **(D).**

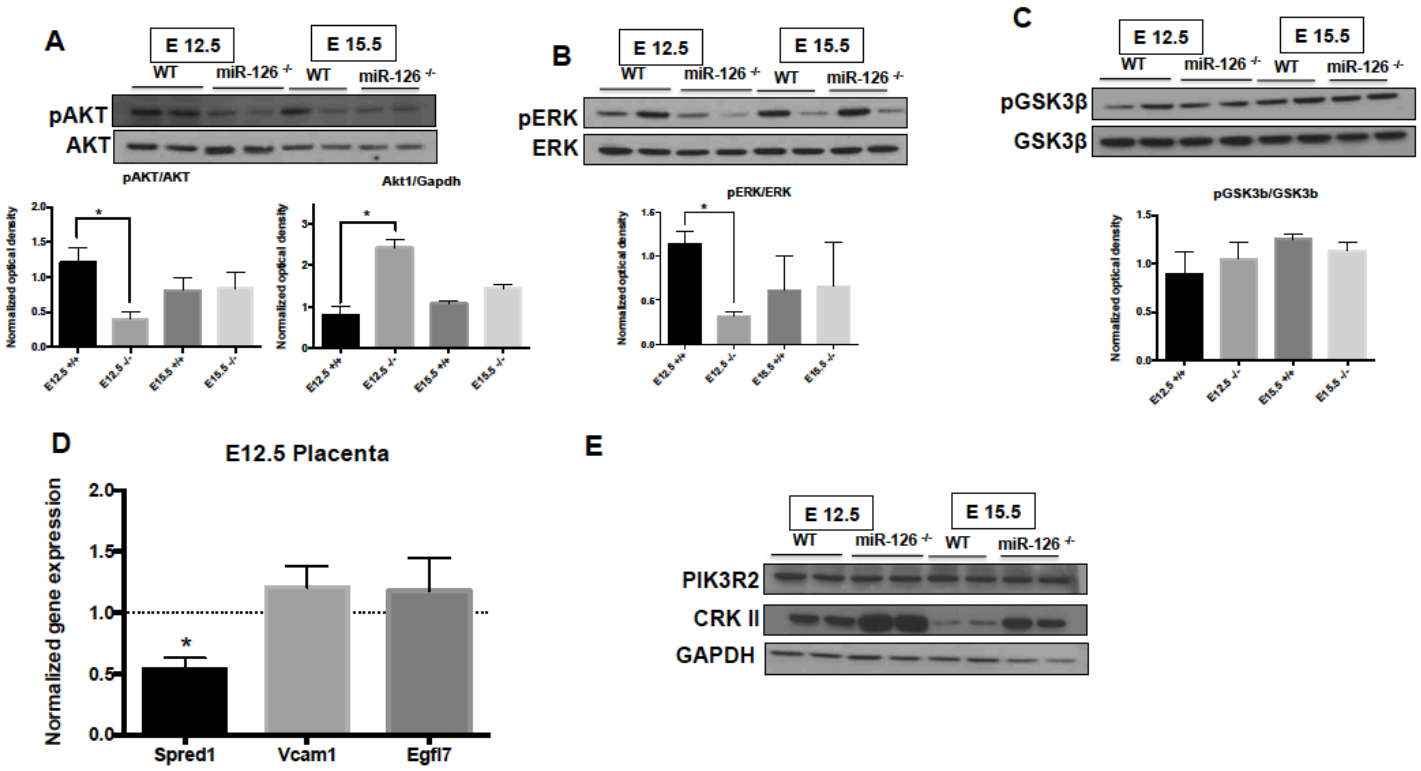


**Figure 3.7 miR-126 regulates PI3K and MAPK pathways in the placenta.** Western blot analysis and quantification of protein expression in tissue lysates by optical density from E12.5 and E15.5 placentas. Membranes were probed with antibodies against pAKT and AKT1 **(A)**. Western blot analysis and quantification of protein expression in tissue lysates by optical density from E12.5 and E15.5 placentas. Membranes were probed with antibodies against pERK and ERK1/2 **(B)**. Western blot analysis and quantification of protein expression in tissue lysates by optical density from E12.5 and E15.5 placentas. Membranes were probed with antibodies against pGSKβ and GSK3β **(C)**. Gene expression levels of *Spred1, Vcam1 and Egfl7* in E12.5 placentas by quantitative RT PCR (n =3, from two litters for each genotype) **(D)**. Western blot analysis of tissue lysates from E12.5 and E15.5 placentas. Membranes were probed with antibodies against PIK3R2, CRKII and GAPDH (loading control) **(E)**.

junctional zone is hypomethylated when compared to the fetal labyrinth (Decato et al. 2017). Future studies that trace maintenance of imprinting in the placenta throughout development will elucidate the cell types and developmental windows in which imprinting is maintained in the placenta.

Our analysis suggested that miR-126 broadly regulates DNA methylation in the placenta by modulating Dnmt1 expression. *Dnmt1* regulates allele specific expression of imprinted genes by maintaining methylation at DMRs (Li et al. 1993; Howell et al. 2001). DNMT1 methylates newly synthesized hemi-methylated DNA during the S phase in dividing cells (Li et al. 1993). Additionally, Dnmt1 loss of function mutants die around E10.5, and as a consequence studies focusing on LOI have utilized placental tissue from E9.5. At mid-gestation, GlyT progenitors undergo a rapid, 250-fold expansion and form tight clusters of mature GlyTs by E14.5 (Coan et al. 2006). We speculate that reduced Dnmt1 expression in miR-126$^{-/-}$ placentas at E12.5 leads to a failure in maintaining allele specific expression of imprinted genes resulting in aberrant increase of GlyT number. Imprinted genes regulating GlyT development potentially have major roles during mid and late gestation in the placenta. However, studying imprinting and DNA methylation in mid and late gestation placentas are challenging due to the lack of techniques that can trace allelic expression in tissues.

*Dnmt1* is regulated at the transcriptional and post-translational levels by several proteins (Lin and Wang 2014; Scott et al. 2014). Based on the absence of canonical binding sites for miR-126 in the Dnmt1 3'UTR, we surmise that miR-126 regulates

Dnmt1 expression indirectly and in a placenta-restricted manner. Furthermore, the dynamic dysregulation of Dnmt1 transcripts and protein along with aberrant signaling of proteins that regulate Dnmt1 expression suggest that miR-126 modulates Dnmt1 expression at both the transcriptional and post-translational level.

miR-126 has a conserved function in regulating PI3K and MAPK signaling. miR-126 modulates PI3K and MAPK signaling in mouse endothelial cells, human hematopoietic stem cells, colorectal and breast cancers by blocking translation of inhibitors of AKT and ERK signaling. miR-126 potentially inhibits trophoblast specific factors that downregulate AKT and ERK signaling in the placenta.

### 3.5 Materials and methods

#### Real Time RT-PCR

Embryos and placentas (E12.5) were isolated in cold PBS and flash frozen in liquid nitrogen. RNA was isolated using Trizol (Invitrogen) and reverse transcribed using SuperScript II (Quanta Biosciences). Gene expression was measured quantitatively using PerfeCTa SYBR Green SuperMix for iQ (Quanta Biosciences). Primer sets are listed in the table below. Differences in target gene expression was quantified using the ΔΔCT method and normalized to ß-actin and 18S rRNA.

| Gene | Forward Primer (5' –> 3') | Reverse primer (5' –> 3) |
|---|---|---|
| Igf2 | AGCAATCGGAAGTGAGCAAAC | GGATGGAACCTGATGGAAACG |
| H19 | GGCTCCCAGAACCCACAAC | GGGTTTTGTGTCCGGATTCA |

| | | |
|---|---|---|
| p57 | GCCGGGTGATGAGCTGGGAA | AGAGAGGCTGGTCCTTCAGC |
| Phlda2 | CCCGCCAAGGAGCTGTTT | CCTTGTAATAGTTGGTGACGATGGT |
| Kcnq1 | CAAAGACCGTGGCAGTAAC | CCTTCATTGCTGGCTACAAC |
| Kcnq1ot1 | GGTCTGAGGTAGGGATCAGG | GGCACACGGTATGAGAAAAGATTG |
| Dnmt1 | CCTAGTTCCGTGGCTACGAGGAGAA | TCTCTCTCCTCTGCAGCCGACTCA |
| Grb10 | AGGATCATCAAGCAACAAGGTCTC | ATTACTCTGGCTGTCACGAAGGA |
| Peg3 | ATGCCCACTCCGTCAGCG | GCTCATCCTTGTGAACTTTG |
| E2f1 | GCCCTTGACTATCACTTTGGTCTC | CCTTCCCATTTTGGTCTGCTC |
| E2f3 | GCCTCTACACCACGCCACAAG | TCGCCCAGTTCCAGCCTT C |
| Rb | ACTCCGTTTTCATGCAGAGACTAA | GAGGAATGTGAGGTATTGGTGACA |
| Spred1 | GCCAAGTCAGCCAGATACCAT | AGGGACCCTAGTTTGGGACTT |
| Vcam1 | GGGACCACATCTACGCTGACA | CCTGTCTGCATCCTCCAGAAA |
| Egfl7 | ATGAGACCATGTGGGGCTC | GGTCTCCGAGATGGAACCTCCG |
| 18s rRNA | AACCCGTTGAACCCCATT | CCATCCAATCGGTAGTAGCG |

**DNA dot blot assay**

Genomic DNA was isolated from E12.5 placentas with phenol and diluted to various concentrations. DNA was denatured with 5µl of 0.1M NaOH, cooled down on ice, neutralized with 1µl of 6.6M-ammonium acetate. 1µl from each DNA dilution was spotted on a nitrocellulose membrane (Immobilon-NY) and air-dried. The membrane was then UV-crosslinked for 5min at 220nm, blocked with 5% milk in TBST for 1 hour and probed with an antibody against 5-methyl cytosine (Cell Signaling). After washing with TBST, the membrane was incubated with [HRP]-conjugated anti-rabbit (1:10000) antibody. Proteins were visualized using ECL Plus (G.E).

**Pyrosequencing assay**

Bisulphite conversion was performed on genomic DNA isolated from decidua free E12.5 placentas. DMRs at the H19 and Kcnq1ot1 loci was amplified with specific primers and sequencing performed to identify methylated CpGs. Biulphite conversion, amplification and sequencing was performed by EpigenDx, Inc.

**Generation of trophoblast stem cells**

Trophoblast stem cells were isolated using the method of Tanaka et al. from blastocysts derived from timed mating of miR-126$^{+/-}$ mice (Tanaka et al. 1998). TSCs were cultured without feeders in 30% TS medium containing RPMI 1640, 20% heat-inactivated fetal bovine serum, 1% sodium pyruvate, 1% penicillin-streptomycin, 1% glutamine, and 100 μM β-mercaptoethanol and 70% conditioned medium isolated from irradiated primary mouse embryonic fibroblasts (MEFs) cultured in TS medium**.**

**Western blot analysis**

Protein was isolated from placentas using radioimmunoprecipitation assay (RIPA) buffer containing a cocktail of protease and phosphatase inhibitors (Sigma). Tissue lysates were mixed with 5x NuPage loading buffer and heated at 70$^0$C for 10min. 20μg of proteins were fractionated on a 4-12% gradient gel and transferred to a nitrocellulose membrane (Bio-Rad). The membrane was blocked in 5% nonfat milk in TBST (0.1% Tween 20 in 1X Tris-buffered saline) and probed with antibodies against DNMT1 (Cell Signaling), pAKT (Santa Cruz), AKT (Santa Cruz), pERK (Santa Cruz), ERK (Santa Cruz), pGSK3b (Cell Signaling) GSK3b (Santa Cruz), p53 (Santa

Cruz), PIK3R2 (Santa Cruz), CRK(R&D), GAPDH (Santa Cruz). After washing with TBST, the membrane was incubated with [HRP]-conjugated anti-rabbit (1:10000). The proteins were visualized using ECL Plus (G.E).

## REFERENCES


Bell AC, Felsenfeld G. 2000. Methylation of a CTCF-dependent boundary controls imprinted expression of the Igf2 gene. *Nature* 405: 482-485.

Charalambous M, Cowley M, Geoghegan F, Smith FM, Radford EJ, Marlow BP, Graham CF, Hurst LD, Ward A. 2010. Maternally-inherited Grb10 reduces placental size and efficiency. *Dev Biol* 337: 1-8.

Coan PM, Conroy N, Burton GJ, Ferguson-Smith AC. 2006. Origin and characteristics of glycogen cells in the developing murine placenta. *Dev Dyn* 235: 3280-3294.

Constancia M, Hemberger M, Hughes J, Dean W, Ferguson-Smith A, Fundele R, Stewart F, Kelsey G, Fowden A, Sibley C et al. 2002. Placental-specific IGF-II is a major modulator of placental and fetal growth. *Nature* 417: 945-948.

Decato BE, Lopez-Tello J, Sferruzzi-Perri AN, Smith AD, Dean MD. 2017. DNA Methylation Divergence and Tissue Specialization in the Developing Mouse Placenta. *Mol Biol Evol* 34: 1702-1712.

Esquiliano DR, Guo W, Liang L, Dikkes P, Lopez MF. 2009. Placental glycogen stores are increased in mice with H19 null mutations but not in those with insulin or IGF type 1 receptor mutations. *Placenta* 30: 693-699.

Ferguson-Smith AC, Tevendale M, Georgiades P, Grandjean V. 2001. Balanced translocations for the analysis of imprinted regions of the mouse genome. *Methods Mol Biol* 181: 41-54.

Fish JE, Santoro MM, Morton SU, Yu S, Yeh RF, Wythe JD, Ivey KN, Bruneau BG, Stainier DY, Srivastava D. 2008. miR-126 regulates angiogenic signaling and vascular integrity. *Dev Cell* 15: 272-284.

Frank D, Mendelsohn CL, Ciccone E, Svensson K, Ohlsson R, Tycko B. 1999. A novel pleckstrin homology-related gene family defined by Ipl/Tssc3, TDAG51, and Tih1: tissue-specific expression, chromosomal location, and parental imprinting. *Mamm Genome* 10: 1150-1159.

Georgiades P, Ferguson-Smith AC, Burton GJ. 2002. Comparative developmental anatomy of the murine and human definitive placentae. *Placenta* 23: 3-19.

Georgiades P, Watkins M, Burton GJ, Ferguson-Smith AC. 2001. Roles for genomic imprinting and the zygotic genome in placental development. *Proc Natl Acad Sci U S A* 98: 4522-4527.

Gicquel C, Rossignol S, Cabrol S, Houang M, Steunou V, Barbu V, Danton F, Thibaud N, Le Merrer M, Burglen L et al. 2005. Epimutation of the telomeric

imprinting center region on chromosome 11p15 in Silver-Russell syndrome. *Nat Genet* 37: 1003-1007.

Green BB, Kappil M, Lambertini L, Armstrong DA, Guerin DJ, Sharp AJ, Lester BM, Chen J, Marsit CJ. 2015. Expression of imprinted genes in placenta is associated with infant neurobehavioral development. *Epigenetics* 10: 834-841.

Guillemot F, Nagy A, Auerbach A, Rossant J, Joyner AL. 1994. Essential role of Mash-2 in extraembryonic development. *Nature* 371: 333-336.

Guo C, Sah JF, Beard L, Willson JK, Markowitz SD, Guda K. 2008. The noncoding RNA, miR-126, suppresses the growth of neoplastic cells by targeting phosphatidylinositol 3-kinase signaling and is frequently lost in colon cancers. *Genes Chromosomes Cancer* 47: 939-946.

Hark AT, Schoenherr CJ, Katz DJ, Ingram RS, Levorse JM, Tilghman SM. 2000. CTCF mediates methylation-sensitive enhancer-blocking activity at the H19/Igf2 locus. *Nature* 405: 486-489.

Harris TA, Yamakuchi M, Ferlito M, Mendell JT, Lowenstein CJ. 2008. MicroRNA-126 regulates endothelial expression of vascular cell adhesion molecule 1. *Proc Natl Acad Sci U S A* 105: 1516-1521.

Himes KP, Koppes E, Chaillet JR. 2013. Generalized disruption of inherited genomic imprints leads to wide-ranging placental defects and dysregulated fetal growth. *Dev Biol* 373: 72-82.

Howell CY, Bestor TH, Ding F, Latham KE, Mertineit C, Trasler JM, Chaillet JR. 2001. Genomic imprinting disrupted by a maternal effect mutation in the Dnmt1 gene. *Cell* 104: 829-838.

Ideraabdullah FY, Thorvaldsen JL, Myers JA, Bartolomei MS. 2014. Tissue-specific insulator function at H19/Igf2 revealed by deletions at the imprinting control region. *Hum Mol Genet* 23: 6246-6259.

Kent LN, Ohboshi S, Soares MJ. 2012. Akt1 and insulin-like growth factor 2 (Igf2) regulate placentation and fetal/postnatal development. *Int J Dev Biol* 56: 255-261.

Kim J, Frey WD, He H, Kim H, Ekram MB, Bakshi A, Faisal M, Perera BP, Ye A, Teruyama R. 2013. Peg3 mutational effects on reproduction and placenta-specific gene families. *PLoS One* 8: e83359.

Lechman ER, Gentner B, van Galen P, Giustacchini A, Saini M, Boccalatte FE, Hiramatsu H, Restuccia U, Bachi A, Voisin V et al. 2012. Attenuation of miR-126 activity expands HSC in vivo without exhaustion. *Cell Stem Cell* 11: 799-811.

Lefebvre L. 2012. The placental imprintome and imprinted gene function in the trophoblast glycogen cell lineage. *Reprod Biomed Online* 25: 44-57.

Lewis A, Mitsuya K, Umlauf D, Smith P, Dean W, Walter J, Higgins M, Feil R, Reik W. 2004. Imprinting on distal chromosome 7 in the placenta involves repressive histone methylation independent of DNA methylation. *Nat Genet* 36: 1291-1295.

Li E, Beard C, Jaenisch R. 1993. Role for DNA methylation in genomic imprinting. *Nature* 366: 362-365.

Lin RK, Wang YC. 2014. Dysregulated transcriptional and post-translational control of DNA methyltransferases in cancer. *Cell Biosci* 4: 46.

Lopez MF, Dikkes P, Zurakowski D, Villa-Komaroff L. 1996. Insulin-like growth factor II affects the appearance and glycogen content of glycogen cells in the murine placenta. *Endocrinology* 137: 2100-2108.

Maher ER, Reik W. 2000. Beckwith-Wiedemann syndrome: imprinting in clusters revisited. *J Clin Invest* 105: 247-252.

Maltepe E, Bakardjiev AI, Fisher SJ. 2010. The placenta: transcriptional, epigenetic, and physiological integration during development. *J Clin Invest* 120: 1016-1025.

Mancini-Dinardo D, Steele SJ, Levorse JM, Ingram RS, Tilghman SM. 2006. Elongation of the Kcnq1ot1 transcript is required for genomic imprinting of neighboring genes. *Genes Dev* 20: 1268-1282.

Messerschmidt DM, Knowles BB, Solter D. 2014. DNA methylation dynamics during epigenetic reprogramming in the germline and preimplantation embryos. *Genes Dev* 28: 812-828.

Mohammad F, Mondal T, Guseva N, Pandey GK, Kanduri C. 2010. Kcnq1ot1 noncoding RNA mediates transcriptional gene silencing by interacting with Dnmt1. *Development* 137: 2493-2499.

Oh-McGinnis R, Bogutz AB, Lefebvre L. 2011. Partial loss of Ascl2 function affects all three layers of the mature placenta and causes intrauterine growth restriction. *Dev Biol* 351: 277-286.

Pant V, Kurukuti S, Pugacheva E, Shamsuddin S, Mariano P, Renkawitz R, Klenova E, Lobanenkov V, Ohlsson R. 2004. Mutation of a single CTCF target site within the H19 imprinting control region leads to loss of Igf2 imprinting and complex patterns of de novo methylation upon maternal inheritance. *Mol Cell Biol* 24: 3497-3504.

Plasschaert RN, Bartolomei MS. 2014. Genomic imprinting in development, growth, behavior and stem cells. *Development* 141: 1805-1813.

Redline RW, Chernicky CL, Tan HQ, Ilan J, Ilan J. 1993. Differential expression of insulin-like growth factor-II in specific regions of the late (post day 9.5) murine placenta. *Mol Reprod Dev* 36: 121-129.

Salas M, John R, Saxena A, Barton S, Frank D, Fitzpatrick G, Higgins MJ, Tycko B. 2004. Placental growth retardation due to loss of imprinting of Phlda2. *Mech Dev* 121: 1199-1210.

Schonherr N, Meyer E, Roos A, Schmidt A, Wollmann HA, Eggermann T. 2007. The centromeric 11p15 imprinting centre is also involved in Silver-Russell syndrome. *J Med Genet* 44: 59-63.

Scott A, Song J, Ewing R, Wang Z. 2014. Regulation of protein stability of DNA methyltransferase 1 by post-translational modifications. *Acta Biochim Biophys Sin (Shanghai)* 46: 199-203.

Sferruzzi-Perri AN, Vaughan OR, Coan PM, Suciu MC, Darbyshire R, Constancia M, Burton GJ, Fowden AL. 2011. Placental-specific Igf2 deficiency alters developmental adaptations to undernutrition in mice. *Endocrinology* 152: 3202-3212.

Smilinich NJ, Day CD, Fitzpatrick GV, Caldwell GM, Lossie AC, Cooper PR, Smallwood AC, Joyce JA, Schofield PN, Reik W et al. 1999. A maternally methylated CpG island in KvLQT1 is associated with an antisense paternal transcript and loss of imprinting in Beckwith-Wiedemann syndrome. *Proc Natl Acad Sci U S A* 96: 8064-8069.

Sun Y, Bai Y, Zhang F, Wang Y, Guo Y, Guo L. 2010. miR-126 inhibits non-small cell lung cancer cells proliferation by targeting EGFL7. *Biochem Biophys Res Commun* 391: 1483-1489.

Tanaka S, Kunath T, Hadjantonakis AK, Nagy A, Rossant J. 1998. Promotion of trophoblast stem cell proliferation by FGF4. *Science* 282: 2072-2075.

Thorvaldsen JL, Duran KL, Bartolomei MS. 1998. Deletion of the H19 differentially methylated domain results in loss of imprinted expression of H19 and Igf2. *Genes Dev* 12: 3693-3702.

Thorvaldsen JL, Mann MR, Nwoko O, Duran KL, Bartolomei MS. 2002. Analysis of sequence upstream of the endogenous H19 gene reveals elements both essential and dispensable for imprinting. *Mol Cell Biol* 22: 2450-2462.

Tunster SJ, Jensen AB, John RM. 2013. Imprinted genes in mouse placental development and the regulation of fetal energy stores. *Reproduction* 145: R117-137.

Tunster SJ, Tycko B, John RM. 2010. The imprinted Phlda2 gene regulates extraembryonic energy stores. *Mol Cell Biol* 30: 295-306.

Tunster SJ, Van de Pette M, John RM. 2011. Fetal overgrowth in the Cdkn1c mouse model of Beckwith-Wiedemann syndrome. *Dis Model Mech* 4: 814-821.

Wang S, Aurora AB, Johnson BA, Qi X, McAnally J, Hill JA, Richardson JA, Bassel-Duby R, Olson EN. 2008. The endothelial-specific microRNA miR-126 governs vascular integrity and angiogenesis. *Dev Cell* 15: 261-271.

Weaver JR, Sarkisian G, Krapp C, Mager J, Mann MR, Bartolomei MS. 2010. Domain-specific response of imprinted genes to reduced DNMT1. *Mol Cell Biol* 30: 3916-3928.

Yang ZZ, Tschopp O, Hemmings-Mieszczak M, Feng J, Brodbeck D, Perentes E, Hemmings BA. 2003. Protein kinase B alpha/Akt1 regulates placental development and fetal growth. *J Biol Chem* 278: 32124-32131.

Zhang J, Du YY, Lin YF, Chen YT, Yang L, Wang HJ, Ma D. 2008. The cell growth suppressor, mir-126, targets IRS-1. *Biochem Biophys Res Commun* 377: 136-140.

Zhou Y, Feng X, Liu YL, Ye SC, Wang H, Tan WK, Tian T, Qiu YM, Luo HS. 2013. Down-regulation of miR-126 is associated with colorectal cancer cells proliferation, migration and invasion by targeting IRS-1 via the AKT and ERK1/2 signaling pathways. *PLoS One* 8: e81203.

## Chapter 4: miR-126 regulates glucose homeostasis

### 4.1 Rationale

Diabetes is a complex metabolic disorder that manifests from a combination of multiple genetic and environmental factors. Complications from Type-2 diabetes mellitus (T2DM) can cause stroke, hypertension, renal failure and myocardial infarction, which is one of the leading causes of morbidity and mortality worldwide. Increased healthcare costs and loss of productivity associated with diabetes in the US has been estimated to be 245 billion USD in 2012 (American Diabetes 2013). Even though diabetes is one of the oldest diseases know to man, the underlying disease mechanism is still incompletely understood and to date a cure is has been elusive. To develop new therapies and improve the efficacy of current treatments, it is critical to develop a thorough understanding of the mechanisms that play a role in the development and progression of diabetes. Mouse models of diabetes have reduced expression levels of miR-126 (Liang et al. 2013) and plasma from type 2 diabetes patients has reduced circulating miR-126 (Zampetaki et al. 2010; Mocharla et al. 2013; Zhang et al. 2015). However, a causative role for miR-126 in T2DM has not been established. Understanding of a possible causative role for miR-126 in T2DM will give us novel insight into the genetic basis for the development of diabetes.

### 4.2 Abstract

Diabetes is a chronic metabolic disease that is the major cause of stroke, hypertension, renal failure and myocardial infarction. There is substantial evidence to suggest that genetic mutations can increase susceptibility to insulin resistance and insulin secretion deficiencies leading to T2DM. We show that loss of a single copy of miR-126 results in fasting hyperglycemia in male and female mice, accompanied by reduced levels of serum insulin. miR-126$^{+/-}$ male but not female mice also display glucose intolerance. A fraction of miR-126$^{+/-}$ male mice also display reduced weight-gain after birth. This data highlights a possible causative role for miR-126 in metabolic dysfunction.

**4.3 Introduction**

Diabetes is a chronic metabolic disease whose incidence has been increasing dramatically over the past few decades. T2DM is the more prevalent form with an estimated 552 million people worldwide expected to have the disease in 2030 (Whiting et al. 2011). T2DM is characterized by hyperglycemia resulting from peripheral organs developing insulin resistance, leading to hyperinsulinemia, and eventually beta cell failure. Importantly T2DM often leads to major pathologies of the cardiovascular system like atherosclerosis resulting from increased breakdown of lipids for energy needs. Poorly managed diabetes is the major cause of stroke, hypertension, renal failure and myocardial infarction. A high-calorie diet and sedentary lifestyle is one of the major causes for the development of obesity and T2DM. There is also substantial evidence to suggest that genetic mutations can

increase susceptibility to insulin resistance and insulin secretion deficiencies leading to T2DM. In support, a high concordance rate in monozygotic twins (Kaprio et al. 1992; Matsuda and Kuzuya 1994) and increased prevalence in offspring of affected patients has been reported (Rich 1990). There are over 40 inheritable genetic variants shown to increase susceptibility to diabetes (Polonsky 2012).

MicroRNAs are a class of evolutionary conserved, non-coding RNAs that repress gene expression post-transcriptionally by targeting the 3'untranslated region (3'UTR) of mRNAs. Multiple microRNAs (miRNAs) have physiological roles in regulating beta cell function (Poy et al. 2004; Joglekar et al. 2009), adipocyte differentiation (Karbiener et al. 2009), and homeostasis in other tissues affected by T2DM (Li et al. 2009; Shan et al. 2010). Although several studies show associations between altered miRNA expression and development of T2DM, few studies have focused on elucidating a possible role for miRNAs in the pathogenesis of the disease (Fernandez-Valverde et al. 2011; Kantharidis et al. 2011).

miR-126 is an evolutionarily conserved endothelial miRNA embedded in intron 7 of *Egfl7* (Campagnolo et al. 2005; Schmidt et al. 2007; Nikolic et al. 2013). *Egfl7* is a largely endothelial cell-restricted gene that encodes a secreted protein that binds to extracellular matrix components (Campagnolo et al. 2005; Schmidt et al. 2007; Nikolic et al. 2013). miR-126 has a conserved role in regulating PI3K and MAPK pathways. miR-126 regulates cell proliferation of colon (Zhou et al. 2013) and breast (Zhang et al. 2008) cancers by targeting members of the PI3K pathway.

Mutations in genes regulated by the PI3K/AKT pathway are known to be associated with hereditary forms of diabetes (Winter and Silverstein 2000; Wang et al. 2002). Mouse models of diabetes have reduced expression levels of miR-126 (Liang et al. 2013) and plasma from type 2 diabetes patients has reduced circulating miR-126 (Zampetaki et al. 2010; Mocharla et al. 2013; Zhang et al. 2015). However, a causative role for miR-126 in T2DM has not been established.

## 4.4 Results and discussion

### 4.4.1 miR-126$^{+/-}$ mice display fasting hyperglycemia and hypoinsulinemia

To examine if miR-126 regulates glucose metabolism, we analyzed glucose and insulin levels of 10-12 weeks old miR-126$^{+/-}$ mice, as miR-126$^{-/-}$ mice in a congenic C57Bl6/J die in utero. We analyzed fasting blood glucose of female miR-126$^{+/-}$ (n=11) and miR-126$^{+/+}$ (n=12) mice, 4hrs after food withdrawal using a glucometer. miR-126$^{+/-}$ male and female mice display significantly elevated levels of fasting blood glucose when compared to miR-126$^{+/+}$ littermates (Fig. 4.1A). We also measured levels of fasting serum insulin from these mice using an ELISA assay. miR-126$^{+/-}$ male (n=7) and female mice (n=3) display a reduction in serum insulin levels compared to miR-126$^{+/+}$ mice without reaching statistical significance (Fig. 4.1B).

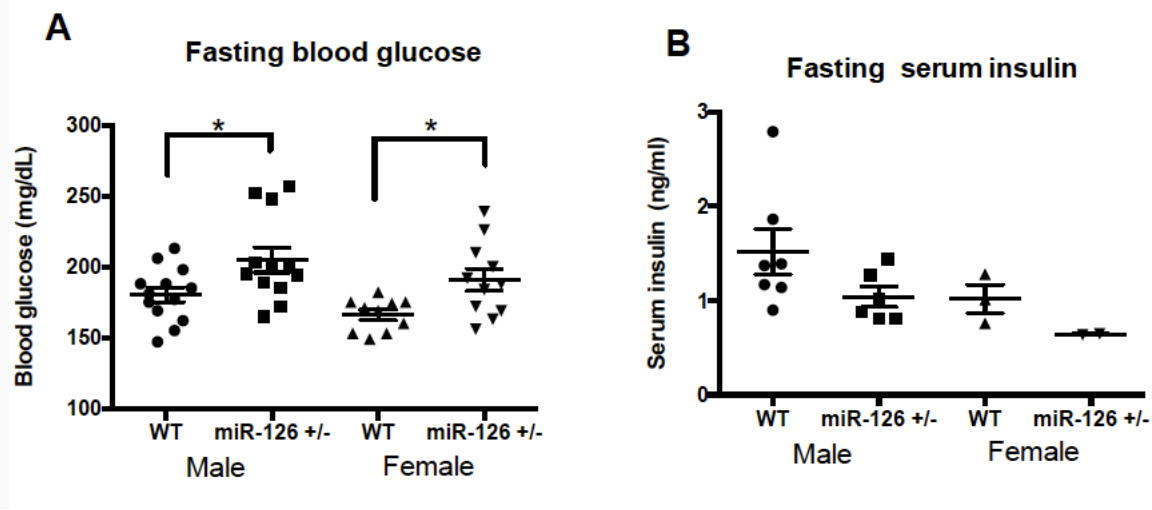


**Figure 4.1 miR-126$^{+/-}$ mice display fasting hyperglycemia and hypoinsulinemia.** Fasting blood glucose levels of 10-12 week old male and female miR-126$^{+/-}$ mice (4hr fast). Error bars indicate SEM. (* $p \leq 0.05$) **(A)**. Fasting serum insulin levels of 10-12 week old male and female miR-126$^{+/-}$ mice measured by ELISA (4hr fast) **(B)**.

### 4.4.2 miR-126$^{+/-}$ mice are glucose intolerant and insulin sensitive

We next tested glucose and insulin sensitivity in these mice by performing glucose and insulin tolerance tests. For the glucose tolerance test, after a 4-hour fast, 10-12 weeks old male and female mice were injected with glucose (1g/kg) intra peritoneally and blood glucose levels were measured at 15, 30, 45, 60 and 120 minutes after the injection. miR-126$^{+/-}$ male mice (n=7) display significantly elevated blood glucose levels at several time points after the glucose injection when compared to miR-126$^{+/+}$ mice (n=7) (Fig. 4.2A). Glucose tolerance test was quantified by area under the curve (Fig. 4.2B). In contrast, there was no significant difference in glucose sensitivity in miR-126$^{+/-}$ female mice (Fig. 4.2C,D). Glucose intolerance in miR-126$^{+/-}$ mice potentially results from insulin resistance in the peripheral organs and/or defective insulin secretion in the pancreas. To test if miR-126$^{+/-}$ were insulin resistant, insulin tolerance test was performed. After a 4-hour fast, 10-12 weeks old male and female mice were injected with human insulin (1U/kg) intra peritoneally and blood glucose levels were measured at 15, 30, 45, 60 and 120 minutes after the injection. miR-126$^{+/-}$male (Fig 4.3A,B) and female mice (Fig 4.3 C, D) do not display significant differences in blood glucose levels when compared to miR-126$^{+/+}$ mice at all time points after the insulin injection. This data demonstrates that miR-126$^{+/-}$ male mice are glucose intolerant and miR-126$^{+/-}$ male and female mice are insulin sensitive.

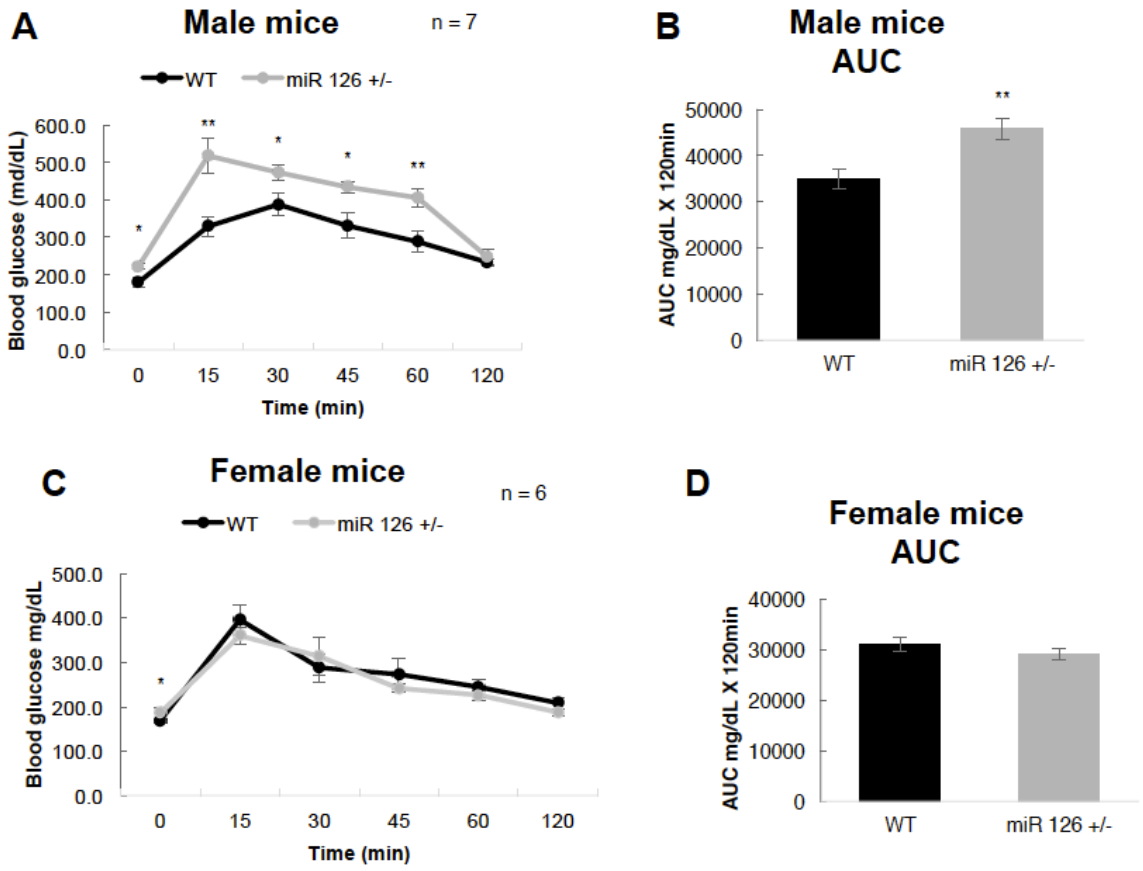


**Figure 4.2 miR-126$^{+/-}$ male, but not female mice display glucose intolerance.** Glucose tolerance test (1g/kg) in 10-12 week old male mice after a 4hr fast. Error bars indicate SEM. (* $p \leq 0.05$) (** $p \leq 0.01$) **(A)**. Area under the curve (AUC) from glucose tolerance test on male mice. Error bars indicate SEM. (** $p \leq 0.01$) **(B)**. Glucose tolerance test (1g/kg) in 10-12 week old female mice after a 4hr fast Error bars indicate SEM. (* $p \leq 0.05$) **(C)**. Area under the curve (AUC) from glucose tolerance test on female mice. Error bars indicate SEM **(D)**.

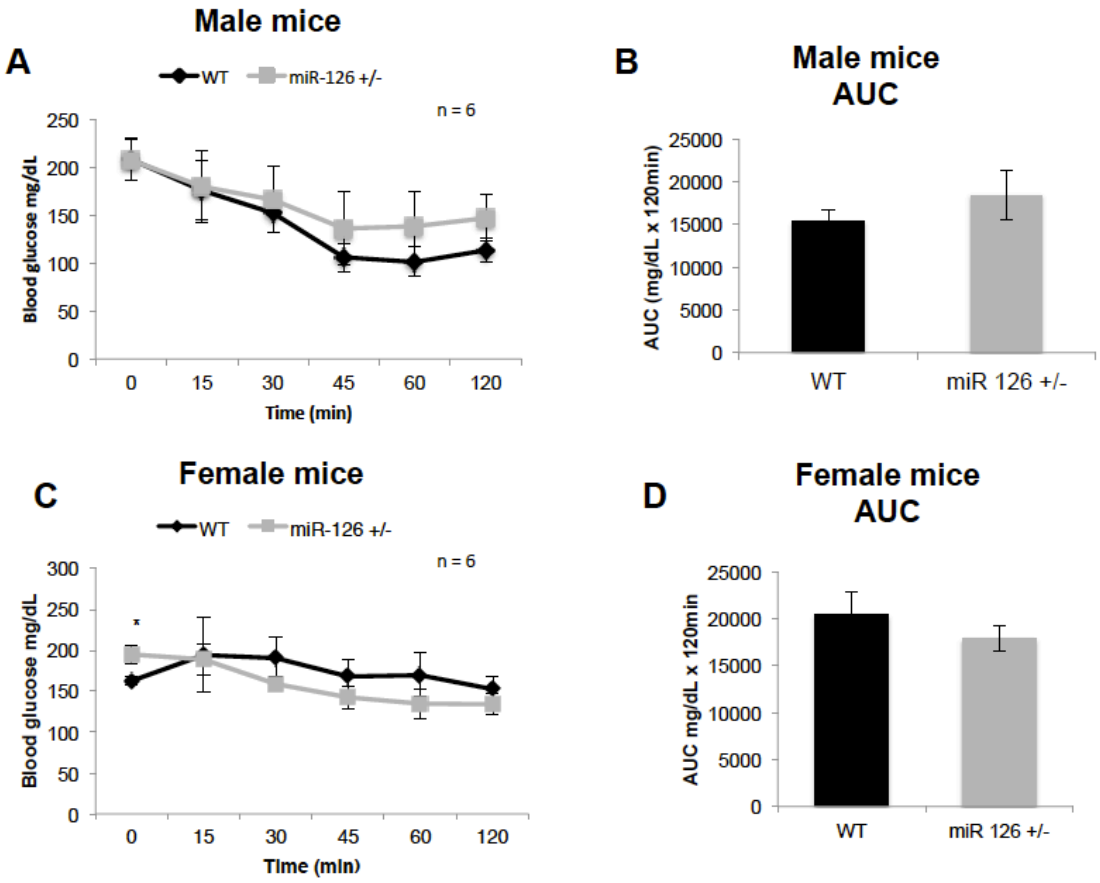


**Figure 4.3 miR-126$^{+/-}$ male and female mice are insulin sensitive.** Insulin tolerance test (1U/kg) in 10-12 week old male mice after a 4hr fast Error bars indicate SEM **(A)**. Area under the curve (AUC) from insulin tolerance test on male mice. Error bars indicate SEM **(B)**. Insulin tolerance test in 10-12 week old female mice (1U/kg) after a 4hr fast Error bars indicate SEM. (* $p \leq 0.05$) **(C)**. Area under the curve (AUC) from insulin tolerance test on female mice. Error bars indicate SEM **(D)**.

### 4.4.3 miR-126$^{+/-}$ male mice display sporadic weight defects

We also measured weights of mice starting at five weeks of age. A fraction of male miR-126$^{+/-}$ mice (20-30%) display sporadic weight defects (Fig. 4.4A). However, the reduced weight phenotype is not completely penetrant in male miR-126$^{+/-}$ mice (Fig. 4.4A). In contrast, female miR-126$^{+/-}$ mice do not display weight gain defects (Fig. 4.4B).

## Discussion

Several genetic and environmental factors have been shown to be important determinants of T2DM. Several genome wide association studies have identified multiple genes that make individuals susceptible to T2DM (Yasuda et al. 2008; Voight et al. 2010; Yamauchi et al. 2010). However, the mechanisms through which these genes contribute to the pathogenesis of the disease are not completely understood. Panels of miRNAs have been identified as potential markers of T2DM (He et al. 2017), however, there are no reports on the functions of individual miRNAs in the pathogenesis of the disease.

It is quite striking that loss of a single copy of miR-126 is sufficient to induce T2DM-like symptoms in an inbred mouse strain. Male and female miR-126$^{+/-}$ mice

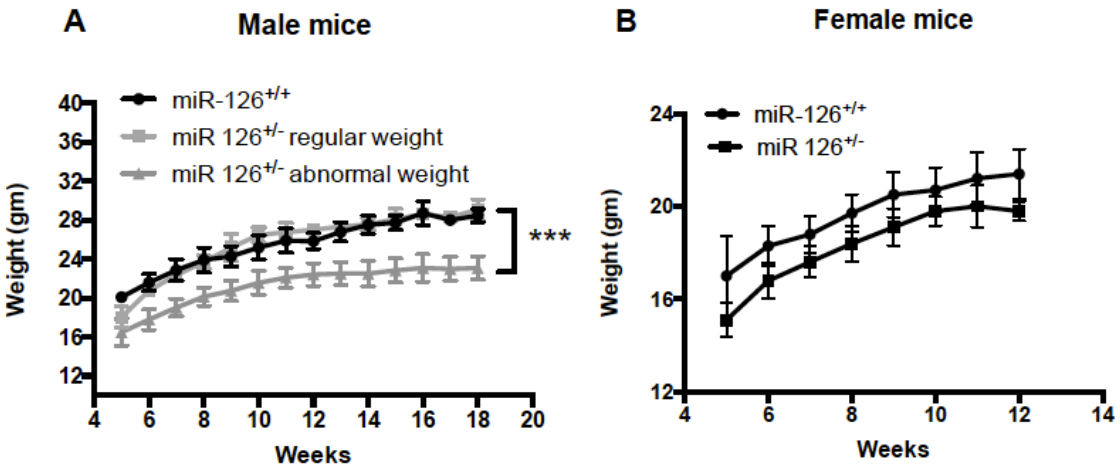


**Figure 4.4 miR-126$^{+/-}$ male but not female mice display weight-gain defects.** Mouse weights of male miR-126$^{+/+}$ (n = 12) and miR-126$^{+/-}$ (n = 4, abnormal weight. n = 8, regular weight) mice starting at 5 weeks of age. Error bars indicate SEM. (*** $p \leq 0.001$) **(A)**. Mouse weights of female miR-126$^{+/+}$ and miR-126$^{+/-}$ starting at 5 weeks of age. Error bars indicate SEM **(B)**.

display fasting hyperglycemia and hypoinsulinemia. This strongly suggests that reduced miR-126 levels not only correlate with, but also are functionally important for controlling blood glucose levels. Interestingly, only male miR-126$^{+/-}$ mice are severely glucose intolerant, and both male and female miR-126$^{+/-}$ mice are insulin sensitive. Sex specific differences in the phenotypes could potentially arise from a protective effect of estrogen on pancreatic beta cell failure in female mice (Liu and Mauvais-Jarvis 2010). This data suggests that loss of miR-126 may lead to a defective glucose stimulated insulin response. Future studies will focus on identifying novel expression domains for miR-126 in the pancreas and other peripheral organs associated with T2DM. Functional studies on pancreatic beta cells from miR-126$^{+/-}$ mice will help characterize insulin secretion defects in these mice.

## 4.5 Materials and methods

**Measurement of fasting blood glucose and serum insulin**.

10-12 weeks old mice were placed in fresh cage without chow for 4 hours. Blood glucose levels were measured using AlphaTrak2 glucometer with blood drawn from the tail vein of mice. For serum isolation, blood from the tail vein was allowed to coagulate at room temperature for 30min and spun at 2500g for 15min at 4C. Supernatant was collected and stored at -80$^{0}$C. Insulin levels were measured using an insulin ELISA kit (R&D).

**Glucose and insulin tolerance tests**

10-12 week old mice, after a 4-hour fast, were injected with either 1g/kg of glucose or 1U/kg of human insulin intra-peritoneally. Blood glucose levels were measured every 15min for 2hrs using AlphaTrak2 glucometer.

**Mouse weights**

Mouse weights were recorded every week on the same day starting at 5 weeks using a standard weighing scale.

## REFERENCES


American Diabetes A. 2013. Economic costs of diabetes in the U.S. in 2012. *Diabetes Care* 36: 1033-1046.

Campagnolo L, Leahy A, Chitnis S, Koschnick S, Fitch MJ, Fallon JT, Loskutoff D, Taubman MB, Stuhlmann H. 2005. EGFL7 is a chemoattractant for endothelial cells and is up-regulated in angiogenesis and arterial injury. *Am J Pathol* 167: 275-284.

Fernandez-Valverde SL, Taft RJ, Mattick JS. 2011. MicroRNAs in beta-cell biology, insulin resistance, diabetes and its complications. *Diabetes* 60: 1825-1831.

He Y, Ding Y, Liang B, Lin J, Kim TK, Yu H, Hang H, Wang K. 2017. A Systematic Study of Dysregulated MicroRNA in Type 2 Diabetes Mellitus. *Int J Mol Sci* 18.

Joglekar MV, Joglekar VM, Hardikar AA. 2009. Expression of islet-specific microRNAs during human pancreatic development. *Gene Expr Patterns* 9: 109-113.

Kantharidis P, Wang B, Carew RM, Lan HY. 2011. Diabetes complications: the microRNA perspective. *Diabetes* 60: 1832-1837.

Kaprio J, Tuomilehto J, Koskenvuo M, Romanov K, Reunanen A, Eriksson J, Stengard J, Kesaniemi YA. 1992. Concordance for type 1 (insulin-dependent) and type 2 (non-insulin-dependent) diabetes mellitus in a population-based cohort of twins in Finland. *Diabetologia* 35: 1060-1067.

Karbiener M, Fischer C, Nowitsch S, Opriessnig P, Papak C, Ailhaud G, Dani C, Amri EZ, Scheideler M. 2009. microRNA miR-27b impairs human adipocyte differentiation and targets PPARgamma. *Biochem Biophys Res Commun* 390: 247-251.

Li S, Chen X, Zhang H, Liang X, Xiang Y, Yu C, Zen K, Li Y, Zhang CY. 2009. Differential expression of microRNAs in mouse liver under aberrant energy metabolic status. *J Lipid Res* 50: 1756-1765.

Liang T, Liu C, Ye Z. 2013. Deep sequencing of small RNA repertoires in mice reveals metabolic disorders-associated hepatic miRNAs. *PLoS One* 8: e80774.

Liu S, Mauvais-Jarvis F. 2010. Minireview: Estrogenic protection of beta-cell failure in metabolic diseases. *Endocrinology* 151: 859-864.

Matsuda A, Kuzuya T. 1994. Relationship between obesity and concordance rate for type 2 (non-insulin-dependent) diabetes mellitus among twins. *Diabetes Res Clin Pract* 26: 137-143.

Mocharla P, Briand S, Giannotti G, Dorries C, Jakob P, Paneni F, Luscher T, Landmesser U. 2013. AngiomiR-126 expression and secretion from circulating CD34(+) and CD14(+) PBMCs: role for proangiogenic effects and alterations in type 2 diabetics. *Blood* 121: 226-236.

Nikolic I, Stankovic ND, Bicker F, Meister J, Braun H, Awwad K, Baumgart J, Simon K, Thal SC, Patra C et al. 2013. EGFL7 ligates alphavbeta3 integrin to enhance vessel formation. *Blood* 121: 3041-3050.

Polonsky KS. 2012. The past 200 years in diabetes. *N Engl J Med* 367: 1332-1340.

Poy MN, Eliasson L, Krutzfeldt J, Kuwajima S, Ma X, Macdonald PE, Pfeffer S, Tuschl T, Rajewsky N, Rorsman P et al. 2004. A pancreatic islet-specific microRNA regulates insulin secretion. *Nature* 432: 226-230.

Rich SS. 1990. Mapping genes in diabetes. Genetic epidemiological perspective. *Diabetes* 39: 1315-1319.

Schmidt M, Paes K, De Mazière A, Smyczek T, Yang S, Gray A, French D, Kasman I, Klumperman J, Rice DS et al. 2007. EGFL7 regulates the collective migration of endothelial cells by restricting their spatial distribution. *Development* 134: 2913-2923.

Shan ZX, Lin QX, Deng CY, Zhu JN, Mai LP, Liu JL, Fu YH, Liu XY, Li YX, Zhang YY et al. 2010. miR-1/miR-206 regulate Hsp60 expression contributing to glucose-mediated apoptosis in cardiomyocytes. *FEBS Lett* 584: 3592-3600.

Voight BF Scott LJ Steinthorsdottir V Morris AP Dina C Welch RP Zeggini E Huth C Aulchenko YS Thorleifsson G et al. 2010. Twelve type 2 diabetes susceptibility loci identified through large-scale association analysis. *Nat Genet* 42: 579-589.

Wang H, Hagenfeldt-Johansson K, Otten LA, Gauthier BR, Herrera PL, Wollheim CB. 2002. Experimental models of transcription factor-associated maturity-onset diabetes of the young. *Diabetes* 51 Suppl 3: S333-342.

Whiting DR, Guariguata L, Weil C, Shaw J. 2011. IDF diabetes atlas: global estimates of the prevalence of diabetes for 2011 and 2030. *Diabetes Res Clin Pract* 94: 311-321.

Winter WE, Silverstein JH. 2000. Molecular and genetic bases for maturity onset diabetes of youth. *Curr Opin Pediatr* 12: 388-393.

Yamauchi T, Hara K, Maeda S, Yasuda K, Takahashi A, Horikoshi M, Nakamura M, Fujita H, Grarup N, Cauchi S et al. 2010. A genome-wide association study in the Japanese population identifies susceptibility loci for type 2 diabetes at UBE2E2 and C2CD4A-C2CD4B. *Nat Genet* 42: 864-868.

Yasuda K, Miyake K, Horikawa Y, Hara K, Osawa H, Furuta H, Hirota Y, Mori H, Jonsson A, Sato Y et al. 2008. Variants in KCNQ1 are associated with susceptibility to type 2 diabetes mellitus. *Nat Genet* 40: 1092-1097.

Zampetaki A, Kiechl S, Drozdov I, Willeit P, Mayr U, Prokopi M, Mayr A, Weger S, Oberhollenzer F, Bonora E et al. 2010. Plasma microRNA profiling reveals loss of endothelial miR-126 and other microRNAs in type 2 diabetes. *Circulation research* 107: 810-817.

Zhang J, Du YY, Lin YF, Chen YT, Yang L, Wang HJ, Ma D. 2008. The cell growth suppressor, mir-126, targets IRS-1. *Biochem Biophys Res Commun* 377: 136-140.

Zhang T, Li L, Shang Q, Lv C, Wang C, Su B. 2015. Circulating miR-126 is a potential biomarker to predict the onset of type 2 diabetes mellitus in susceptible individuals. *Biochemical and biophysical research communications* 463: 60-63.

Zhou Y, Feng X, Liu YL, Ye SC, Wang H, Tan WK, Tian T, Qiu YM, Luo HS. 2013. Down-regulation of miR-126 is associated with colorectal cancer cells proliferation, migration and invasion by targeting IRS-1 via the AKT and ERK1/2 signaling pathways. *PLoS One* 8: e81203.

## Chapter 5: Conclusions and future perspectives

### 5.1 Summary

miR-126 has a functional role in regulating glycogen trophoblast proliferation in the murine placenta and glucose metabolism in adult mice in a C57Bl6\J background. In Chapter2, using a miR-126 loss of function mouse model, I have demonstrated that deletion of miR-126 results in aberrant glycogen trophoblast proliferation in the placenta and IUGR of embryos. In chapter 3, as a potential mechanism for regulating glycogen trophoblasts, I have shown that miR-126 regulates DNA methylation and imprinted gene expression in placenta by regulating DNMT1 expression. In chapter 4, I have shown that loss of a single copy of miR-126 can result in fasting hyperglycemia, glucose intolerance and sporadic weight defects in adult male mice. Results form this study provides insights into the role of miR-126 in placental development and metabolic dysfunction.

### 5.2 Implications of miR-126 signaling in placental development

The placenta is indispensable during development and despite several disease pathologies associated with the placenta, human placental development has not been extensively studied. Research on human placentas mainly relies on post partum tissue or choriocarcinoma cell lines. The use of transgenic mouse models has greatly aided identification of several genes and pathways that regulate human placental development. Research on miRNAs in placental development has been restricted to

studying their roles in *in vitro* and *ex vivo* trophoblast cultures or as biomarkers in placental pathologies. A large majority of miRNA knockout mice have subtle or no phenotypes and analysis of their placentas are largely ignored. miR-126 is one of the very few miRNAs with a lethal loss-of-function phenotype. Using a miR-126$^{-/-}$ mouse model, the studies described in chapters 2 and 3 give an insight into the role of miR-126 in placental development.

miR-126 deletion results in aberrant imprinted gene expression, methylation changes at ICRs and dysregulation of glycogen trophoblasts. However, there is no direct evidence to demonstrate loss of imprinting in miR-126$^{-/-}$ placentas. Assays used to quantify allele specific expression of imprinted genes rely on the presence of parent-specific single nucleotide polymorphisms (SNPs). Since miR-126$^{-/-}$ mice are in a congenic background, future studies will involve crossing miR-126$^{-/-}$ mice into a *Mus castaneus* mouse line. miR-126$^{-/-}$ placentas from miR-126$^{+/-}$ *Mus musculus* and *Mus castaneus* intercrosses will be used to quantify expression levels of imprinted genes from *musculus* and *castaneus* alleles and determine if deletion of miR-126 results in loss of imprinting in the placenta.

miR-126$^{-/-}$ embryos display pervasive hemorrhaging, reduced numbers of proliferating endothelial cells and defective angiogenesis as previously reported (Kuhnert et al. 2008; Wang et al. 2008). We hypothesized that loss of miR-126 would also result in deficient angiogenesis in the placenta. Surprisingly, miR-126$^{-/-}$ placentas have no defects in numbers of proliferating endothelial cells and vascular coverage in

the fetal labyrinth. However, miR-126$^{-/-}$ placentas display increased numbers of glycogen trophoblasts in the junctional zone. We have also identified a novel expression domain for miR-126 in trophoblast stem cells and all the differentiated trophoblast subtypes in the placenta. This data suggests that the junctional zone phenotypes in miR-126$^{-/-}$ placentas are cell autonomous. However, this does not eliminate the possibility that, endothelial cells of miR-126$^{-/-}$ placentas act in cell non-autonomous ways to affect trophoblasts. To delineate the role of miR-126 in junctional zone trophoblasts and endothelial cells, future experiments will use a conditional deletion of miR-126 (miR126$^{fl/fl}$). Endothelial specific deletion of miR-126 will be done by crossing miR126$^{fl/fl}$ and VE Cadherin-Cre mice (Alva et al. 2006). To study the role of miR-126 specifically in the junctional zone trophoblasts of the placenta, future experiments will use utilize miR-126$^{fl/fl}$ and Tpbpa-Cre (Simmons et al. 2007) mouse lines. miR126$^{fl/fl}$ mice will also be used to investigate if defects in the embryo contribute to placental phenotypes. To test if the loss of miR-126 in the embryo contributes to phenotypes of the extraembryonic tissues, Mox-2-Cre (MORE) mice (Tallquist and Soriano 2000) will be used to delete miR-126 specifically in the epiblast.

Both Egfl7 and miR-126 are expressed by trophoblasts of the placenta and endothelial cells of the placenta and embryo (Fitch et al. 2004; Lacko et al. 2014). EGFL7 and miR-126 loss-of-function mutants display complementary phenotypes in endothelial cells of the embryo and placenta during development. Global loss of EGFL7 does not result in major vascular defects in the embryo, whereas global loss of

miR-126 results in pervasive vascular defects in the embryo. In the placenta, loss of EGFL7 results in constricted vessels and aberrant vascular patterning, whereas loss of miR-126 results in no major vascular defects in the placenta. It is plausible, that redundant pathways exist for functions performed by Egfl7 (Rossi et al. 2015), but not miR-126 in the embryonic vasculature, and redundant pathways exist for functions performed by miR-126 but not Egfl7 in the placental vasculature. Egfl7 is a secreted protein, and could potentially have autocrine and paracrine effects, whereas miR-126 would mostly have intercellular functions. It is plausible that both vascular beds use distinct molecular mechanisms during angiogenesis. This result may also reflect the fact that the endothelial cell lineage in the fetal labyrinth is derived from the extraembryonic mesoderm of the allantois whereas all embryonic and adult endothelial cells are derived from the mesoderm of the embryo proper. The transcriptome of the placental endothelium is unique when compared to that of other vascular beds (Nolan et al. 2013).

Intronic miRNAs are proposed to have an antagonistic or synergistic effect on the function of the host gene. Egfl7 expression is unaffected in miR-126$^{-/-}$ embryos and placentas, and 3'UTR of EGFL7 does not contain binding sites for miR-126. Any synergistic or antagonistic roles of miR-126 on Egfl7 signaling would be through indirect mechanisms.

Future experiments will identify intersecting pathways between Egfl7 and miR-126 signaling. Gene expression analysis comparing embryonic and placental

vasculature from both Egfl7$^{-/-}$ and miR-126$^{-/-}$ mice will provide insights into overlapping and unique pathways regulated by Egfl7 and miR-126 during developmental angiogenesis in both vascular beds. Similarly gene expression analysis on Egfl7$^{-/-}$ and miR-126$^{-/-}$ trophoblast stem cells and their differentiated progenitors will be used to identify overlapping and unique pathways in trophoblasts.

miR-126 is proposed to be generated from alternatively spliced Egfl7 transcripts (Wang et al. 2008). The promoter of *Egfl7,* and intron 7, where miR-126 is located, contain multiple conserved CpG islands (Fig. 5.1). Epigenetic therapies on human cancer cell lines have been shown to modulate *Egfl7* and miR-126 expression (Saito et al. 2009). Our data from the murine placenta indicate that miR-126 controls imprinted gene expression in part by regulating *Dnmt1* expression. Recent evidence suggests that *Dnmt1* is imprinted in the human placenta (Das et al. 2013). It is plausible that DNA methylation of Egfl7 promoter and intron 7 regulates biogenesis of miR-126. Future experiments will explore the possibility of an autoregulatory loop between DNMT1 and miR-126 (Model in Fig 5.1)

Assisted reproductive technology (ART) has been associated with increased incidences of imprinting disorders in humans, potentially resulting in long-term adverse health outcomes in offspring (Odom and Segars 2010; Eroglu and Layman 2012; Chiba et al. 2013). In mouse models, ART procedures including superovulation, embryo transfer and culture of fertilized blastocysts cumulatively increase DNA methylation defects, loss of imprinting and morphological abnormalities in the

placenta (de Waal et al. 2014; de Waal et al. 2015). These studies also highlight the increased susceptibility of the placenta to methylation defects after ART procedures. It is not clear what culture conditions and mechanisms make the trophoblasts in the blastocyst vulnerable to methylation defects. We have shown that miR-126 regulates DNA methylation specifically in the trophoblasts of the placenta and more importantly, trophoblast stem cells, but not the embryo. It is plausible that environmental insults and cues trigger a miR-126 dependent DNA methylation response. Future experiments will identify upstream signaling factors that are part of the machinery controlling DNA methylation through miR-126 in trophoblasts.

### 5.3 Implications of miR-126 signaling in glucose metabolism

Type-2 diabetes is a chronic metabolic disorder that manifests from a combination of environmental and genetic factors. Although several studies show associations between altered miRNA expression and development of T2DM, few studies have focused on elucidating a possible role for miRNAs in the pathogenesis of the disease (Fernandez-Valverde et al. 2011; Kantharidis et al. 2011). Strikingly, loss of even a single copy of miR-126 leads to fasting hyperglycemia, hypoinsulinemia and severe glucose intolerance. To our knowledge this is the first example in which haploinsufficiency in a single miRNA results in metabolic dysfunction.

Collectively, data from the metabolic studies suggests that miR-126$^{+/-}$ mice have a defective insulin response. Future studies will involve functional assays on

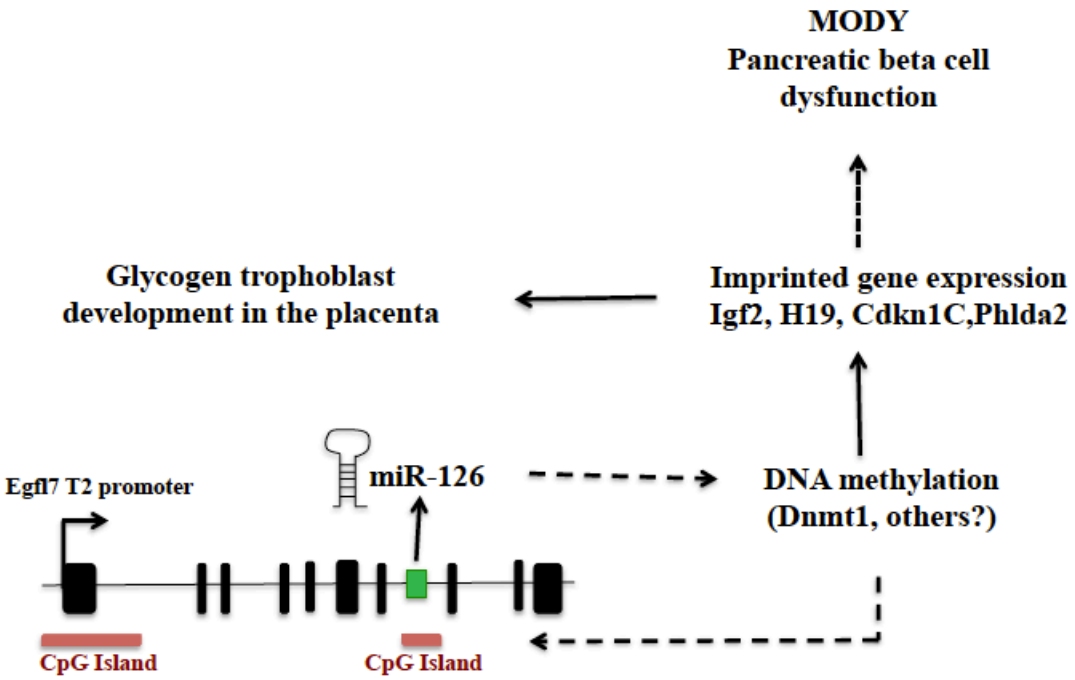


**Figure 5.1 Putative model for miR-126 in the placenta and pancreas.** miR-126 controls glycogen trophoblast numbers in the placenta by regulating DNA methylation and imprinted gene expression. miR-126 potentially regulates pancreatic beta cell function by regulating genomic imprinting at the Kcnq1 locus. (MODY – Maturity Onset Diabetes of the Young).

isolated pancreatic islets from these mice to identify any defects in insulin secretion. To measure islet response to glucose stimulation *in vivo*, a hyperglycemic clamp will be used. Islets isolated from miR-126$^{+/-}$ and miR-126$^{+/+}$ will also be used to perform *ex vivo* glucose stimulated insulin secretion assays.

A number of rare autosomal dominant, monogenic forms of diabetes termed maturity onset diabetes (MODY) have been identified in humans. Fourteen MODY subtypes are listed by the Online Mendelian Inheritance in Man (OMIM) database, four of which account for 80–90% of diagnosed cases (Shields et al. 2010). Of particular importance for our experiments, is the identification of Kcnq1 imprinted cluster as a susceptibility locus (Travers et al. 2013). Kcnq1 mutations in humans that cause loss of imprinting of CDKN1C on the paternal allele result in early onset diabetes accompanied by growth restriction (Kerns et al. 2014). Mouse models have demonstrated that deletion of Kcnq1 has no effect on mice, but loss of imprinting in that region results in reduced pancreatic beta cell mass and onset of diabetes (Asahara et al. 2015). Since miR-126 regulates CDKN1C expression by regulating DNA methylation in the placenta, it is plausible that miR-126 performs similar roles in the pancreas. Future experiments will analyze pancreatic islets isolated from miR-126$^{+/-}$ mice to identify potential defects in beta cell mass and imprinting.

The functional role of glycogen trophoblasts in the placenta is not known. It has been speculated that these cells provide nutrition to the embryo during late gestation, when energy demands become high. Importantly, studies in mice have

shown that the development and differentiation of this cell type is intricately liked to imprinted gene expression in the placenta. In human placentas, abnormal glycogen deposition is observed in pregnancies with gestational diabetes. Women treated with insulin have similar glycogen content to healthy women whereas women with a diet-based intervention have abnormal glycogen content in the placenta (Desoye et al. 1992; Desoye et al. 2002). This suggests that placenta serves as a buffer for excess fetal glucose during gestation. Increased placental glycogen in miR-126$^{-/-}$ placentas could potentially arise from a combination of pancreatic defects in pregnant miR-126$^{+/-}$ mice, resulting in hyperglycemia, and the inability of miR-126$^{-/-}$ placentas to buffer excess glucose. To test maternal contribution to placental phenotypes, blastocysts from miR-126$^{+/-}$ intercrosses will be transferred to miR-126$^{+/+}$ and miR-126$^{+/-}$ mice.

### 5.4 Conclusions

The studies presented in my thesis have used a loss-of-function mouse model to elucidate a miR-126 specific role in placental development and glucose metabolism. miR-126 regulates extra embryonic energy stores and DNA methylation specifically in the placenta. These findings uncover a novel mechanism for miRNA-based regulation of DNA methylation in extra embryonic tissue and raise the possibility of using miR-126 as a marker for non-invasive detection imprinting disorders. Furthermore, its role in regulating glucose metabolism may provide a novel angle for therapeutic targeting to treat insulin secretion defects in diabetes. Future studies on the roles of miR-126 in

placental development and glucose metabolism will determine its potential uses as a biomarker and as a therapeutic agent.

## REFERENCES

Alva JA, Zovein AC, Monvoisin A, Murphy T, Salazar A, Harvey NL, Carmeliet P, Iruela-Arispe ML. 2006. VE-Cadherin-Cre-recombinase transgenic mouse: a tool for lineage analysis and gene deletion in endothelial cells. *Dev Dyn* 235: 759-767.

Asahara S, Etoh H, Inoue H, Teruyama K, Shibutani Y, Ihara Y, Kawada Y, Bartolome A, Hashimoto N, Matsuda T et al. 2015. Paternal allelic mutation at the Kcnq1 locus reduces pancreatic beta-cell mass by epigenetic modification of Cdkn1c. *Proc Natl Acad Sci U S A* 112: 8332-8337.

Chiba H, Hiura H, Okae H, Miyauchi N, Sato F, Sato A, Arima T. 2013. DNA methylation errors in imprinting disorders and assisted reproductive technology. *Pediatr Int* 55: 542-549.

Das R, Lee YK, Strogantsev R, Jin S, Lim YC, Ng PY, Lin XM, Chng K, Yeo G, Ferguson-Smith AC et al. 2013. DNMT1 and AIM1 Imprinting in human placenta revealed through a genome-wide screen for allele-specific DNA methylation. *BMC Genomics* 14: 685.

de Waal E, Mak W, Calhoun S, Stein P, Ord T, Krapp C, Coutifaris C, Schultz RM, Bartolomei MS. 2014. In vitro culture increases the frequency of stochastic epigenetic errors at imprinted genes in placental tissues from mouse concepti produced through assisted reproductive technologies. *Biol Reprod* 90: 22.

de Waal E, Vrooman LA, Fischer E, Ord T, Mainigi MA, Coutifaris C, Schultz RM, Bartolomei MS. 2015. The cumulative effect of assisted reproduction procedures on placental development and epigenetic perturbations in a mouse model. *Hum Mol Genet* 24: 6975-6985.

Desoye G, Hofmann HH, Weiss PA. 1992. Insulin binding to trophoblast plasma membranes and placental glycogen content in well-controlled gestational diabetic women treated with diet or insulin, in well-controlled overt diabetic patients and in healthy control subjects. *Diabetologia* 35: 45-55.

Desoye G, Korgun ET, Ghaffari-Tabrizi N, Hahn T. 2002. Is fetal macrosomia in adequately controlled diabetic women the result of a placental defect?--a hypothesis. *J Matern Fetal Neonatal Med* 11: 258-261.

Eroglu A, Layman LC. 2012. Role of ART in imprinting disorders. *Semin Reprod Med* 30: 92-104.

Fernandez-Valverde SL, Taft RJ, Mattick JS. 2011. MicroRNAs in beta-cell biology, insulin resistance, diabetes and its complications. *Diabetes* 60: 1825-1831.

Fitch MJ, Campagnolo L, Kuhnert F, Stuhlmann H. 2004. Egfl7, a novel epidermal growth factor-domain gene expressed in endothelial cells. *Dev Dyn* 230: 316-324.

Kantharidis P, Wang B, Carew RM, Lan HY. 2011. Diabetes complications: the microRNA perspective. *Diabetes* 60: 1832-1837.

Kerns SL, Guevara-Aguirre J, Andrew S, Geng J, Guevara C, Guevara-Aguirre M, Guo M, Oddoux C, Shen Y, Zurita A et al. 2014. A novel variant in CDKN1C is associated with intrauterine growth restriction, short stature, and early-adulthood-onset diabetes. *J Clin Endocrinol Metab* 99: E2117-2122.

Kuhnert F, Mancuso MR, Hampton J, Stankunas K, Asano T, Chen CZ, Kuo CJ. 2008. Attribution of vascular phenotypes of the murine Egfl7 locus to the microRNA miR-126. *Development* 135: 3989-3993.

Lacko LA, Massimiani M, Sones JL, Hurtado R, Salvi S, Ferrazzani S, Davisson RL, Campagnolo L, Stuhlmann H. 2014. Novel expression of EGFL7 in placental trophoblast and endothelial cells and its implication in preeclampsia. *Mech Dev* 133: 163-176.

Nolan DJ, Ginsberg M, Israely E, Palikuqi B, Poulos MG, James D, Ding BS, Schachterle W, Liu Y, Rosenwaks Z et al. 2013. Molecular signatures of tissue-specific microvascular endothelial cell heterogeneity in organ maintenance and regeneration. *Dev Cell* 26: 204-219.

Odom LN, Segars J. 2010. Imprinting disorders and assisted reproductive technology. *Curr Opin Endocrinol Diabetes Obes* 17: 517-522.

Rossi A, Kontarakis Z, Gerri C, Nolte H, Holper S, Kruger M, Stainier DY. 2015. Genetic compensation induced by deleterious mutations but not gene knockdowns. *Nature* 524: 230-233.

Saito Y, Friedman JM, Chihara Y, Egger G, Chuang JC, Liang G. 2009. Epigenetic therapy upregulates the tumor suppressor microRNA-126 and its host gene EGFL7 in human cancer cells. *Biochem Biophys Res Commun* 379: 726-731.

Shields BM, Hicks S, Shepherd MH, Colclough K, Hattersley AT, Ellard S. 2010. Maturity-onset diabetes of the young (MODY): how many cases are we missing? *Diabetologia* 53: 2504-2508.

Simmons DG, Fortier AL, Cross JC. 2007. Diverse subtypes and developmental origins of trophoblast giant cells in the mouse placenta. *Dev Biol* 304: 567-578.

Tallquist MD, Soriano P. 2000. Epiblast-restricted Cre expression in MORE mice: a tool to distinguish embryonic vs. extra-embryonic gene function. *Genesis* 26: 113-115.

Travers ME, Mackay DJ, Dekker Nitert M, Morris AP, Lindgren CM, Berry A, Johnson PR, Hanley N, Groop LC, McCarthy MI et al. 2013. Insights into the molecular mechanism for type 2 diabetes susceptibility at the KCNQ1 locus from temporal changes in imprinting status in human islets. *Diabetes* 62: 987-992.

Wang S, Aurora AB, Johnson BA, Qi X, McAnally J, Hill JA, Richardson JA, Bassel-Duby R, Olson EN. 2008. The endothelial-specific microRNA miR-126 governs vascular integrity and angiogenesis. *Dev Cell* 15: 261-271.